

Enzymatic Synthesis and Microbial Degradation of β -Amino Acids via Transaminases

Zur Erlangung des akademischen Grades eines
DOKTORS DER NATURWISSENSCHAFTEN (Dr. rer. nat.)

Fakultät für Chemie- und Biowissenschaften
Karlsruhe Institut für Technologie (KIT)

genehmigte DISSERTATION

von

M. Sc. Sarah-Marie Dold

aus Überlingen

KIT-Dekan: Prof. Dr. Willem M. Klopper

Referent: Prof. Dr. Stefan Bräse

Korreferent: Prof. Dr. Christoph Syldatk

Tag der mündlichen Prüfung: 19.07.2016

Erklärung

Hiermit erkläre ich, dass ich die vorliegende Arbeit selbstständig angefertigt und keine anderen als die darin angegebenen Quellen und Hilfsmittel benutzt sowie die wörtlich oder inhaltlich übernommenen Stellen als solche kenntlich gemacht und die Satzung des Karlsruher Institut für Technologie (KIT) zur Sicherung guter wissenschaftlicher Praxis in der gültigen Fassung beachtet habe und dass die elektronische Version der Arbeit mit der schriftlichen übereinstimmt.

Ich versichere außerdem, dass ich diese Dissertation nur in diesem und keinem anderen Promotionsverfahren eingereicht habe und, dass diesem Promotionsverfahren keine endgültig gescheiterten Promotionsverfahren vorausgegangen sind.

Ort, Datum

Unterschrift

ABSTRACT

Enantiopure β -amino acids are of great importance as components of antibiotics or other drugs. Chemical synthesis of β -amino acids requires chiral precursors, hazardous materials and metallic catalyst loading. Enzymatic kinetic resolution of racemic β -amino acid esters is used in industrial processes. Transaminases and their wide substrate scope were found to be a suitable biocatalyst for this synthesis. In this work, aminotransferases were examined for asymmetric synthesis and were immobilized for easy downstream processes.

For this purpose, an aminotransferase from *Variovorax paradoxus*, which is described in literature and able to convert β -amino acids, was synthesized. A His-tag was coupled to the aminotransferase's coding gene and the resulting sequence was ligated into an expression plasmid. The successful heterologous expression in *Escherichia coli* was examined via nickel chelate-affinity chromatography and SDS-PAGE. The activity of the expressed enzyme was determined by biotransformation with several β -amino acids.

The His-tagged aminotransferase was immobilized out of the crude cell extract using magnetic M-PVA (polyvinyl alcohol) beads. Thereby, a one-step purification and immobilization approach of aminotransferases was performed for the first time. The immobilized aminotransferase exhibits long term stability with a residual activity of 50 % after 38 days, a 90 % residual activity after 7 cycles of recycling and higher temperature as well as pH stability. Due to immobilization using magnetic beads, it is now an easy downstream processing to recover the enzyme. Activity was determined for kinetic resolution of several enantiopure aromatic β -amino acids.

Asymmetric synthesis of enantiopure aromatic β -amino acids was to be conducted by a lipase and aminotransferase enzyme cascade. This is necessary due to the thermodynamic unfavoured prochiral educt, the β -keto acid, which is freshly prepared via hydrolysis of stable β -keto acid ester. The lipase from *Candida rugosa*, *Thermomyces lanuginosus* and *Rhizomucor miehei* were found to successfully hydrolyze the β -keto acid esters with an exhibited activity toward ethyl benzoylacetate and the, at the phenyl ring *para*-substituted, derivatives. Hence, both enzymes for asymmetric synthesis of β -amino acids through an enzyme cascade are provided.

The *Burkholderia phytofirmans* strain BS115 exhibits transaminase activity. To characterize the responsible enzyme and to investigate how the strain BS115 metabolize β -amino acids, several experiments were conducted. The establishment of a fermentation process was necessary as the enzyme is not overexpressed. Thereby high amounts of biomass are needed for its purification. As a first attempt shaking flask experiments were conducted with several

concentrations of *rac*- β -phenylalanine and glucose. These experiments provided preliminary results about the conversion of (*R*)- and (*S*)- β -phenylalanine and it was observed that acetophenone was formed. The (*S*)-enantiomer was completely consumed after 21 h in this time the acetophenone concentration increased. After total conversion of the (*S*)-enantiomer the (*R*)-enantiomer was consumed. The (*R*)-enantiomer may be converted via oxidative deamination. During biotransformation with crude cell extract and the purified enzyme with *rac*- β -phenylalanine only the (*S*)-enantiomer was converted. Hence, the conversion of the (*S*)-enantiomer is catalyzed by a (*S*)-selective ω -transaminase. The (*S*)-selective transaminase is also able to convert several aromatic β -amino acids with F, Cl, NO₂, CH₃O, OH and Br as residues at the phenyl ring.

Purification of the enzyme responsible for transaminase activity in *Burkholderia phytofirmans* strain BS115 was performed via ammonium sulfate precipitation and anion exchange chromatography. With this process a purification factor of 10 was achieved for the (*S*)-selective transaminase.

ZUSAMMENFASSUNG

Enantiomerenreine β -Aminosäuren sind von erheblicher Bedeutung als Bestandteile zahlreicher Antibiotika und andere Medikamente. Da zur chemischen Synthese von β -Aminosäuren chirale Vorstufen, toxische Materialien und metallische Katalysatoren benötigt werden, werden sie industriell mit enzymatisch katalysierter kinetischer Resolution racemischer β -Aminosäureestern hergestellt. Transaminasen besitzen einige Vorteile, die sie für die Synthese von β -Aminosäuren geeignet machen, zum Beispiel besitzen sie ein breitgefächertes Substratspektrum. Diese Enzyme wurden in dieser Arbeit für die asymmetrische Synthese zur Herstellung von enantiomerenreinen β -Aminosäuren untersucht, sowie die Wiederverwendbarkeit dieser Enzyme mittels Immobilisierung erreicht werden konnte.

Das Gen, einer in der Literatur beschriebenen Aminotransferase aus *Variovorax paradoxus* wurde synthetisiert, ein His-Tag angefügt und in einen Expressionsvektor kloniert. Die erfolgreiche heterologe Expression in *Escherichia coli* wurde mittels Nickelchelat-Affinitätschromatography und SDS-PAGE überprüft und die Aktivität des Enzyms mittels Biotransformation mit mehreren β -Aminosäuren nachgewiesen.

Die Immobilisierung erfolgte aus dem Zellrohextrakt an magnetische M-PVA Beads, sodass hier erstmals für Aminotransferase eine kombinierte Reinigungs- und Immobilisierungsmethode realisiert werden konnte. Die immobilisierte Aminotransferase zeigt Langzeitstabilität in einem Zeitraum von 38 Tagen, mit einer Restaktivität von 50 %. Außerdem ist sie mindestens 7 Mal wiederverwendbar mit einer Restaktivität von 90 %, ist stabil bei höheren Temperaturen und bei höheren pH-Werten. Durch die Immobilisierung an magnetischen Beads ist die Abtrennung des Enzyms aus der Reaktion erheblich erleichtert. Die Aktivität wurde durch kinetische Resolution mehrerer enantiomerenreinen aromatischen β -Aminosäuren bestimmt.

Für die asymmetrische Synthese von enantiomerenreinen aromatischen β -Aminosäuren sollte eine Enzymkaskade verwendet werden, die aus einer Lipase und einer Aminotransferase besteht. Dies ist erforderlich, da das benötigte prochirale Edukt, die β -Ketosäure thermodynamisch instabil ist und durch Hydrolyse eines stabilen β -Ketosäureesters hergestellt wird. Die Lipasen aus *Candida rugosa*, aus *Thermomyces lanuginosus* und aus *Rhizomucor miehei* wurden erfolgreich für die Hydrolyse von β -Ketosäureester eingesetzt und zeigten Aktivität für das Substrat Ethyl Benzoylacetat und seine am Phenylring in *para*-Stellung substituierten Derivate, so dass nun Enzyme für beide Teilreaktionen der Kaskade zur Verfügung stehen.

Transaminaseaktivität wurde in einem *Burkholderia phytofirmans* BS115 Stamm nachgewiesen. Deshalb sollte das verantwortliche Enzym näher charakterisiert werden und die Aufnahme von β -Aminosäuren in die Zelle untersucht werden, da es bisher kaum Informationen zum β -Aminosäuremetabolismus in Bakterien gibt. Dazu wurde ein Fermentationsprozess etabliert. Zuerst wurden Schüttelkolbenexperimente mit verschiedenen Konzentrationen von *rac*- β -Phenylalanin und Glukose durchgeführt. Dies brachte erste Erkenntnisse zum Abbau des (*R*)- und (*S*)- β -Phenylalanins und zeigte, dass bei der Reaktion Acetophenon entsteht. Das (*S*)-Enantiomer wurde nach 21 h bereits vollständig aufgebraucht, in dieser Zeit steigt die Konzentration an Acetophenon an. Nachdem das (*S*)-Enantiomer abgebaut wurde, sinkt die Konzentration des (*R*)-Enantiomers. Dieses könnte durch oxidative Desaminierung abgebaut worden sein. Da bei der Biotransformation mit Rohextrakt oder mit aufgereinigtem Enzym mit *rac*- β -Phenylalanine nach Zugabe von PLP und des Aminoakzeptors nur der Abbau des (*S*)-Enantiomers beobachtet werden konnte, kann man davon ausgehen, dass eine (*S*)-selektive Aminotransferase für den Abbau verantwortlich ist. Die (*S*)-selektive Aminotransferase ist auch geeignet um andere aromatische β -Aminosäuren, die am Phenylring in *para*-Stellung substituiert sind (mit F, Cl, NO₂, CH₃O, OH, Br) enantioselektiv abzubauen.

Zur Aufreinigung des für die Transaminaseaktivität in *Burkholderia phytofirmans* BS115 verantwortlichen Enzyms wurden eine Ammoniumsulfatfällung und eine Anionenaustauschchromatographie durchgeführt. Ein Aufreinigungsfaktor von insgesamt 10 konnte für die Transaminase erzielt werden.

PUBLICATIONS

Publications

Dold, S.-M., Syldatk, C., Rudat, J., Transaminases and Its Applications, in: Patel, R. (Ed.), Green Biocatalysis, 1. ed., WILEY-VCH Verlag, 2016, 715–746.

Dold, S.-M., Cai, L., Rudat, J. One-step purification and immobilization of a β -amino acid aminotransferase using magnetic (M-PVA) beads, *Eng. Life Sci.*, 2016, 16, 568–576

Buss, O., Jager, S., **Dold, S.-M.**, Zimmermann, S., Hamacher, K., Schmitz, K., Rudat, J., Statistical Evaluation of HTS Assays for Enzymatic Hydrolysis of β -Keto Esters, *PLOS One*, 2016, 11

Conference Publications

Dold, S.-M., Syldatk, C., Rudat, J., Synthesis of β -amino acids via Lipase/Transaminase reaction cascade, *Chem. Ing. Tech.* (special issue), 2014, pp. 1411-1412

Lecture

Dold, S.-M., Syldatk, C., Rudat, J., Synthesis of chiral β -amino acids via Lipase / Transaminase reaction cascade, Annual Conference of the Association for General and Applied Microbiology (VAAM) and Conference of the German Society for Hygiene and Microbiology, 2014, Biotechnology-Enzyme Catalysis (BTV20)

Poster

Dold, S.-M., Litty, D., Rudat, J, Beta beware – microbial degradation of aromatic β -amino acids, Annual Conference of the Association for General and Applied Microbiology (VAAM), 2016, Biospektrum (BDP02)

Dold, S.-M., Rudat, J, β -Amino acid production by a lipase/transaminase enzyme cascade 2 Increasing the stability and enabling recyclability of a β -transaminase, Annual Conference of the Association for General and Applied Microbiology (VAAM), 2016, Biospektrum (BTP30)

Dold, S.-M., Buss, O., Syldatk, C., Rudat, J., β -amino acid production by employing an enzyme reaction, Biotrans Wien, 2015, (PS-8)

Dold, S.-M., Syldatk, C., Rudat, J., β -amino acid production by a transaminase/lipase enzyme cascade, "Transam 2.0 - Chiral Amines Through (Bio)Catalysis" conference, 2015

Dold, S.-M., Syldatk, C., Rudat, J., Lipase- catalyzed hydrolysis of β -keto acid esters as precursor for synthesis of β -amino acids, Summer School RWTH Aachen, 2013

Dold, S., Maur, J., Syldatk, C., Rudat, J., Novel transaminases responsible for transformation of aromatic β -amino acids, 1st International Symposium on Transaminase Biocatalysis (Stockholm, S), 2013

Dold.S, Andre, M., Syldatk, C., Rudat, J., Chemische Acylierung enzymatisch synthetisierter Oligopeptide, Dechema Jahrestagung, 2012, Biotransformations

DANKSAGUNG

Folgenden Personen und Institutionen möchte ich meinen Dank aussprechen, da sie alle zum Gelingen dieser Arbeit beigetragen haben:

Herrn Prof. Christoph Syldatk für die Möglichkeit in seiner Arbeitsgruppe an diesem spannenden Thema zu arbeiten, für die wissenschaftlichen Diskussionen und das Interesse am Forschungsfortschritt.

Herrn Prof. Stefan Bräse für die freundliche Übernahme des Referates.

Herrn Dr. Jens Rudat für die Konzeption der Arbeit, zahlreichen Diskussionen, fachlichem Input und die Unterstützung und Motivation, wenn mal wieder nichts funktioniert hat.

Vielen Dank an meine Studenten Dennis, Nils-„Schnilsi“, Jonas, Raphael-„Michi“, Georg, Liyin, Bryan und Olli, die mit ihrem unermüdlichen Einsatz, ihrem unvoreingenommenen fachlichen Beitrag und den lustigsten Stunden in und außerhalb des Labors einen wertvollen Beitrag geleistet haben. Es war eine schöne Zeit mit euch!

Ein großer Dank geht auch an alle Kollegen, die mit ihrem fachlichem Wissen, ihrer immerwährenden Unterstützung, sowie lustigen Plaudereien auf dem Flur und im Büro eine Wohlfühlatmosphäre geschaffen haben: Ines, Marius, Pascal, Laura, Florian, Sascha, Ulrike, Katrin, Alba, Daisy, Deepansh, Julia und Judit. Janina und Michaela für die Beantwortung aller Fermentationsfragen, Sandra, für die Unterstützung an der ÄKTA und vielem mehr, Werner, für deine Hilfe und Unterstützung, wenn die HPLC mal wieder ausgefallen ist und ich am Verzweifeln war, Stefan (X-Ucker) und Olli, für die Gespräche und lustigen Zeiten. Johann Schäli, Dr. Pörnbein und MP, ich bin froh euch kennengelernt zu haben.

Danke Herrn Prof. Matthias Franzreb, für die Bereitstellung der magnetischen Partikel und fachlichem Beitrag.

Danke Dr. Kersten Rabe, für das bereitwillige Engagement bei der Aufreinigung und wissenschaftliche Unterstützung.

Ich danke dem BMBF für die Förderung innerhalb des MIE- Forschungsprojekts.

Herzlichen Dank an meine Familie und Manu für die immerwährende Unterstützung und Rückhalt! Ganz besonderen Dank an Christin, Carmi und Darja, für alle lustigen Stunden, für Diskussionen und Albernheiten, für hilfreiche Tipps und Ausraster.

TABLE OF CONTENT

Abstract	i
Zusammenfassung.....	iii
Publications	v
Danksagung	vii
Table of Content.....	viii
Abbreviations.....	xiii
1 Introduction	1
1.1 Transaminases	1
1.1.1 Classification as pyridoxal-5'-phosphate dependent enzymes	2
1.1.2 Classification based on substrate scope	3
1.1.3 Mechanism	3
1.1.4 Enantioselectivity.....	6
1.1.5 Synthesis strategy	6
1.2 β -amino acids	9
1.2.1 Chemical synthesis of β -amino acids	10
1.2.2 Enzymatic synthesis of β -amino acids.....	11
1.3 Protein Purification with Immobilized Affinity Ligands	13
1.3.1 Mechanism and choice of adsorbents and ions	13
1.3.2 Specifically bound proteins – His-tag.....	14
1.4 Immobilization and purification using magnetic (M-PVA) beads	15
1.5 <i>Burkholderia phytofirmans</i> spec. as model organism	16
1.5.1 General properties and characteristics	16
1.5.2 Previous applications and research.....	17
1.5.3 Novel applications	17
2 Research proposal.....	19
3 Material and Methods	20
3.1 Material	20
3.1.1 Devices.....	20
3.1.2 Chemicals and materials.....	21

3.1.3	Enzymes.....	22
3.1.4	Strains, plasmids and gene Sequence	23
3.1.5	Media.....	23
3.1.5.1	Solutions for cultivation.....	25
3.1.6	Buffers and solutions.....	25
3.1.6.1	Biotransformation buffer	25
3.1.6.2	Immobilized metal ion affinity chromatography (IMAC)	26
3.1.6.3	Immobilization on magnetic beads.....	26
3.1.6.4	HPLC buffer and solutions	27
3.1.6.5	Agarose gel elektrophoresis.....	27
3.1.6.6	SDS-polyacrylamid gel elektrophoresis	28
3.1.6.7	Silver nitrate solution	28
3.2	Analytical Methods	28
3.2.1	HPLC Analysis by precolumn derivatization.....	28
3.2.2	HPLC analysis without derivatization.....	29
3.2.3	Analysis with gas chromatography	29
3.2.4	Calculation of enzyme activity, purification, μ , t_d and consumption rate.....	30
3.3	Molecularbiological methods.....	30
3.3.1	Gene synthesis and introduction of a His-tag.....	30
3.3.2	Transformation	31
3.3.3	Plasmid preparation	31
3.3.4	Digestion by restriction enzymes	31
3.3.5	Agarose gel elektrophoresis	31
3.4	Microbiological methods.....	32
3.4.1	Strain maintenance	32
3.4.2	Preculture	32
3.4.3	Cultivation.....	32
3.4.3.1	Expression of aminotransferase gene in BL21DE.....	32
3.4.3.2	Shaking flask experiment with <i>Burkholderia phytofirmans</i>	32
3.4.4	Fermentation	33
3.4.4.1	Preculture.....	33
3.4.4.2	Fermentation.....	33

3.4.5	Cell harvesting.....	34
3.4.6	Cell disruption.....	34
3.5	Biochemical methods	35
3.5.1	Determination of protein concentration.....	35
3.5.2	Glucose assay.....	35
3.5.3	SDS-polyacrylamid gel electrophoresis	36
3.5.4	Protein purification via immobilized metal ion affinity chromatography (IMAC)	36
3.5.5	Desalting.....	37
3.5.6	Immobilization on magnetic M-PVA beads.....	38
3.5.7	Purification via magnetic M-PVA beads.....	39
3.5.8	Recycling of magnetic M-PVA beads	39
3.5.9	Fractionated ammonium sulfate precipitation.....	40
3.5.10	Ion exchange chromatography	40
3.6	Biotransformation.....	41
3.6.1	Kinetic resolution	41
3.6.1.1	Testing of optimal temperature and temperature stability	41
3.6.1.2	Testing of different pH values for pH optimum and stability	42
3.6.1.3	Substrate scope (β -amino acids)	42
3.6.1.4	Amino acceptors.....	42
3.6.1.5	Different concentrations of magnetic M-PVA beads.....	43
3.6.1.6	Incubation of magnetic M-PVA beads with various protein concentrations ..	43
3.6.1.7	Long-term stability	43
3.6.1.8	Recyclability of immobilized aminotransferase	44
3.6.2	Asymmetric synthesis	44
3.6.2.1	Hydrolysis of β -keto acid esters via lipases	44
3.6.2.2	Cascaded enzyme reaction.....	44
3.6.2.3	Asymmetric synthesis with 3-oxo-3-phenyl propionate as substrate	45
4	Results	46
4.1	Kinetic Resolution of β -amino acids.....	46
4.1.1	Introduction of a polyhistidin tag	46
4.1.2	Expression and activity of the His-tagged aminotransferase	47
4.1.3	Purification via immobilized metal ion affinity chromatography.....	50

4.1.4	Purification via magnetic M-PVA beads.....	53
4.1.5	One-step purification and immobilization using magnetic M-PVA beads	55
4.1.5.1	Influence of bivalent metal ions	56
4.1.5.2	Influence of the temperature	57
4.1.5.3	Influence of the pH	58
4.1.5.4	Influence of different amino acceptors	59
4.1.5.5	Substrate scope.....	60
4.1.5.6	Influence of various bead and crude cell extract concentrations.....	62
4.1.5.7	Storage stability and recyclability	63
4.2	Asymmetric synthesis of β -amino acids.....	65
4.2.1.1	Hydrolysis of β -keto acid esters	66
4.2.1.2	Asymmetric synthesis of β -amino acids via enzyme cascade.....	68
4.2.1.3	Asymmetric synthesis of β -amino acids with 3-oxo-3-phenyl propionate	71
4.3	Characterization of Transaminase Activity of <i>Burkholderia phytofirmans</i> spec.	72
4.3.1	Cultivation of <i>Burkholderia phytofirmans</i> spec. with β -amino acid as nitrogen source	73
4.3.2	Fermentation of <i>Burkholderia phytofirmans</i> spec.....	77
4.3.3	Substrate scope and choice of amino acceptor to characterize the transaminase activity of <i>Burkholderia phytofirmans</i> spec.....	79
4.3.4	Protein enrichment via ammonium sulfate precipitation.....	81
4.3.5	Protein enrichment via anion exchange chromatography	83
5	Discussion.....	86
5.1	Kinetic Resolution of β -amino acids.....	86
5.1.1	Expression and activity of the His-tagged aminotransferase	86
5.1.2	Purification of the β -amino acid aminotransferase	87
5.1.3	One-step purification and immobilization using magnetic M-PVA beads	89
5.1.3.1	Influence of bivalent metal ions	89
5.1.3.2	Influence of temperature and pH on immobilized aminotransferase.....	90
5.1.3.3	Influence of amino acceptors	92
5.1.3.4	Substrate scope.....	92
5.1.3.5	Influence of various beads and crude cell extract concentrations.....	94
5.1.3.6	Storage stability and recyclability	96
5.2	Asymmetric synthesis of β -amino acids via enzymatic cascade.....	97

5.2.1	Hydrolysis of β -keto acid esters	97
5.2.2	Asymmetric synthesis via enzyme cascade	98
5.3	Characterization of Transaminase Activity of <i>Burkholderia phytofirmans</i> spec.	100
5.3.1	Cultivation of <i>Burkholderia phytofirmans</i> spec with β -amino acid as sole nitrogen source	101
5.3.2	Fermentation of <i>Burkholderia phytofirmans</i> spec.....	103
5.3.3	Substrate scope and choice of amino acceptor of the transaminase from <i>Burkholderia phytofirmans</i> spec	106
5.3.4	Protein enrichment	108
6	References.....	111
7	Appendices	121
7.1	Sequence of the β -amino acid aminotransferase	121
7.2	Plasmid card	122
7.3	Freezing and thawing	122
7.4	Conversion of rac- β -phenylalanine with β -amino acid aminotransferase	123
7.5	Activity of the aminotransferase in the presence of DMSO	123
7.6	Asymmetric synthesis starting with the prochiral ketone 3-oxo-3-phenyl propionate	124
7.7	SDS-PAGE after incubation of the immobilized enzyme on magnetic beads at 90 °C	124
7.8	Acetophenone and rac- β -phenylalanine as carbon source	125
Figure Legend		cxxvi
Table Legend.....		cxxix

ABBREVIATIONS

ad	adjust
AEX	anion exchange chromatography
<i>ddH₂O</i>	demineralized water
BCA	Bicinchoninic acid
DMSO	dimethylsulfoxide
DNA	deoxyribonucleic acid
<i>E. coli</i>	<i>Escherichia coli</i>
EDTA	ethylenediaminetetraacetic acid
ee	enantiomeric excess
E-PLP	enzyme-pyridoxal-5'-phosphate complex
E-PMP	enzyme-pyridoxalmonophosphate complex
FTIR ATR	Fourier transform infrared spectroscopy- attenuated total reflectance
GC	gas chromatography
h	hour
HIC	hydrophobic interaction chromatography
HPLC	high performance liquid chromatography
IBLC	isobuturyl-L-cysteine
IDA	iminodiacetic acid
IMAC	immobilized metal ion affinity chromatography
IPTG	isopropyl β -D-1-thiogalactopyranoside
kb	kilo base
kDa	kilo dalton
K_M	Michaelis-Menten constant
KU	kilo units
LB	lysogeny broth
lpm	liter per minute
m	Mass, meter
MeOH	methanol
mM	milli molare = millimol per litre
M-PVA	magnetic-polyvinylalcohol
MTP	microtiter plate
MWCO	molecular weight cut off
μ_{max}	maximum growth rate
NaPP	sodium phosphate
ND	not determined

nm	nano meters
NTA	nitrilotriacetic acid
OD ₆₀₀	optical density at 600 nm
OPA	<i>ortho</i> -phtaldialdehyde
PLP	pyridoxal-5'-phosphate
PMP	pyridoxalmonophosphate
R	consumption rate
<i>rac</i>	racemic
<i>rac</i> -β-(Br)PA	3-amino-3-(4-bromphenyl)propionic acid
<i>rac</i> -β-(Cl)PA	3-amino-3-(4-clorophenyl)propionic acid
<i>rac</i> -β-(F)PA	3-amino-3-(4-fluorophenyl)propionic acid
<i>rac</i> -β-(<i>iso</i> propyl) PA	3-amino-3-(4-isopropylphenyl)propionic acid
<i>rac</i> -β-(NO ₂)PA	3-amino-3-(4-nitrophenyl)propionic acid
<i>rac</i> -β-(OCH ₃)PA	3-amino-3-(4-methoxyphenyl)propionic acid
<i>rac</i> -β-PA	3-amino-3-phenylpropionic acid
<i>rac</i> -β-(OH)PA	3-amino-3-(4-hydroxyphenyl)propionic acid
<i>rac</i> -β-hPA	β-homophenylalanine
RP	reversed phase
rpm	rounds per minute
rRNA	ribosomal ribonucleic acid
s	second
SDS	sodium dodecyl sulfate
SEC	size exclusion chromatography
<i>sp</i>	<i>species</i>
TB	terrific broth
TBE	Tris-aminomethan/borate/EDTA
t _d	doubling time
TFA	trifluoroacetic acid
TSB	tryptic soy broth
UV	Ultra violet
vvm	volume per volume per minute
% (v/v)	volume/volume (volume percent)

1 INTRODUCTION

Section 1.1 and 1.2 are published in Green Biocatalysis (Editor: Ramesh Patel): chapter 29 “Transaminases and Its Applications” -copyright 2016, John Wiley and Sons, Inc [1].

Section 1.5.1 and 1.5.2 are derived from the master thesis of Judit Maur [2].

1.1 TRANSAMINASES

Since their discovery, firstly published by Needham et al., transaminases or aminotransferases (EC 2.6.1.X) have received much attention as biocatalysts for the transformation of a keto acid to the corresponding amino acid/amine or vice versa [3]. Transaminases play an important role in amino acid metabolism and are ubiquitous in microbes and eukaryotic cells. They are pyridoxal-5'-phosphate (PLP)-dependent enzymes and are qualified as biocatalysts, due to their wide substrate scope, high enantio- and regioselectivity, high reaction rates, and stability [4]. As pictured in Figure 1.1, the amino group of the amino donor is transferred to the carbonyl group of the amino acceptor. Due to the aforementioned benefits of transaminases, they are utilized for the synthesis of optically pure amines, amino acids, and amino alcohols. These products are used as building blocks for fine chemicals and pharmaceutical agents or for food and agriculture. Furthermore, unusual amino acids, for example, β -amino acids, offer higher stability against proteases and thus are deployed in peptidomimetics. For the synthesis of non-canonical amino acids or bulky amines, novel ω -transaminases are used [5–9]. A variety of synthesis strategies were established and optimized for transaminases, facing the challenges of product and substrate inhibition and the need to shift the equilibrium toward the product.

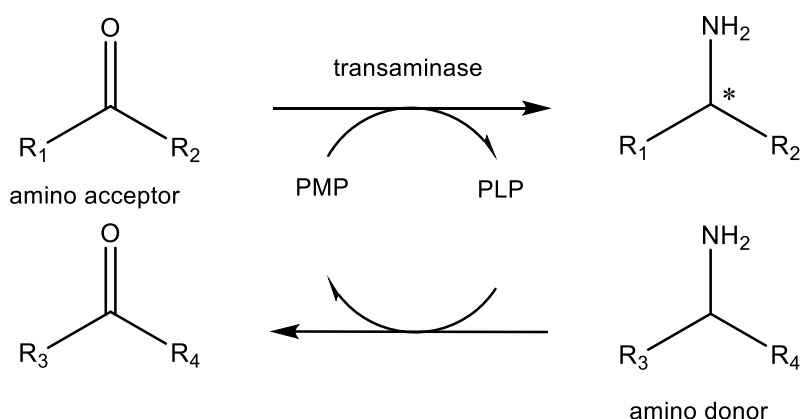


Figure 1.1: Transaminase catalyzed reaction mechanism.

1.1.1 Classification as pyridoxal-5'-phosphate dependent enzymes

Aminotransferases (AT) or transaminases (TA) comprise a major group of enzymes with different substrate spectra correlating with the sequence and the fold types of the different enzymes. Transaminases belong to the pyridoxal-5'-phosphate (PLP) dependent enzymes, which consist of seven fold types of enzymes on the basis of amino acid sequence comparisons (latest update: <http://bioinformatics.unipr.it/B6db>) [8]. Transaminases can be found within the fold types I und IV (table 1.1) [9-11]. According to the Pfam-database - a database of protein families, where families correlate sharing high sequence similarity of defined protein regions - transaminases are divided in six subgroups [12]. The typical transaminases in fold type I are the well-known and described aspartate aminotransferase and other (S)-selective transaminases. Recently a branched-chain aminotransferase from the thermophilic archaeon *Thermococcus sp.* CKU-1 has been discovered and classified to fold type I due to its high homology to the fold type I transaminases known so far [13]. Interestingly this enzyme reaches its maximum activity not until 95 °C. Furthermore it is noteworthy that this transaminase is active towards isoleucine and valine, which is not described for other transaminases in this fold type. In the division of fold type IV transaminases, lately an (R)-selective ω -transaminase from *Aspergillus terreus*, has been described [14], as well as branched chain aminotransferases.

Table 1.1: Classification of transaminases based on their evolutionary relationship as pyridoxal-phosphate dependent enzymes.

Pfam subgroup	fold type	Enzyme
		Aspartate AT
I/II	I	Aromatic AT
III	I	ω -TA
		Branched chain AT
IV	IV	(R)-selective AT
V	I	Phosphoserine AT
VI		
(DegT_DnrJ_EryC1)	I	Sugar AT

Enzymes of fold type I/IV are active as homodimers with two active sides, a larger domain, with a seven-stranded β -sheet in the center and a smaller domain, containing the C-terminus of the amino acid chain. Pyridoxal-5'-phosphate is covalently bound to the larger domain via the ϵ -amino group of a lysine residue. The difference between the two fold types is based on the mirror inverted binding of the phosphate in the active side. For fold type I classified enzymes the *re* face of the enzyme is exposed to the solvent, rather than the *si* side of enzymes of fold type IV [11, 15].

1.1.2 Classification based on substrate scope

A possible classification of transaminases is based on their differing substrate scope [10, 11]. The amino donor for the transamination, catalyzed by transaminases, can be classified in three chemically different groups, differing in the presence and position of the functional groups, usually a negatively charged carboxylate group. Thus transaminases are divided into α -transaminases, ω -transaminase, and amine transaminases. Since α -transaminases need substrates with the α -carboxylic group adjacent to the amino, carbonyl, or keto-substituted α -carbon atom, these enzymes usually catalyze the transamination of proteinogenic amino acids in the metabolism and are industrially established for the production of canonic amino acids. The next group of transaminases - the ω -transaminases - accepts substrates with carbon atoms between the carbonyl and the carboxylate group and substrates with the ketone or aldehyde function on the terminal carbon atom. Therefore the aminotransferases of this group are high in demand for the synthesis of various building blocks for pharmaceuticals, like chiral amines. Amine transaminases convert ketones into amines and do not require substrates with any carboxylic group. This is a huge benefit to produce sterically challenging amines like rivastigmine [12] or sitagliptin [13], among other amines. A very important difference between α -transaminases and amine transaminases is concerning the reaction equilibrium. The equilibrium of α -transaminase-catalyzed reactions is close to unity, whereas the production of alanine is strongly favored using amine transaminase as biocatalyst, indicating the need to shift the equilibrium toward the product side.

1.1.3 Mechanism

The reaction mechanism of transaminases is well understood and examined in detail due to structure determination of the aspartate aminotransferase [14–18]. The transfer of the amino group is supported by the external cofactor pyridoxal-5'-phosphate (PLP) forming a Schiff base with the ϵ -amino group of the lysine in the active side of the enzyme (Lys-E), called internal aldimine. The internal aldimine keeps the PLP in a highly reactive condition, due to the positively charged nitrogen of the protonated imine which is far more electrophilic than the aldehyde or ketone. Further conversion leads to pyridoxamine-5'-phosphate (PMP) reacting as an intermediate via the ping-pong bi-bi reaction mechanism [19]. The reversible reaction is accomplished in two reaction steps: In the first step PLP reacts with the L-aspartate to PMP and oxaloacetate. In the second reaction step, the amino acceptor, for example, α -ketoglutarate, regenerates the PLP, and the product L-glutamic acid is created (details are shown in Figure 1.2.). More precisely, the internal aldimine undergoes transamination with the amino group of the substrate to create the external aldimine. But it is important that either the internal aldimine is protonated and the amino group is not or the internal aldimine is deprotonated and the amino group is protonated for the extra proton that can be transferred

between the amino group of the substrate and the imine nitrogen of the aldimine [18]. The formed Michaelis–Menten complex possesses the proton on the imine nitrogen and the free amino group of the substrate. This leads to a rapid attack of the free amino group and a geminal diamine mediated by 3'-oxygen of PLP. The diamine collapses into the external aldimine intermediate and the free amino residue of the lysine in the active side of the enzyme as the leaving group. The step after the external aldimine is the formation of the corresponding α -carbanionic intermediate (quinonoid) by loss of the substrate's α -hydrogen bond through deprotonation catalyzed by the free base of the lysine of the active side (Lys-E). This quinonoid possesses the electron pair from the α -hydrogen bond delocalized onto the pyridine nitrogen. Protonating the C4' is leading to the ketimine intermediate. The ketimine reacts to the carbinolamide intermediate by addition of water to the C α atom catalyzed by Lys-E. Finally, deprotonation of the carbinolamide leads to the PMP/ oxaloacetate Michaelis complex, which dissociates to the free enzyme and the product. The reverse of the same steps with α -ketoglutarate as substrate leads to L-glutamic acid as amino acid product. The influence of the PLP cofactor concerning the activity and stability of transaminases and their catalyzed reactions was shown for ω -transaminases as well [20–22].

The main limitation in the described transamination reaction is inhibition by the substrates utilized and the formed products. It is noteworthy that substrate inhibition results from both amine enantiomers. For example, the (*R*)-enantiomer can form a Michaelis–Menten complex with PLP leading to dead-end complexes, whereas the (*S*)-enantiomer is able to convert PLP to PMP [23]. This indicates that the substrate inhibition and therefore the wide substrate range are caused by the promiscuous binding pockets of the enzyme. Conversely, it is possible that the product forms a Michaelis–Menten complex with PLP of the free enzyme. Thus, the place for the substrate is taken and fast conversion rates are inhibited. Another limitation for amination with transaminases is the equilibrium of the reaction. Due to the reversibility of all steps in the reaction mechanism, it is necessary to shift the equilibrium toward the product side to reach high conversion yields.

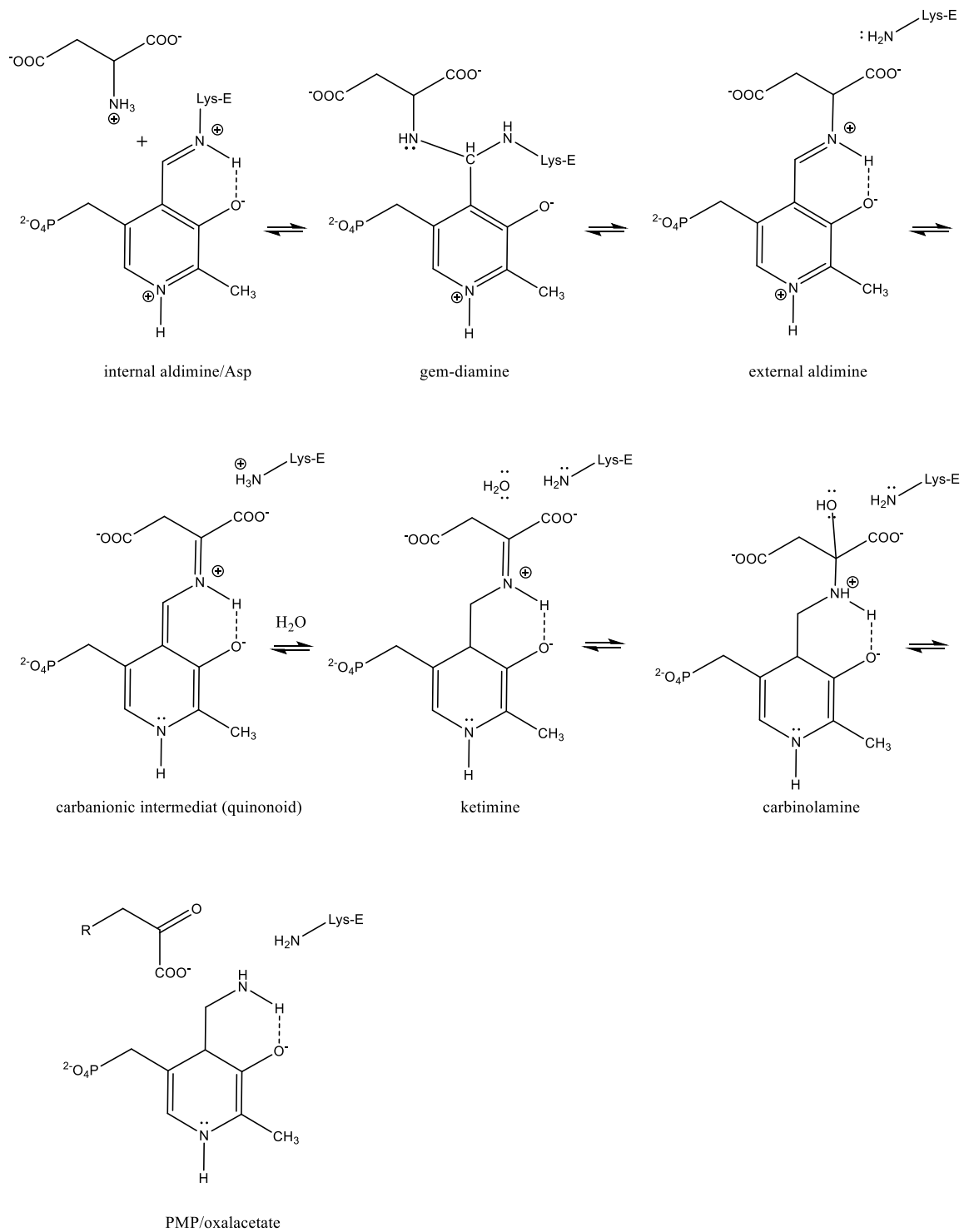


Figure 1.2: Reaction mechanism of transaminases with pyridoxal-5'-phosphate (PLP) as external co-factor via a ping-pong bi-bi mechanism. A two-step reaction, starting with an internal aldimine creating an external aldimine to pyridoxamine-5'-phosphate (PMP). Modified after Toney et al [16].

1.1.4 Enantioselectivity

The most described transaminases are showing high enantioselectivity for the chiral carbon atom with the carboxylic group at the α -position or the chiral center at the β -position. To determine the mechanism towards enantioselectivity of transaminases a structure analysis is necessary. The crucial factor is the architecture of the active side of the enzyme, which gives the substrate the required orientation into the binding pockets [24]. Since the discovery of transaminases numerous (*S*)-selective enzymes have been isolated. To expand the applications for biocatalysis, (*R*)-selective transaminases are in demand as well. The most convenient tool to reveal (*R*)-selective transaminases is computational design or protein engineering [25]. In the last years various transaminases with (*R*)-enantiopreference have been discovered. A recently published study has determined the structure of an (*R*)-selective amine:pyruvate aminotransferase from *Nectria haematococca*, which has the ability to convert (*R*)-methylbenzylamine and several (*R*)-amines and ketones [26]. Furthermore (*R*)-selective amine transaminases from *Aspergillus terreus* und *Aspergillus fumigatus* have been characterized lately [26, 27]. For the β -selectivity of aminotransferases no binding mode has been reported so far. Wybenga et al. showed that the active side of the aminotransferase from *Mesorhizorium sp.* evolved specifically to receive both, β - and α - amino acids [28]. This aminotransferase is enantioselective towards (*S*)- β -phenylalanine, and (*R*)-3-amino-5-methylhexanoic acid, and toward (*R*)-3-aminobutyric acid, due to their stereo configuration of the functional groups on the C- β -atom. The architecture of the active sides showed that the orientation of the substrates is forced to bind the carboxylic group at the arginine in the P-pocket, the side chain in the O-pocket and the groups associated with the amino group on the *si*-face of the β -carbon of the keto acid. Moreover the O-pocket binding the aliphatic and hydrophilic side chains of β -amino acids is also capable of binding the α -carboxylic groups of α -amino acids.

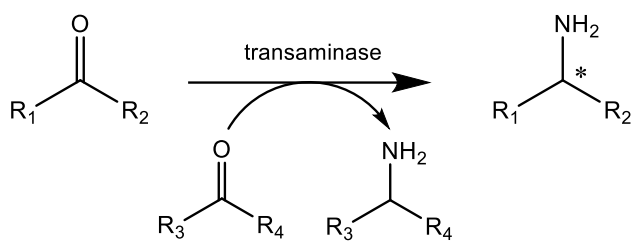
Consequently, it is important to gain further knowledge about the structure and the mechanism of the relevant enzymes to facilitate in protein engineering in order to expand the substrate and thus the product range, leading to the desired optically pure enantiomers.

1.1.5 Synthesis strategy

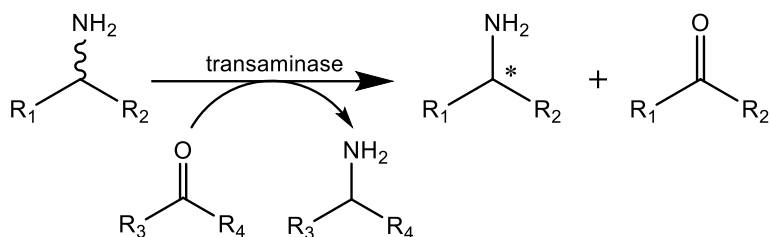
Transaminases are well established as biocatalysts in the production of a wide variety of chiral amines and amino acids. The use of the latter as building blocks in pharmaceuticals, like in antiarrhythmics, cancer or diabetes treating drugs and agrochemicals, makes it particularly important to find enzymatic approaches for their production and to overcome the limitations which are accompanied with the chemical synthesis methods known so far [29, 30]. The synthesis of enantiopure amines has been the main challenge of chemical, synthetic routes,

since protective groups, toxic transition metal catalysts, harsh reaction conditions and multiple reaction steps are needed [31, 32]. Reactions catalyzed by transaminases offer advantages like a promiscuous substrate spectrum, no need of external co-factors, high enantio- and stereo- selectivity, mild reaction conditions and good reaction yields. Only catalytical amounts of pyridoxal-5'-phosphate (PLP) are needed as a co-factor to stabilize and to form the active dimer [6, 8, 29, 33]. Transaminases can either be utilized in kinetic resolution or asymmetric synthesis (see Figure 1.3.). Asymmetric synthesis, starting with a prochiral ketone substrates can theoretically lead to 100 % conversion and is usually the preferred way to generate chiral products (Figure 1.3 A). Furthermore high enantiomeric purity is not dependent on conversion rates, whereas a kinetic resolution (Figure 1.3 B) needs 50 % conversion for a high enantiomeric excess (*ee*). However, kinetic resolution is thermodynamically favoured, if pyruvate is the amino acceptor, compared to asymmetric synthesis where the equilibrium lies on the substrate side [7, 34]. To achieve 100 % conversion, dynamic kinetic resolution serves as an alternative with spontaneous deracemization or the initiation with a suitable racemase for enantiomerically pure substrates (Figure 1.3 C). Deracemization in a one-pot two-step reaction with an (*S*)- and (*R*)-selective transaminase respectively is a further method of choice, but for that purpose two enantiocomplementary enzymes are needed (Figure 1.3 D) [35]. Therefore deracemization with a dehydrogenase in the kinetic resolution step and a transaminase in the following step is an option [36]. But overall the major challenges of transaminase-catalyzed reactions still are product and substrate inhibition for each described synthesis strategy and the necessity to shift the reaction equilibrium toward the product in order to achieve high reaction yields.

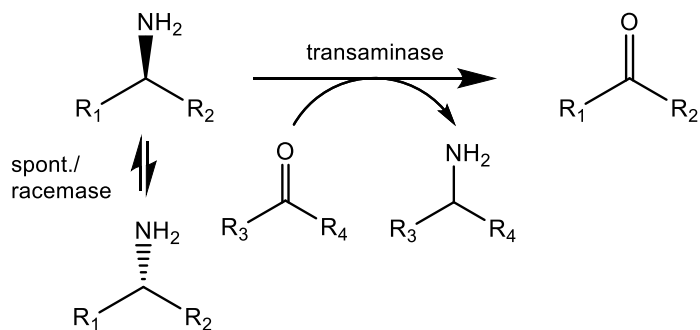
A Asymmetric Synthesis with Transaminase



B Kinetic Resolution with Transaminase



C Dynamic Kinetic Resolution with Transaminase



D One pot two step Deracemization with Transaminase

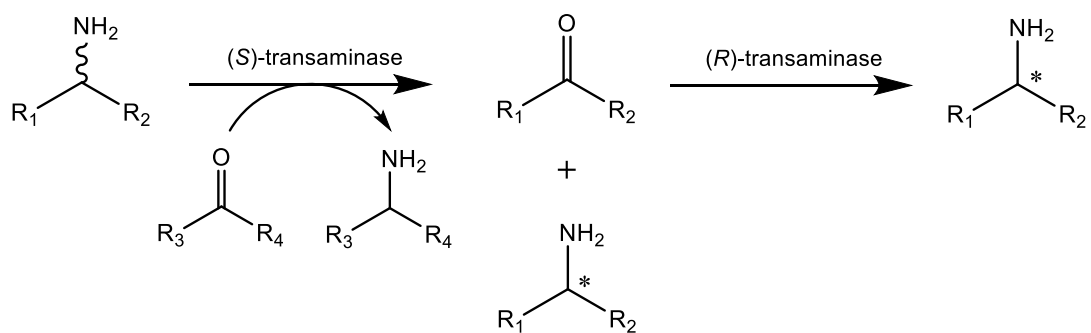


Figure 1.3: General synthesis strategies for transaminase-catalyzed reactions.

1.2 β -AMINO ACIDS

Considering the growing importance of β -amino acids as building blocks for peptidomimetics and bioactive compounds, there is the need of new synthesis strategies for their production in enantiopure form. As shown in Figure 1.4., the amine group of β -amino acids is attached to the β -carbon atom compared to α -amino acids. There are β^3 , β^2 - and $\beta^{2,3}$ -substituted amino acids, classified by the position and number of their residues [37–39].

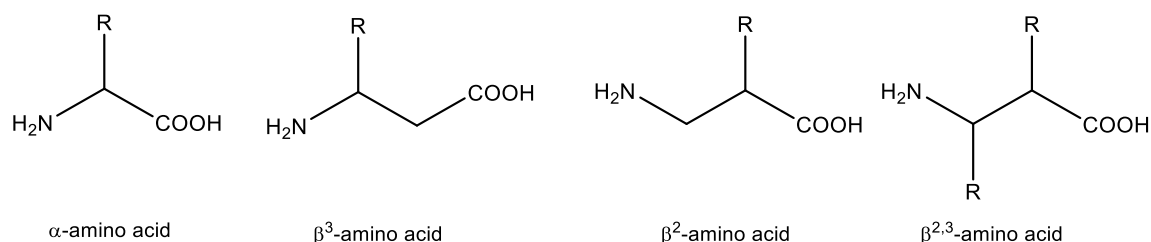


Figure 1.4: The structures of α - and β -amino acids.

Various β -amino acids occur naturally as free metabolites in metabolic pathways or as key intermediates in biosynthetic products. For example β -alanine, the simplest β -amino acid appears in pantothenic acid, a precursor of the coenzyme A. Further examples are (2*R*,3*S*)-*N*-benzoyl-3-phenylisoserine derived from (*R*)- β -phenylalanine, which serves as a compound in the antitumor agent paclitaxel from *Taxus brevifolia* [40] or as a building block in β -lactam antibiotics [41] and in jasplakinolide, an antifungal compound [42]. A few examples of the in this work utilized β -amino are shown in Figure 1.5.

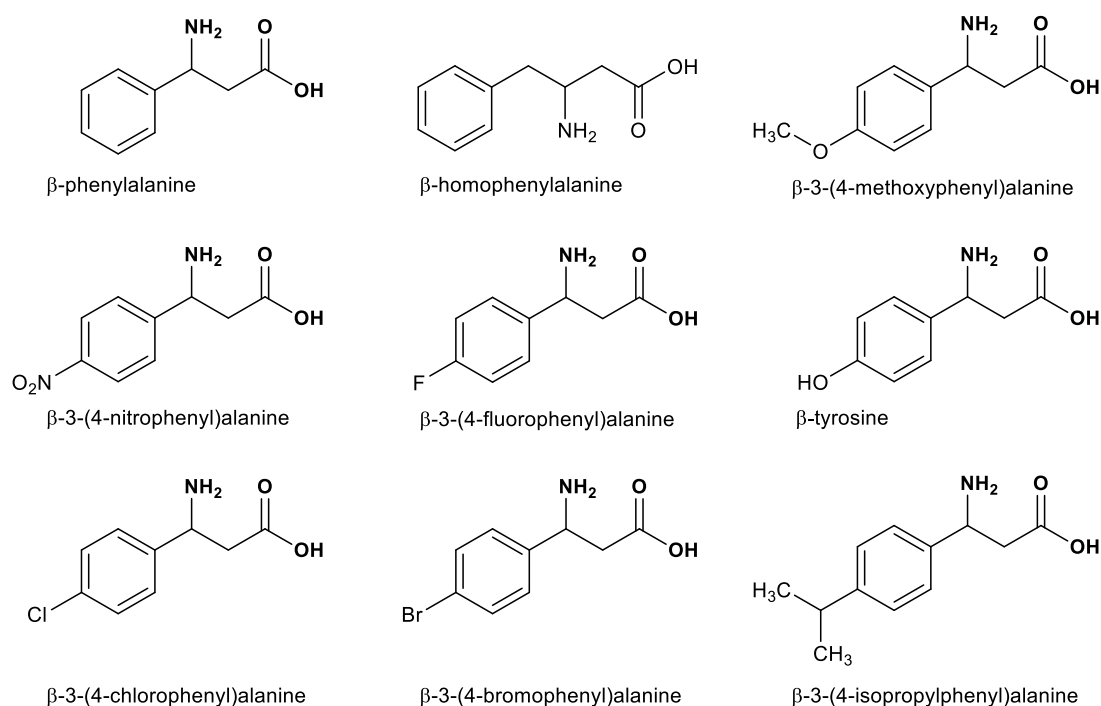


Figure 1.5: Overview of the β -amino acids examined in this work.

Additionally, β -amino acids possess the ability to form β -peptide analogs to α -peptides. These secondary structures are highly stable against cleavage of proteolytic enzymes [43, 44]. Furthermore, it was noticed that mixed peptides containing α - and β -amino acids seemed to be more protected against proteolytic digestion [45].

1.2.1 Chemical synthesis of β -amino acids

The chemical synthesis of β -amino acids has been described in several reviews in the last years [46–48].

Arndt-Eistert homologation

An attempt for the chemical synthesis of β -amino acids is the homologation of α -amino acids, which has the advantages of low costs and high enantiopurity of the substrates. Seebach and his coworkers synthesized β -peptides with this method. *N*-protected α -amino acids are used to create an anhydride with triethylamine and ethylchloroformate. After adding diazomethane, the enantiopure diazoketone is formed. To produce the β -amino acid a Wolff rearrangement has to be achieved by UV light or with catalytic amounts of silver benzoate in triethylamine and methanol. The diazoketone can as well be entrapped with another carboxyl protected β -amino acid for the direct formation of a β -peptide. [49]

Curtius rearrangement

Further succinates can be used as precursors for the synthesis of β -amino acids, by transforming the carboxylic group into an amine group with a Curtius rearrangement. For the synthesis of *N*-Boc-protected iturinic acid and 2-methyl-3-aminopropanoic acid functionalized succinic acid are used. First alkylation at the α -carbon with sodium bis(trimethylsilyl)amide to the imide takes place. After selective removal of the imide by hydrolyzation with lithium peroxide or trifluoroacetic acid (TFA) and Curtius rearrangement, *N*-protected β -amino acids are provided. These can be deprotected with another Curtius rearrangement to isomeric β -amino acids. [50]

Asymmetric Mannich-reaction

This method involves the condensation of an imine and an ester enolate. For the preparation of (*R*)- β -phenylalanine and (*S*)-ethyl- β -3-pyridinepropanoate diastereoselective addition of sodium enolate to chiral sulfinimine are carried out. Sulfinimine is treated with $\text{CH}_3\text{CO}_2\text{Me}$ and sodium bis(trimethylsilyl)amide and TFA to get the desired product. [51, 52]

Conjugate addition

In this field, various protocols for the synthesis of β -amino acids exist. In this overview, diastereoselective conjugated addition of metalized amines (chiral nucleophiles) will be amplified. For example lithium *N*-benzyl-phenylethylamide is subjected to different enolates,

after debenzoylation with a Pearlmans catalyst (palladium hydroxide on carbon) and hydrolysis of β -amino acids and α -methyl-substituted β -amino acids occurs with high enantiomeric purity [53]. Furthermore after hydroxylation of the intermediate enolate, α -hydroxy β -amino acids can be synthesized [54].

Reductive amination

One attempt for reductive amination is the chemoselective reduction of a β -enamino ester with sodium tricacetoxyborohydride in acetic acid. The intermediate formed by ligand exchange between the β -enamino ester and the acetoxy ligand is converted with acetic acid to the final product [55].

Catalytic hydrogenation

Another approach for enantiopure β -amino acid derivatives is the catalytic hydrogenation of nitriles and acrylic acids. For example, the synthesis of β -amino acid esters via hydrogenation of 3-aminoacrylate was catalyzed by a rhodium catalyst. With this reaction, a spectrum of aliphatic β -amino esters were synthesized, but only the β -(acyl-amino) acrylates with a phenyl substitute was brought to a successful conclusion with a modest ee of 65-66%. The reaction was carried out under high H_2 pressure and in toluene. The chosen rhodium catalysts were Rh-BICP and Rh-DuPhos [56].

Friedel-Crafts reaction

The asymmetric Friedel-Crafts reaction is an effective route to construct chiral centers on the α - or β - position of aromatic systems. Liu and coworkers added a 2-methoxyfuran to an aromatic nitro olefin in an asymmetric Friedel-Crafts reaction with a diphenylamine-tethered bisoazoline Zn(II) complex in xylene. The product of this reaction is an intermediate which can form, treated with diazomethane, the β -nitro ester leading to the corresponding β^2 -amino acid. [57]

Despite the numerous ways for chemical synthesis of β -amino acids many challenges remain, concerning the application in large industrial scales. Drawbacks include high costs of silver, rhodium, and other catalysts, as well as a narrow range of chiral α -amino acids, the necessity of hazardous reagents for the reaction and long reaction times. This is leading to another option for the synthesis of β -amino acids, the enzymatic route. Advantages for this route are the aqueous milieu for the reaction and thus no hazardous reagents, short reaction times and low costs for the biocatalyst.

1.2.2 Enzymatic synthesis of β -amino acids

Various ways for the enzymatic synthesis of β -amino acids are described so far. For example the acylation of racemic aliphatic β -amino acid esters with a lipase from *Candida antartica*,

with 2,2,2- trifluoroethyl butanoate in diisopropyl ether and with butyl butanoate towards an enantiopure β -amino acid ester was described [58, 59]. In the last two decades, several approaches for the enzymatic synthesis of enantiopure β -amino acids were pursued [8, 47]. Starting from *N*-acetylated ethyl esters lipases [43], aminomutases [60, 61], acylases [62], monooxygenases [63] and amidases [64] were applied.

But in this work, however enzymatic synthesis of β -amino acids catalyzed by a transaminase is discussed.

Kinetic Resolution

The advantage of kinetic resolution of β -amino acids is the shift of the equilibrium towards the product side, due to the spontaneous decarboxylation of the β -keto acid by-product. For the synthesis of *D*-amino-*N*-butyric acid with a ω -transaminase from *Alcaligenes denitrificans* and pyruvate as amino acceptor conversion rates of 53 % and >99 % ee were obtained [65]. Mathew and his group produced chiral β -amino acids with a ω -transaminase from *Burkholderia graminis* via kinetic resolution [66]. For the synthesis of chiral β -amino acids with conversion rates of about 50 % and ee of >99 % different amino acceptors (benzaldehyde amongst others) were tested.

Furthermore the kinetic resolution of racemic β -phenylalanine catalyzed by the ω -transaminase from *Burkholderia phytofirmans* has been examined recently [67].

Asymmetric synthesis

For the challenging asymmetric synthesis of β -amino acids, caused by the unstable, prochiral β -ketone acid substrate, a coupled reaction combining the hydrolysis of the β - keto acid ester by a lipase from *Candida rugosa* and the transamination with a β -transaminase isolated from *Mesorhizobium sp* has been proposed [68]. With conversion rates of 20 % and >99 % ee for the (*S*)-enantiomer of 3-amino-3-phenylpropionic acid, this coupled reaction was successful. The equilibrium was favoured due to 3-aminobutyric acid as amino donor, converting into the volatile acetone with acetaldehyde as an intermediate. At first, the β - keto acid ester has been considered as amino donor for the transamination reaction, but no formation of the corresponding β -amino acid ester was noticed, assuming that, transaminases possess no ability for the amination of β -keto acid esters. The same working group showed in 2015 the asymmetric synthesis of 10 different β -amino acids with the same enzyme cascade, but with an optimized ratio of lipase and transaminase of 4:3.3 and (*S*)-methylbenzylamine as amino donor leading to an enhanced yield of up to 99 % [69].

Various ω -transaminases have been found to be suitable for asymmetric synthesis and kinetic resolution of amino acids with high conversion rates and high enantiomeric excess, often in

combination with other enzymes to shift the equilibrium. A huge benefit of the latter enzymes is the wide substrate range, thus even amino acids with bulky side chains can be converted.

To gain a stable and reusable biocatalyst for the synthesis of β -amino acids, immobilization is suitable technique. In this work, an immobilization approach for a His-tagged aminotransferase was established which is based on the IMAC principle. The enzyme is immobilized out of the crude cell extract, giving the advantage of a low cost immobilized biocatalyst.

1.3 PROTEIN PURIFICATION WITH IMMOBILIZED AFFINITY LIGANDS

For rapid and extensive purification of proteins, affinity chromatography with immobilized metal ions (IMAC) has gained much attention over the recent years. Covalently bound chelating compounds were used on a solid insoluble matrix with entrapped metal ions. These metal ions were used as affinity ligands for a variety of proteins, exhibiting certain amino acid residues on their surface. [70] This purification technique offers some advantages even for the application in industrial processes, like ligand stability, mild elution conditions, simple regeneration and low costs [71].

1.3.1 Mechanism and choice of adsorbents and ions

The principal of IMAC purification is the coordination of the metal ions and the corresponding electron donor groups, residing on the surface of the protein. Common metal ions employed in IMAC are Cu^{2+} , Ni^{2+} , Co^{2+} , Zn^{2+} and Fe^{3+} , which are electron pair acceptors and can be considered as Lewis acids. Electron donor atoms are, for example, N, S and O, available on the compounds attached to the support matrix. These compounds could be tetradentate or tridentate, which is dependent on the number of disposable coordination bonds (figure 1.6). [70, 72] The remaining sites are occupied by water molecules, which are replaced by corresponding sites of the protein during the purification process. These corresponding sites are either the amino groups or special amino acids with electron donor atoms in their side chains (histidine, cysteine, tryptophane, phenylalanine [73]). An attempt to replace the bound amino acid side chain groups is the ligand exchange carried out with imidazole at neutral pH, which is specified for histidyl groups.

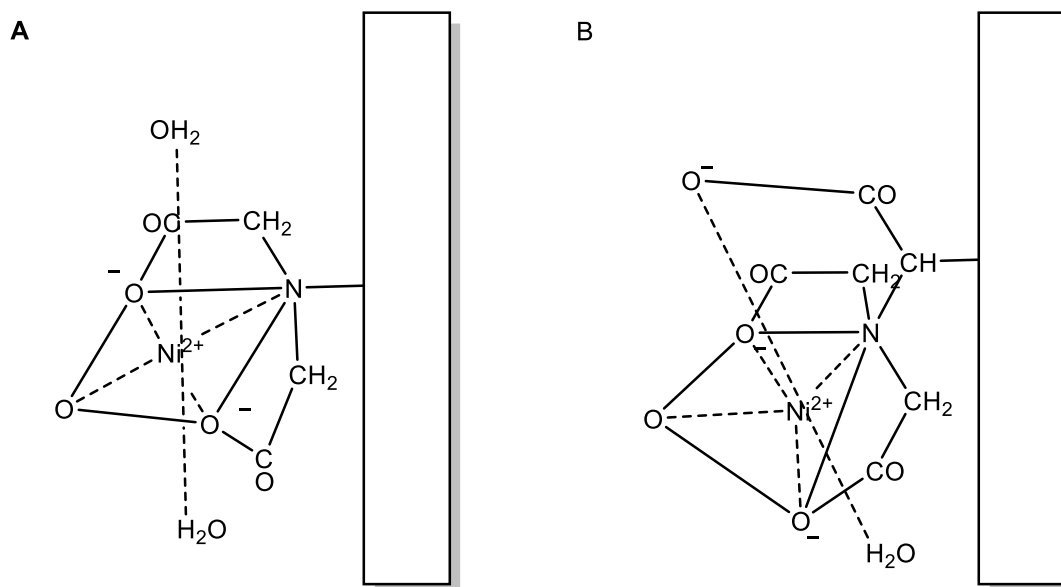


Figure 1.6: Solid matrix functionalized with iminodiacetic acid (IDA) (tridentate) and covalently bound nickel (A) and functionalized with nitrilotriacetic acid (NTA) (tetradentate) with a covalently bound nickel (B). Modified after Garberc-Porekar et al [70].

Even if tetradentate adsorbents like nitrilotriacetic acid (NTA) have a higher affinity to metal ions, the most used adsorbent for IMAC purification is the tridentate iminodiacetic acid (IDA), due to weaker binding to the protein of tetradentate adsorbents caused by the loss of a condensation site. [72, 74–76]

1.3.2 Specifically bound proteins – His-tag

The IMAC technique was used for proteins naturally presenting histidine residues. This was changed by Hochuli et al, who invented recombinant enzymes with attached histidine residues at the N- or C-terminus [72, 76]. Histidin-tags can be incorporated in any expression vector and can be added to the target gene by site- directed mutagenesis or by polymerase chain reaction. Furthermore, the DNA fragment consisting of oligonucleotides, coding for the polyhistidine- tag can be created synthetically and cloned into the desired position [77]. Normally, the polyhistidine tail is introduced at the C-terminus of the recombinant protein; therefore no interference with the translation occurs. Introduction of the His-tag at the N-terminus, on the other hand, was also reported [78]. The concept of using polyhistidine-tags is based on enhancing the binding to the functionalized matrix by multiple histidine residues. Khan and coworkers increased the binding to the matrix and therefore achieved higher purification yields by a double hexahistidin- tag [79]. Another option is the His₁₀-tag which is also improving the purification scheme and can be removed by stringent washing steps [80]. However, the most attention lies on His₆-tags, described very well in literature for a wide range of applications. Beitzinger and coworkers described His₆-tagged proteins that showed enhanced binding capacity to antigens, which are used to intoxicate cells [81]. Thus, the broadest field using polyhistidin tags is purification of enzymes and other proteins. [82–85]

1.4 IMMOBILIZATION AND PURIFICATION USING MAGNETIC (M-PVA) BEADS

In the last decade enzyme immobilization became an important field in biocatalysis. The advantages of immobilized enzymes are their reusability and the enhanced stability toward pH and temperature changes. Especially for application in industrial processes, long-term stability, reusability and easy down-stream processing are presupposed to lower the overall costs. [86, 87] Since magnetic separation is an interesting option for the removal of the biocatalyst from the reaction media, non-porous polyvinyl alcohol (M-PVA) micro beads have been considered as carriers to covalently bind enzymes [88, 89]. The small diameter of these micro beads reduces mass transfer limitations, and in some cases, the K_M values are lower, due to the decreased charge density in the electrical double layer [90].

Another advantage of magnetic M-PVA beads is their ability to be differently functionalized, giving a variety of options for immobilization of enzymes. Jia and coworkers immobilized a ω -transaminase on magnetic PVA- Fe_3O_4 beads via glutaraldehyde cross-linking [91]. Another possibility is a surface covered with chloroalkane binding enzymes with a Halo-tag. The Halo-tag is fused to a lipase, which can be immobilized directly from the crude cell extract and the lipase shows high activity and high storage stability [92]. This is a major step for immobilization of enzymes. Traditionally, purified enzyme solutions were required for immobilization. The sometimes necessary precipitation and chromatographic purification out of the crude cell extract in order to achieve high purities are associated with high costs. A major step toward the immobilization is the integration of affinity tags to the enzyme and the preparation of suitable carriers. In figure 1.7, the surface of magnetic beads is functionalized with IDA, building a chelating complex with a bivalent metal ion (in this case nickel). The histidines of the polyhistidin tag are binding to this chelating complex and a stable immobilization of the enzymes is achieved. This immobilization technique offers the benefit of one-step immobilization and purification directly from the crude cell extract.

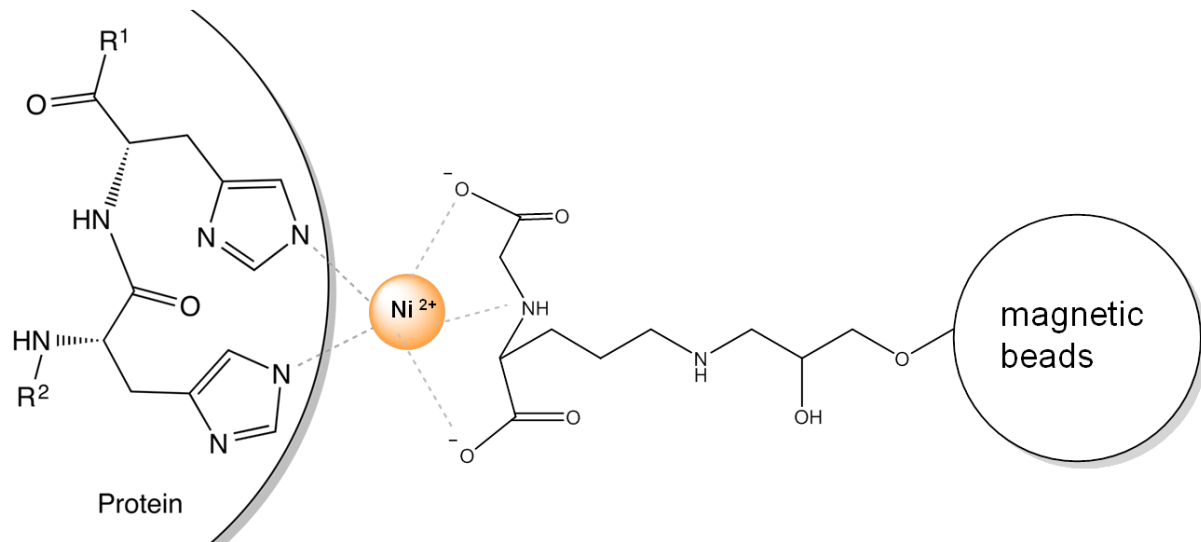


Figure 1.7: Protein with His-tag, binding onto nickel-chelate complex with functionalized magnetic beads.

1.5 *BURKHOLDERIA PHYTOFIRMANS SPEC. AS MODEL ORGANISM*

1.5.1 General properties and characteristics

Strain *Burkholderia phytofirmans* PsJN was firstly mentioned in a work from Frommel and coworkers in 1991 [93]. Based on several biochemical and physiological tests the *Burkholderia phytofirmans* was erroneously taken as *Pseudomonas spec.* After 16S rRNA sequencing it was determined as *Burkholderia phytofirmans* PsJN, which belongs to the β -proteobacteria and comprises more than 30 species so far [94]. It is a gram-negative, non-sporulating, rod-shaped, motile bacterium with a single polar flagellum [94]. It was originally isolated from an onion root infected by *Glomus vesiculiferum* and is shown as a highly efficient plant-conductive bacterium. This bacterial strain is able to form rhizosphere and endophytic populations associated with various plants [95]. The bacterium is able to stimulate the growth of the plants, including tomatoes, potatoes, maize and grapevines. The significant changes of bacterized plant compared to non-bacterized plants are the increased root numbers and increased weight of the roots. Furthermore, the lignin content of the plants inoculated with the bacterium is higher, secondary roots develop and the leaf hair formation is enhanced [93, 96]. The inoculation with the bacterium induces developmental changes, leading to better water management [97] and enhanced resistance resulting in low levels of pathogens [98]. The plants inoculated with this species seem to have an increased level of the phytohormones cytokinin and indole-3-acetic acid (IAA) and enhanced activity of phenylalanine ammonia lyase, which is hypothesized to be responsible for the enhanced growth of infected plants [93, 98, 99]. [2]

1.5.2 Previous applications and research

As described in 1.5.1, *Burkholderia phytofirmans* PsJN is an endophyte with a beneficial effect toward various plants. These plant growth-promoting rhizobacteria (PGPR) are able to lower biotic and abiotic stress [95]. Enhanced growth after inoculation with this PGPR is thought to be influenced by choline-phosphoribosyltransferase (QPRT) and 1-amino cyclopropane-1-carboxylate (ACC) deaminase. ACC deaminases are commonly found in PGPR and cleave the plant's ethylene ACC, leading to a decreased ethylene level of a stressed or developing plant. QPRT is involved in the *de novo* biosynthesis of NAD⁺, which could be used by the plant. [94, 100]

Inoculation of *Vitis vinifera* L. cv. Chardonnay with *Burkholderia phytofirmans* PsJN results in increased growth of the grapevine and increased physiological activity at lower temperatures. A major effect is observed at root growth and plantlet biomass at an ambivalent temperature of 26 °C and 4 °C. Furthermore, the bacterized plants enhance the CO₂ fixation and O₂ evolution and increase levels of starch, proline and phenolics. Modification of the carbohydrate metabolism and a non-stomatal limitation of photosynthesis (under cold conditions) are observed to correlate with the enhancement of cold tolerance. [101–103] The tolerance of cold temperatures after inoculation with PsJN is observed for *Arabidopsis thaliana* as well [104]. The photosynthesis is enhanced after exposure to -3 °C, and thickening of the cell wall is observed. Another abiotic stress is water abstraction (drought). The effects of inoculation with PsJN of maize is examined by Naveed and coworkers [105]. Maize showed reduced effects of drought stress on growth and photosynthesis. Drought stress effectuates oxidative burst in plants as a primary immune response, including increased production of reactive oxygen species (ROS). Increased production of ROS leads to extensive cellular damage and cell death and provokes upregulation of genes involved in detoxification of ROS in strain PsJN. Furthermore oxidative phosphorylation is activated in strain PsJN, generating energy for almost all vital processes. [106] The positive effects of endophytes like *Burkholderia phytofirmans* PsJN on plants exposed to abiotic stress, could be a solution for challenges in the growing demand of energy and food stock, due to the enhanced plant growth and control of plant diseases [107, 108]. An advantage for application in these fields is the complete sequencing of the genome of PsJN [109]. [2]

1.5.3 Novel applications

Biocatalysis

A new application of endophyte *Burkholderia phytofirmans* is the deployment in biocatalysis. A novel class of hydroxynitril lyases (HNL) was found in *Burkholderia phytofirmans* strain PsJN [110]. This new enzyme shows activity with acetone cyanohydrin and Cl-substituted mandelonitril, as well as with *meta*-phenoxybenzaldehyde cyanohydrin. High activity was also

observed for the synthesis of mandelonitril by converting benzaldehyde. The synthesis is regioselective in the (*R*) direction with an ee of 89 %. An imidase isolated from *Burkholderia phytofirmans* strain DSM 17436 is capable to hydrolyze 3-substituted glutarimide stereoselectively to synthesize 3-substituted glutaric acid monoamide [111]. This chemoenzymatic reaction can be deployed for the synthesis of 3-substituted gamma-aminobutyric acid (GABA), used in human therapeutics, like for the treatment of spasticity or autism disorders [112, 113]. The imidase was found to hydrolyze 3-isobutyryl glutarimide to (*R*)-3-isobutyryl glutaric acid monoamide with an ee of 95 %. Furthermore, the imidase is able to hydrolyze 3-(4-chlorophenyl) glutarimide to (*R*)-3-(4-chlorophenyl) glutaric acid monoamide.

Biodegradation

Another application of *Burkholderia phytofirmans* arises from the ability of this strain to biodegrade novel substrates. Vu and coworkers investigated the biodegradation of thiocyanate, a toxic contaminant of gold mine tailings and a waste product of the steel and chemical industry [114]. This finding could provide a new tool for the bioremediation of thiocyanate to protect soil and water. The strain is able to oxidize sulfur in thiocyanate to sulfate with acetate as carbon source. The sulfate decreases after 2 days of incubation, which can be explained with the assimilatory sulfate reduction occurring in other *Burkholderia species* [115]. The strain *Burkholderia phytofirmans* is also capable of converting unnatural aromatic β -amino acids, which was investigated in 2010 by Brucher [67]. A range of bacterial strains were examined to convert these novel amino acids as sole nitrogen source in minimal media. The conversion of aromatic β -amino acids was only possible when the enzyme, responsible for the conversion, is expressed by adding β -amino acids to the medium. The enzyme responsible for the conversion is a transaminase, strictly enantioselective, converting only the (*S*)-enantiomer.

2 RESEARCH PROPOSAL

β -Amino acids as building blocks for peptidomimetics and bioactive compounds are of great importance. A variety of β -amino acids can be found in nature, in metabolic pathways or key intermediates in biosynthetic products. For instance, an (*R*)- β -phenylalanine derivative serves as a component in the antitumor agent Taxol™. For the production of enantiopure β -amino acids pyridoxal-5'-dependent ω -transaminases recently attracted attention due to their wide substrate scope. Two basic strategies are known for the synthesis of enantiopure amines and amino acids. Kinetic resolution is starting from a racemic substrate which converts to the optical pure product with high ee for complete substrate conversion. Asymmetric synthesis of amines and amino acids is starting with a prochiral ketone substrate transforming to the chiral product with high ee, even for poor conversion rates. Both synthesis strategies need an amino donor and acceptor pair which should be kinetically favored by the chosen biocatalyst.

In this work transaminases able to convert β -amino acids are to be found. A suitable transaminase is to be applied for the kinetic resolution and asymmetric synthesis of enantiopure β -amino acids. For asymmetric synthesis an enzyme cascade has to be established consisting of a lipase and a transaminase. The enzyme cascade is necessary, due to the unstable prochiral substrate for β -amino acid synthesis. Therefore, the reaction has to start with a stable β -keto acid ester which is hydrolyzed by a lipase to freshly prepare the required β -keto acid for the transamination.

To obtain a long-term stable, recyclable, temperature and pH stable biocatalyst which can be easily removed from the reaction mixture, an immobilization method should be established. Since their magnetic properties, M-PVA beads are suitable to achieve easy downstream processing and a reusable biocatalyst.

Furthermore, a transaminase activity determined before in *Burkholderia phytofirmans* strain BS115 is to be characterized and the responsible enzyme is to be identified and purified.

To gain high amount of cell protein for the purification of the enzyme revealing transaminase activity from the strain *Burkholderia phytofirmans* BS115, a fermentation process has to be established as well. Furthermore, the microbial metabolism of β -amino acids is to be examined. Since almost no details are known how β -amino acids are metabolized in bacterial cells.

3 MATERIAL AND METHODS

3.1 MATERIAL

3.1.1 Devices

Table 3.1: Devices.

Device	Type	Supplier
Autoclave	V-150	Systemec, Wetzlar, DE
	HX-430	Thermo Fisher Scientific, Waltham, US
Centrifuge	5415D Rotor: F45-24-11	Eppendorf Wesseling-Berzdorf, DE
Centrifuge	Avanti J-300	Beckman Coulter, Brea, US
Centrifuge	Heraeus Multifuge X3 FR	Thermo Fisher Scientific, Waltham, US
Clean bench	Lamin Air	Heto-Holten A/S, Allerød, DK
DNA-gel electrophoresis	Minigel-Sub® cell GT Power supply: 200/2.0	Bio-Rad Laboratories, Hercules, US
FPLC	Äkta™ explorer 100	Amersham Biosciences AB, Uppsala, SE
Gel electrophoresis	Minigel-Twin Power Pack P25	Biometra GmbH, Göttingen, DE
HPLC	1260 Series	Agilent Technologies, Santa Clara, US
Incubator	BBD 6220	Thermo Fisher Scientific, Waltham, US
Incubator	Multitron	Infors HT, Bottmingen, CH
Magnetic separation	Dynal®, invitrogen bead separations	Thermo Fisher Scientific, Waltham, US
Magnetic stirrer	MR 3001 K	Heidolph Instruments GmbH & Co. KG, Schwabach, DE
PCR	Mastercycler Gradient	Eppendorf Wesseling-Berzdorf, DE
pH-meter	InoLab pH Level 1	WTW, Weilheim, DE
Pipette	Research plus	Eppendorf Wesseling-Berzdorf, DE
Balance	BP3100S, BP61S	Sartorius AG, Göttingen, DE
Spectrophotometer	Epoch	BioTek Instruments, Winooski, US
Spectrophotometer	Ultrospec 1100 <i>pro</i> UV/Vis	GE Healthcare, Chalfont, St. Giles, UK
ThermoMixer®	Comfort, compact, C	Eppendorf Wesseling-Berzdorf, DE
Ultrapure water system	Purelab Plus	USF Seral, Ransbach-Baumbach, DE
Vortex	D-6012	neoLab®, Heidelberg, DE

3.1.2 Chemicals and materials

Chemicals were of reagent grade and from commercial sources if not stated otherwise.

Table 3.2: *Rac*- β -Amino acids.

Substance	CAS-No ^a	CAS-No ^b
(<i>S</i>)-3-amino-3-phenylpropionic acid	614-19-7	83649-48-2
(<i>R</i>)-3-amino-3-phenylpropionic acid	614-19-7	83649-47-3
(<i>S</i>)-3-amino-3-(4-chlorophenyl)propionic acid	19947-39-8	131690-60-3 R 131690-61-4
(<i>S</i>)-3-amino-3-(4-fluorophenyl)propionic acid	325-89-3	151911-33-0
3-amino-3-(4-bromophenyl)propionic acid	39773-47-2	-
3-amino-3-(4-nitrophenyl)propionic acid	35005-61-9	-
3-amino-3-(4-methoxyphenyl)propionic acid	5678-45-5	-
3-amino-3-(4-hydroxyphenyl)propionic acid	6049-54-3	-
3-amino-4-phenylbutyric acid	3060-41-1	-
3-amino-3-(4-isopropylphenyl)propionic acid	117391-53-4	-

^a) of the racemate

^b) of the enantiopure form

All amino acids in table 3.2 in their racemic form, utilized for biotransformation are purchased from Sigma Aldrich (St.Louis, US). All enantiopure amino acids are purchased from PepTech Corporation (Bedford, US).

Table 3.3: Deployed amino acceptors.

Substance	Supplier	CAS-No
α -ketoglutarate	Roth	328-50-7
Pyruvate	Sigma Aldrich	113-24-6
Acetophenone	Sigma Aldrich	98-86-2
Oxaloacetate	Roth	328-42-7

Table 3.4: Deployed amino donors.

Substance	Supplier	CAS-No
(<i>R</i>)/(<i>S</i>)-methylbenzylamine	Sigma Aldrich	3886-69-9 /2627-86-3
Isopropylamine	Sigma Aldrich	75-31-0
3-aminobutanoic acid	Sigma Aldrich	541-48-0

M-PVA beads are purchased from Perkin Elmer Chemagen (Baesweiler, DE) functionalized with iminodiacetic acid ligands. The mean size of the beads is 2-3 μm and their magnetization is 40 A m²/kg.

Table 3.5: Columns for enzyme purification.

Column	Model	Supplier
Desalting	HiPrep 26/10 Desalting	Amersham Biosciences AB, Uppsala, SE
Nickel-Sepharose	HisTrap™ HP	GE Healthcare Bio-Sciences AB,Uppsala, SE
Q-Sepharose	HiTrap Q HP	GE Healthcare Bio-Sciences AB,Uppsala, SE

Table 3.6: General substances for biotransformation and regeneration of magnetic beads.

Substance	Supplier	CAS-No
Pyridoxal-5-phosphate (PLP)	Roth	853645-22-4
Sodium dodecyl sulfate (SDS)	Roth	151-21-3
Na ⁺ 3-oxo-3-phenyl propanoate	AKos	-

Table 3.7: β-Keto acid esters.

Substance	Supplier	CAS-No
Ethyl benzoylacetate	Sigma Aldrich	94-02-0
Ethyl-(4-fluorobenzoyl)acetate	Sigma Aldrich	1999-00-4
Ethyl-(4-chlorobenzoyl)acetate	Sigma Aldrich	2881-63-2
Ethyl-(4-nitrobenzoyl)acetate	Sigma Aldrich	838-57-3
Ethyl (4-methylbenzoyl)acetate	Sigma Aldrich	27835-00-3

3.1.3 Enzymes

Table 3.8: Deployed enzymes.

Enzyme	Strain	Source
Lipase	<i>Rhizomucur miheii</i>	Sigma Aldrich
Lipase	<i>Candida rugosa</i>	Sigma Aldrich
Lipase	<i>Thermomyces lanuginosus</i>	Sigma Aldrich
Aminotransferase	<i>Variovorax paradoxus</i>	Crismaru et al [116]
Aminotransferase	<i>Burkholderia phytofirmans</i>	Brucher et al [117]

3.1.4 Strains, plasmids and gene Sequence

Table 3.9: Strains with activity toward β -amino acids.

Strain	Source
<i>Variovorax paradoxus</i>	Crismaru et al [116]
<i>Burkholderia phytofirmans</i>	Brucher et al [117]

Table 3.10: Expressing strain and introduced plasmids.

Strain	Plasmid
BL21DE	pET21b *
	pET11a *

*see appendix 7.2

The sequence of the aminotransferase discovered by Crismaru and coworkers [116] and the introduced His-tag are specified in the appendix 7.1.

3.1.5 Media

Before use, the medium was autoclaved for 20 min at 121 °C. Heat unstable ingredients were filtered with Rotilabo® syringe filter (0.22 μ m, sterile, Carl Roth, Karlsruhe, DE) and afterwards added to the autoclaved medium. For the preparation of agar plates, 10 g/l of agar were added to the corresponding medium, before autoclaving.

TB (terrific broth) medium: (pH 7)

Tryptone	12 g	KH ₂ PO ₄	0.17 M
Yeast extract	24 g	K ₂ HPO ₄	0.72 M
Glycerol	4 ml		
ddH ₂ O	ad 900 ml	ddH ₂ O.	ad 100 ml

The two components were autoclaved separately.

LB (lysogeny broth) medium: (pH 7)

Tryptone	10 g
Yeast extract	5 g
NaCl	10 g
ddH ₂ O	ad 1 l

TB and LB medium were used for the cultivation of BL21DE.

TSB (tryptic soy broth) medium: pH 7.3

Casein peptone	17 g
K ₂ HPO ₄	2.5 g
Glucose	2.5 g
NaCl	5 g
Soya peptone	3 g
<i>ddH₂O</i>	ad 1 l

Modified M1 minimal medium: (pH 7)

Substance	MW / g/mol	Concentration (end) / mM	Stock Solution / mM	Mass / g	
Glucose	180.16	100	1000	90,08 g in 0,5 l	A
KH ₂ PO ₄	136.086	5.8	580	7.89 g in 100ml	A
Na ₂ HPO ₄ x 2 H ₂ O	177.99	4.1	410	7.29 g in 100ml	A
MgSO ₄ x 7 H ₂ O	246.48	1	100	2.4648 g in 100ml	A
CaCl ₂ x 2 H ₂ O	147.02	0.5	50	0.7351 g in 100ml	A
FeCl ₂ x 4 H ₂ O	198,81	0.01	50	0.0298 g in 3ml	F
Vitamin B ₆	247.14	0.001	20	4,9 mg in 1ml	F
Vitamin B ₁₂	1355.37	0.001 μM	100 μM	1,3 mg in 10 ml	F
β-Phenylalanine. <i>ddH₂O</i>	165.19	10	50	1 l	F A

A autoclaving

F filtrating with sterile Rotibalo® filter

All components were dissolved in *ddH₂O*.

TSB medium was purchased from Sigma Aldrich. TSB and modified M1 minimal medium were used for the cultivation of *Burkholderia phytofirmans*.

3.1.5.1 Solutions for cultivation

The following solutions were filtrated with a sterile Rotibalo® filter, before adding to the medium.

<u>Ampicillin stock solution</u>	100 mg	<u>IPTG</u>	100 mM
<i>ddH₂O</i>	1 ml	<i>ddH₂O</i>	
		<u>IPTG</u>	

IPTG was added as an induction solution, after a certain OD₆₀₀ was reached.

3.1.6 Buffers and solutions

Buffers used for HPLC (solvent buffer) were filtrated with a nitrocellulose 0.2 µm filter (Merck Millipore, Darmstadt, DE) and subsequently degassed via sonication. All buffers were stored at 4° C. All buffers components were dissolved in *ddH₂O*.

3.1.6.1 Biotransformation buffer

100 mM NaCO₃ buffer: (pH 9.1/10.8)

NaHCO₃ 8.4 g

Na₂CO₃ 10.6 g

100 mM NaPP buffer: (pH 7)

Na₂HPO₄ x 2 H₂O 17.8 g

NaH₂PO₄ x 2 H₂O 15.6 g

100 mM citrate buffer: (pH 4)

Citric acid 19.2 g

ad ddH₂O 0.5 l

Sodium citrate x H₂O 29.4 g

Both buffer components of the relevant buffer were mixed together until the required pH was reached. These buffers were utilized for biotransformation with the aminotransferase as the catalyst.

3.1.6.2 Immobilized metal ion affinity chromatography (IMAC)

Binding buffer: (pH 8)

TRIS	20 mM
NaCl	500 mM
Imidazole	5 mM
HCl	

Elution buffer: (pH 8)

TRIS	20 mM
NaCl	500 mM
Imidazole	500 mM
HCl	

HCl was used to adjust the pH, ddH₂O was used to dissolve all components.

3.1.6.3 Immobilization on magnetic beads

Loading buffer 1: (pH 8)

NiSO ₄ x 6 H ₂ O	50 mM
NaCl	200 mM

Loading buffer 2: (pH 8)

CuSO ₄ x 5 H ₂ O	50 mM
NaCl	200 mM

Loading buffer 3: (pH 8)

CoSO ₄ x 7 H ₂ O	50 mM
NaCl	200 mM

Binding buffer: (pH 8)

NaH ₂ PO ₄ x 2 H ₂ O	20 mM
NaCl	200 mM

Elution buffer: (pH 8)

Imidazole	200 mM
NaCl	200 mM

Washing buffer:

Imidazole	10 mM
NaCl	300 mM
Na ₂ HPO ₄ x 2 H ₂ O	50 mM

3.1.6.4 HPLC buffer and solutions40 mM NaPP buffer: (pH 6.5)

Na₂HPO₄ x 2 H₂O 7.1 g

NaH₂PO₄ x 2 H₂O 6.2 g

Pre column derivatizationBorate buffer: (pH 10.4)

H₃BO₃ 133 mM
NaOH adjust the pH

IBLC 100 mM

Ad with borate buffer

OPA 100 mM

ad MeOH

3 % acetic acid (v/v)

3.1.6.5 Agarose gel electrophoresisTBE buffer (50x): (pH 8)

TRIS 89 mM
EDTA 2 M
Boric acid 89 mM

3.1.6.6 SDS-polyacrylamid gel elektrophoresis

SDS-sample buffer (5x)

TRIS	225 mM
BPB	0.05 %
DTT	250 mM
Glycerol	50 %
SDS	5 %

SDS-electrophoresis buffer (10x)

TRIS	250 mM
Glycerol	1.92 M
SDS	35 mM

0.625 TRIS/HCl buffer: (pH 6.8)

1.88 M TRIS/HCl buffer: (pH 8.8)

3.1.6.7 Silver nitrate solution

Fixation solution

Acetic acid 10 %
Methanol 20 %

Reduction solution

Ethanol 30 %
Glutaraldehyde 0.5 %
Sodium thiosulfate 0.2 %
Sodium acetate 0.5 M

Dying solution

Silver nitrate 0.1 %
Formaldehyde
0.01 %

Developing solution

Sodiumcarbonate 2.5 %
Formaldehyde 0.01 %

3.2 ANALYTICAL METHODS

3.2.1 HPLC Analysis by precolumn derivatization

Precolumn derivatization with *ortho*-phthaldialdehyde is established for detection and separation of α - and β - amino acids since the 1980s [118]. The analysis was provided with a 1200 series (Agilent) and with a reversed phase (RP) HPLC column 50 x 4.6 mm HyperClone 5 μ m ODS (C18) (Phenomenex Inc., Torrance, US) and isocratic flow of 1 ml/min. For

enantiomer separation precolumn derivatization was used with *o*-phthalaldehyde and *N*-isobutryl-L-cysteine (chapter 3.1.6.4.). These two components were mixed together and diluted in borate buffer (the ratio was modified after Brucher et al [119]). Due to the instable derivatives, the derivatization was carried out directly in the injection needle. The needle draws 2 μ l borate buffer, 3 μ l mixed IBLC/OPA and 0.5 μ l of the sample. After mixing and a short reaction time of 2.5 min, 2 μ l acetic acid was used to adjust the pH. Subsequently 7.5 μ l were injected. The mobile phase consists of 55 % (v/v) MeOH and 45 % (v/v) 40 mM NaPP buffer pH 6.5 (for β -PA, β -(F)PA, β -(CH₃)PA, β -(NO₂)PA, β -homophenylalanine), 65 % (v/v) MeOH and 35 % (v/v) 40 mM NaPP pH 6.5 (β -(*iso* pentyl)PA) and 50 % (v/v) MeOH and 50 % 40 mM NaPP pH 6,5 (β -(Br)PA, β -(Cl)PA, β -(CH₃)PA, β -(OH)PA). The detection wavelength was 337 nm and the column temperature was set to 25° C.

3.2.2 HPLC analysis without derivatization

For the analysis of underivatized substances, like acetophenone and ethylbenzoylacetate with various residues (table 3.7), the same column and the same HPLC system were used. A NaPP buffer pH 6.5 and methanol were used as solvents. For the analysis of ethylbenzoylacetate and derivatives a gradient was established. Starting from 40 % MeOH to 50 % in 25 min and from 50 % to 70 % in 30 min. The detection wavelength was 250 nm and column temperature was set to 25 °C. For the detection of acetophenone an isocratic method with a flow of 1 ml/min was chosen, and the wavelength was set to 250 nm.

3.2.3 Analysis with gas chromatography

The detection of ethanol (EtOH) was provided via a temperature gradient by gas chromatography. A polar DB-wax column (30 m / 0.25 mm, 0.25 μ m, Agilent) was used. The upstream isothermal phase was set for 2 min. The parameters are shown in table 3.11 and the temperature program is shown in table 3.12.

Table 3.11: Parameters for analysis of ethanol with GC.

<u>Parameters</u>	
Column	DB-Wax
Pressure	1.012 bar
Gas- flow	1.3 ml/min
Split-ratio	27.0:1
Injection (volume)	1 μ l
Inlet temperature	220 °C

Table 3.12: Temperature program (GC).

<u>Temperature program</u>		<u>Time</u>
Start	50 °C	1 min
Temperature-gradient	17 °C/min	
Highest temperature	220 °C	5 min

3.2.4 Calculation of enzyme activity, purification, μ , t_d and consumption rate

Specific activity correlates with activity / protein and activity / beads.

$$\frac{\text{Activity}}{\text{Protein}} \left[\frac{\text{U}}{\text{mg}} \right] = \frac{\frac{\text{Substrate Concentration } [\mu\text{mol}]}{\text{Time } [\text{min}]}}{\text{Protein Concentration } [\text{mg}]}$$

$$\frac{\text{Activity}}{\text{Beads}} \left[\frac{\text{U}}{\text{mg}} \right] = \frac{\frac{\text{Substrate Concentration } [\mu\text{mol}]}{\text{Time } [\text{min}]}}{\text{Bead Concentration } [\text{mg}]}$$

$$\text{Recovery } [\%] = \frac{\text{Total Activity after purification } [\text{U}] \times 100}{\text{Total Activity before purification } [\text{U}]}$$

$$\text{Purification fold} = \frac{\text{Specific Activity after purification } \left[\frac{\text{U}}{\text{mg}} \right]}{\text{Specific Activity before purification } \left[\frac{\text{U}}{\text{mg}} \right]}$$

$$\mu \left[\frac{1}{\text{h}} \right] = \frac{\ln(\text{OD}_{600} t_n) - (\ln(\text{OD}_{600} t_{n-1}))}{t_n - t_{n-1}}$$

$$t_d [\text{h}] = \frac{\ln 2}{\mu}$$

$$\text{Consumption rate } (R) \left[\frac{\text{g}}{\text{h}} \right] = \frac{m(t_0) - m(t)}{t - t_0}$$

$$ee [\%] = \frac{\text{conversion of } (S) - \text{conversion of } (R)}{\text{conversion of } (S) + \text{conversion of } (R)} \times 100$$

3.3 MOLECULARBIOLOGICAL METHODS

3.3.1 Gene synthesis and introduction of a His-tag

The gene of the aminotransferase from *Variovorax paradoxus* was identified by Crismaru and coworkers [116] and is synthesized by Invitrogen Life Technologies. The His₆-tag was introduced as well. The complete sequence is shown in appendix 7.1A. The plasmids used in this work were pET11a (without His-tag) and pET21b (with His-tag). Both plasmids were stored

at the institute. The two vectors with the included aminotransferase gene are shown in appendix 7.2.

3.3.2 Transformation

The plasmids were cloned into *E. coli* strains XLpBlue (Stratagene) for subcloning and BL21DE (institutes strain collection) for expression of the gene. For the transformation 200 µl of chemical competent strain XLpBlue was incubated for 20 min on ice with 5 µl of the plasmid containing the aminotransferase gene, followed by a heat shock for 90 s at 42° C. Subsequently, 1 ml of preheated LB-medium (chapter 3.1.5) was added and incubated at 37° C for 30-45 min and 500 rpm. Afterwards the mixture was plated on an LB agar plate containing 100 µg/ml ampicillin and incubated over night at 37° C. The same protocol was carried out for the transformation into the strain BL21DE.

3.3.3 Plasmid preparation

For extraction of plasmid DNA the peqGOLD Miniprep Kit I (C line) was employed (VWR International GmbH, Erlangen, Germany). The isolation of the plasmid DNA was performed according to the manufacturer's instructions.

3.3.4 Digestion by restriction enzymes

Restriction enzymes from Fermentas (table 3.13) (Thermo Scientific Inc., Waltham, US) were used to perform DNA digestion. The suggested protocol of the manufacturer is usually 16 µl of nuclease-free water, 2 µl of recommended enzyme buffer, 1 µl of substrate DNA and 2 µl of certain restriction enzyme, to receive a total volume of 20 µl. The digestion was usually conducted for ~ 16 h at 37° C.

Table 3.13: Restriction enzymes for DNA digestion

Restriction enzyme	Cutting site	Supplier
Nde I	CATATG	Fermentas
Xho I	CTCGAG	Fermentas
BamH I	GGATCC	Fermentas

3.3.5 Agarose gel electrophoresis

Gel electrophoresis was conducted to verify if the plasmids carry the aminotransferase gene. Therefore, a gel electrophoresis chamber and a power supply were used. For the preparation of the 1 % agarose gel, 1 g agarose was dissolved in 100 ml 1 X TBE buffer, under extreme heat (microwave). To visualize the DNA under UV light after gel electrophoresis 5 µl Roti@gel stain (Roth, Karlsruhe, DE) were added after the gel solution cooled down for a few minutes.

The final agarose gel solution was poured into a gel chamber and left until solidified. Subsequently the gel was covered with 1 X TBE buffer in the chamber, before the DNA samples and 5 μ l of 1 kb marker (New England Biolabs, Ipswich, US) was loaded in the gel pockets. Afterwards the power supply was adjusted to 80 V and the gel chamber was energized until the DNA was sufficiently separated. The DNA loaded gel was then observed under UV light.

3.4 MICROBIOLOGICAL METHODS

3.4.1 Strain maintenance

Short-term storage of all strains employed in this work was at 4° C plated on agar plates consisting of certain media (chapter 3.1.5). For a longer storage period, 850 μ l of a culture with an OD₆₀₀ of ~ 1 were mixed with 150 μ l sterile glycerol (100 %) and stored at -80° C.

3.4.2 Preculture

For the preculture of *E. coli* strain BL21DE containing the plasmid with the aminotransferase gene sequence the preculture TB media was used with added ampicillin. 20 ml of media were inoculated from the agar plate or glycerol stocks and incubated over night at 37° C and 120 rpm. *Burkholderia phytofirmans* was incubated in M1 minimal medium (from TSB agar plate or glycerol stock) or TSB media for at least 30 h at 30° C and 120 rpm.

3.4.3 Cultivation

3.4.3.1 Expression of aminotransferase gene in BL21DE

The preculture of the *E. coli* strain was added to 400 ml of TB media containing 100 μ g/ml ampicillin. The culture had an OD₆₀₀ of 0.1 and was incubated at 37° C and 100 rpm. At an OD₆₀₀ between 5 and 6 the expression of the aminotransferase gene was induced by adding 1 mM IPTG. After induction, the temperature was lowered to 30° C and the shaking speed to 90 rpm. The culture was incubated overnight.

3.4.3.2 Shaking flask experiment with *Burkholderia phytofirmans*

The preculture of *Burkholderia phytofirmans* was used for inoculation of shaking flasks. The inoculation OD₆₀₀ was 0.1. The shaking flask (triplicate) was inoculated and incubated at 30° C for several hours with rpm adjusted to the used shaking flask. Every hour 2 ml samples were taken until no further growth of the bacteria was observed. The period of growth examined in this experiment was about 40-50 h, due to the growth in mineral medium containing only β -amino acids as sole nitrogen source. The samples were centrifuged at 13200 rpm and stored

at -20°C until further investigations of glucose, acetophenone and β -amino acids concentration.

3.4.4 Fermentation

The cultivation was also performed in a 2.5 l benchtop bioreactor with a nominal containing capacity of 1.5 l (Minifors, HT Infors, Bottmingen, CH). The bioreactor was equipped with a pH electrode (Mettler-Toledo Inc, Greifensee, CH), a pO_2 electrode (Oxyferm, Hamilton Bonaduz, AG, Bonaduz, CH), a temperature sensor and a rushton turbine. The system was regulated via IRIS (HT Infors, Bottmingen, CH).

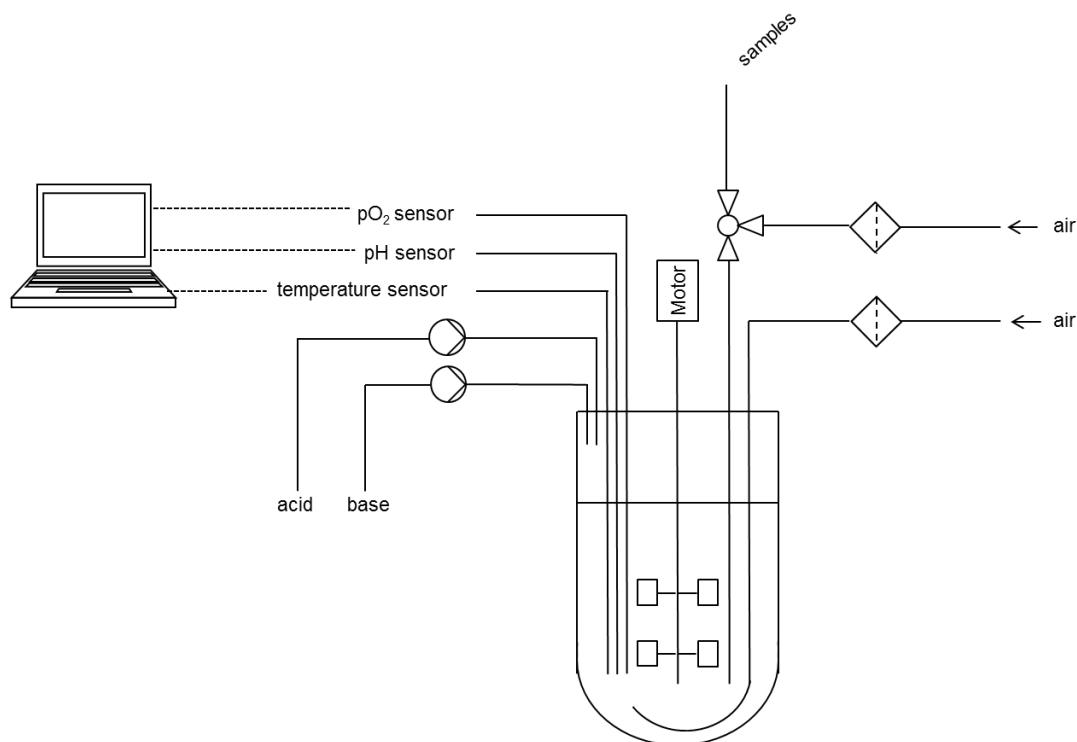


Figure 3.1: Bioreactor (Minifors, HT Infors, Bottmingen, CH) containing a Rushton turbine, a pH sensor, a pO_2 sensor and a temperature sensor. The system was regulated via IRIS (HT Infors, Bottmingen, CH).

3.4.4.1 Preculture

The preparation of the preculture utilized for the cultivation in a bioreactor is equal to the preparation of the preculture used for shaking flask experiments, except for the fact that the volume had been adjusted to 100 ml, due to the larger amount of preculture needed for the bioreactor and minimal medium was used for every cultivation.

3.4.4.2 Fermentation

The cultivation in a bioreactor was conducted at 30°C . The airflow was adjusted to 1 lpm and the stirrer was regulated to 120 rpm. The pO_2 was not controlled but permanently monitored. The pH was not regulated, but to prevent strong pH fluctuations a strong acid (4 M H_3PO_4) and

a strong base (4 M NaOH) were connected to the reaction vessel. The cultivation (triplicate) was conducted for 55 h. Samples were taken from the reaction broth every hour during the day and every three hours during the night. The growth of the culture was observed via OD₆₀₀ measurement. The samples were centrifuged at 13.200 rpm and stored at -20° C for further investigations, like glucose, acetophenone and β-amino acid concentration.

3.4.5 Cell harvesting

The harvesting of the cells was carried out for all used strains as described in the following section. To stop the cultivation, the culture was filled in Beckman® centrifuge tubes and centrifuged for 10 min at 4 °C and 10.000 rpm. The pellet was resuspended in as much saline 0.9 % as needed, decanted in 50 ml plastic tubes (Greiner Bio One, Kremsmünster, A) and centrifuged again for 75 min at 4 °C and 4700 rpm. The supernatant was removed and the cell pellet was measured (wet bio mass). Subsequently the pellet was deep-freezed with liquid nitrogen and stored at -20 °C until further use.

3.4.6 Cell disruption

E. coli cells with pET21b vector

The frozen pellets were thawed and resuspended in 5 ml Bugbuster® (primary amine-free) extraction reagent (Merck Millipore, Darmstadt, DE) per g wet bio mass. Bugbuster® was laced with 1 mM PLP, 25 units Benzonase® Nuclease and 1 KU r Lysozyme™ solution (both from Merck Millipore, Darmstadt, DE). The resuspended cell solution was incubated for 20 min at room temperature, slightly shaking. After 20 min the suspension was centrifuged for 20 min at 4° C and 10000 rpm. The supernatant was decanted in a new Falcon tube and was either frozen with liquid nitrogen or stored at -20° C or was immediately used.

Burkholderia phytofirmans cells

Deep-freezed pellets were thawed and resuspended in 3 ml Tris/HCl buffer pH 8 per g wet bio mass. The buffer was laced with 1 mM PLP. After resuspension, disruption of the cells was carried out via sonification with rhythms of 30 s on and 30 s off and amplitude of 20 % for 2 x 8 min until the solution was slightly clear. The cell solution was stored on ice the whole time. Subsequently the cell solution was centrifuged 20 min at 4° C and 10.000 rpm. The supernatant was decanted in a new Falcon tubes and was frozen with liquid nitrogen and stored at -20° C or was immediately used.

3.5 BIOCHEMICAL METHODS

3.5.1 Determination of protein concentration

The protein concentration of the crude cell extract was determined with a BCA assay (Uptima, Interchim, Clichy, F). For ecological reasons the measurements were carried out in MTP due to a decreased amount of the needed reagents. For the photometric assay the BCA assay reagents were mixed in a ratio of 50:1 and 200 μl of the mixture had to be added to 25 μl of the sample. The samples (triplicates) were diluted to a protein concentration within the calibration range (0; 0.2; 0.4; 0.6; 0.8 and 1 mg/ml of BSA standard). The reaction mixture was incubated for 30 min at 37° C and 350 rpm. After incubation, the mixture cooled to room temperature and was measured photometrically at 562 nm.

3.5.2 Glucose assay

To determine the consumption of D-glucose throughout the cultivation of *Burkholderia phytofirmans*, another photometric enzymatic assay (R-biopharm AG, Darmstadt, DE) was conducted. The assay is based on an enzymatic reaction of two cascaded enzymes. The emerging NADPH has its adsorption maximum at 340 nm, which is equivalent to the adsorption maximum of D-glucose. The assay was performed in a cuvette, where 250 μl of solution 1 was mixed with 25 μl sample solution and 475 μl *ddH*₂O. After 3 min of incubation the extinction was measured (E1). Subsequently, 5 μl of the enzyme solution was added and after 15 min the extinction was measured again (E2). A blank was measured as well. For the determination of ΔE , the following formula was used:

$$\Delta E = (E_2 - E_1)_{\text{sample}} - (E_2 - E_1)_{\text{blank}}$$

The following formula is derived from the Lambert-Beer law and was used to calculate the concentration of D-glucose.

$$c \left[\frac{\text{g}}{\text{l}} \right] = \frac{V * \text{MW}}{\epsilon * d * v * 1000} * \Delta E$$

V	total volume / ml
v	sample volume /ml
MW	molecular weight / g/mol
d	light path /cm
ϵ	extinction coefficient of NADPH at 340 nm 340 nm = 6.3 / 1/mmol x cm

3.5.3 SDS-polyacrylamid gel electrophoresis

SDS-polyacrylamid gel electrophoresis (SDS-PAGE) [120] was conducted to test the purity of enzymes after purification via IMAC, or via magnetic beads, as well as after ammonium sulfate precipitation and to control whether the expressed enzyme is the desired one. The preparation of two gels is shown in Table 3.14.

Table 3.14: SDS-gel preparation for 2 gels.

	Separation gel (12.5 %)	Stacking gel (6 %)
1.88 M Tris/HCl buffer pH 8.8	2.4 ml	-
0.625 M Tris/HCl buffer pH 6.8	-	800 µl
10 % SDS	120 µl	40 µl
ddH ₂ O	4.48 ml	2.5 ml
30 % Bis-Acrylamide	5 ml	660 µl
10 % APS	60 µl	20 µl
TEMED	10 µl	4 µl

The samples were prepared by determination of the protein concentration to ensure, that all pockets of the SDS-gel contain 20 µg of protein. The total volume of 80 µl was divided by the protein concentration and this amount of protein was added to 16 µl of sample buffer (see chapter 3.1.6.6). The solution was poured in with *ddH₂O*. Subsequently, the mixture was thoroughly mixed and incubated for 10 min at 95° C and 500 rpm. In the meantime the prepared gels were stacked in the chamber and filled with SDS-gel electrophoresis buffer. After incubation, the samples were centrifuged at 13200 rpm for 10 s, cooled to room temperature and 20 µl of the solution was filled into the pockets. Furthermore, 5 µl of a protein standard PageRuler™ Prestained Protein Ladder, 10 to 180 kD (Thermo Fisher Scientific, Waltham, US) was filled into the pockets as well. The chambers were closed with a lid connected to the power supply and adjusted to 120 V for ~ 1.5 h depending on gels and chambers. After the solvent front was reaching the end of the gel, the chamber was opened and the gel was stained with Imperial™ Protein Stain solution (Thermo Fisher Scientific, Waltham, US) for at least 2 h and subsequently washed over night with *ddH₂O*.

3.5.4 Protein purification via immobilized metal ion affinity chromatography (IMAC)

The crude cell extract containing the aminotransferase expressed in *E. coli* was purified via IMAC. This purification method is suitable to purify enzymes with an added recombinant tag. In this case, a polyhistidin-tag was introduced. The histidines form a covalent complex binding to the bivalent nickel ions of the stationary phase. For IMAC purification an ÄKTA Explorer Chromatographic System (GE Healthcare Bio-Sciences AB, Uppsala, S) and as a stationary

phase a HisTrap™ HP column was used. The system was controlled by Unicorn software 5.31. (Amersham Bio-Sciences AB, Uppsalla, S). The complete chromatographic system was constantly cooled at 4° C. An UV-detector (UV-900) and a conductivity detector were used throughout the experiment. The detection wavelength was 280 nm and the flow rate was adjusted to 1 ml/min. Before starting, the system was flushed with either binding or elution buffer (composition see chapter 3.1.6.2) and the HisTrap column was flushed with 5 times of the column volume. The binding of the histidine residues increases when adding 1 % (% v/v) elution buffer to the crude cell extract. Subsequently the column was loaded with the crude cell extract and washed 5 times the column volume with binding buffer. The elution starts by switching to the elution buffer. The best enzyme yield was obtained with a gradient (see Figure 3.2.). Within 75 min the content of elution buffer increased to 50 %, after 75 min the content of elution buffer concentration increased to 100 % and stayed at 100 % for another 25 min. This led to imidazole concentrations of 5 mM (0 % elution buffer) and 500 mM (100 % elution buffer) during the elution of the enzyme. During elution protein peaks were detected via UV (280 nm). The activity of the collected fractions was tested toward β -amino acids and the purity was analyzed via SDS-PAGE gel electrophoresis. All samples and fractions were constantly stored on ice.

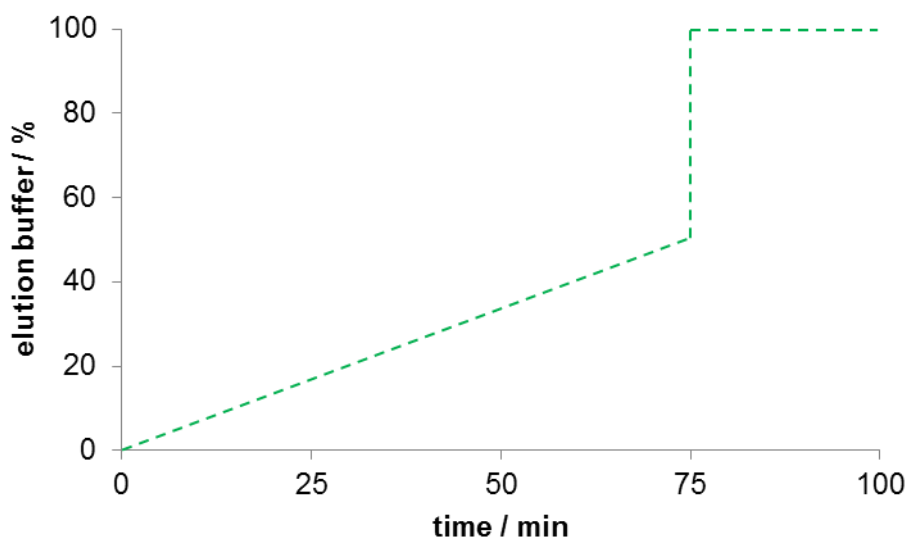


Figure 3.2.: Gradient for elution of the enzyme via IMAC purification of the His-tagged aminotransferase.

3.5.5 Desalting

Containing a high concentration of imidazole, the elution buffer had to be removed after enzyme elution off the stationary phase. High levels of imidazole could interact with the enzyme and may lower the enzyme activity and stability. Hence, all collected fractions were desalted or more precisely an exchange of buffer was carried out via SEC (size exclusion chromatography). The same ÄktaExplorer system with controlling program Unicorn 5.31 and

UV detector was used for desalting as for purification, described in section 3.5.4. A 53 ml HiPrep 26/10 desalting column (Amersham Bio-Sciences AB, Uppsalla, S) containing cross linked dextran was utilized with a flow rate of 2.5 ml/min. The mobile phase was 100 mM Tris/HCl buffer pH 8. The complete system was flushed with Tris/HCl buffer. Furthermore, it was necessary to let the column equilibrate with buffer, 5 times the column volume. All samples and desalted fractions were stored on ice during the process and stored at -20° C until further use.

3.5.6 Immobilization on magnetic M-PVA beads

M-PVA beads were purchased from Perkin Elmer Chemagen (Baesweiler, DE) and functionalized with iminodiacetic acid ligands. The mean size of the beads was 2-3 μm and their magnetization was 40 A m²/kg.

The beads used for experiments in this thesis are functionalized with imino diacetic acid (IDA), which forms a chelating complex with bivalent metal ions, based on the same mechanism as IMAC. During long storage at 4° C the beads formed lumps; therefore, the beads were sonicated for at least 2 min before usage. After sonication the beads were washed several times with binding buffer (recipe see section 3.1.6.3) and diluted to specific bead concentrations in mg/ml (described in section 3.6). Subsequently the beads were washed with loading buffer (section 3.1.6.3) containing certain bivalent metal ions, like nickel, copper or cobalt and incubated in loading buffer for 20 min at room temperature and 950 rpm. After incubation the beads were washed at least 3 times with binding buffer, to remove surplus metal ions. The metal ions are charged after washing with binding buffer; hence the enzymes with an added His-tag are able to bind to the magnetic beads. This was conducted by incubating the functionalized and charged beads with 1.5 ml crude cell extract mostly 30 mg/ml (with certain protein concentrations, described in section 3.6) for 20 min at room temperature and 950 rpm. The crude cell extract was stored on ice until it was needed for incubation. It was necessary to add 1 % of elution buffer to the crude cell extract. The containing imidazole prevents unspecific binding of proteins with histidine residues. Three washing steps followed the incubation. This time the beads were washed with the buffers needed for biotransformation. The buffers used in biotransformation are described in section 3.1.6.1. All fractions of the washing steps were stored for activity tests and determination of protein concentration at -20° C. The beads with immobilized enzymes were stored at 4° C or -20° C for several days, but to be sure that the highest activity of the enzyme was given, the freshly prepared immobilized enzymes were used for all further experiments.

3.5.7 Purification via magnetic M-PVA beads

Another way to purify a His-tagged enzyme is the elution of the immobilized enzyme off magnetic M-PVA beads. In this method the enzyme was immobilized as described in the latter section 3.5.6. After immobilization, the beads were washed several times with biotransformation buffer. Subsequently the beads were treated with elution buffer (recipe in section 3.1.6.2) three times at room temperature for 5 min and 950 rpm. After every elution, elution buffer was removed and decanted in 1.5 ml Eppendorf Tubes® (Eppendorf AG, Hamburg, DE). The three supernatants were pooled and a buffer change to biotransformation buffer, due to the imidazole in the elution buffer, was conducted with VivaSpin tubes with a polyethersulfone (PES) membrane and a MWCO of 30.000 kDa (Sartorius, Göttingen, DE). The pooled enzyme solution was filled in the filter tubes and centrifuged at 4700 rpm at 4° C for several minutes. After a few minutes the centrifuge was stopped and 2 ml of biotransformation buffer was filled into the filter tube and centrifuged again. This was performed at least three times. When the elution buffer was removed the filter tubes were centrifuged again until the enzyme solution was concentrated to an acceptable enzyme concentration and volume. The protein concentration was determined before and after buffer change and the purity was defined by SDS-gel electrophoresis. The enzymes in biotransformation buffer were treated with liquid nitrogen and stored until further use at -20° C

3.5.8 Recycling of magnetic M-PVA beads

The beads, used for immobilization of enzymes, were reused after every experiment. To remove the enzymes completely, the beads were incubated with 1 % SDS ultra pure at 90° C for 20 min and 950 rpm. After incubation the beads were cooled to room temperature and 1 % SDS was decanted to a micro test tube (Eppendorf AG, Hamburg, DE). Subsequently, the beads were washed with washing buffer until SDS was removed completely (no foam after shaking). For storing the beads they were washed several times with binding buffer and kept at 4° C until further use. To determine the bead concentration for the next experiments, 3 micro test tubes were dried in a heating chamber at 60° C overnight and measured. Furthermore, 250 µl of the bead suspension (after 2 min sonication) were filled in these micro test tubes and again dried at 60° C overnight. After measuring the filled tubes, the bead concentration of the suspension was determined. The enzyme concentration in 1 % SDS was determined via BCA assay and this concentration was used to calculate the specific activity of the aminostransferase.

3.5.9 Fractionated ammonium sulfate precipitation

For a first purification of the aminotransferase out of strain *Burkholderia phytofirmans* an ammonium sulfate precipitation was carried out. A saturated ammonium sulfate solution of 3.8 M was prepared; which should be as cold as possible throughout the experiment. The precipitation was performed according to Protein Purification (3rd edition) edited by Scopes [121]. With the following formula the needed amount of saturated 3.8 M ammonium sulfate solution was calculated.

$$V \text{ [ml]} = \frac{10(C_2 - C_1)}{100 - C_2}$$

- V volume of ammonium sulfate needed for x % of ammonium sulfate in solution
C1 x % of ammonium sulfate already in solution
C2 x % desired ammonium sulfate in solution

Firstly, 10 ml of crude cell extract after cell disruption via sonication were filled in a beaker which was kept on ice throughout the precipitation. Ammonium sulfate concentrations of 0 %, 25 %, 50 %, 75 % and 95 % were desired. For an ammonium sulfate concentration of 25 % 3.3 ml of 3.8 M ice cold ammonium sulfate solution was added dropwise by a burette. The solution was stirred for 15 min and subsequently centrifuged at 4° C for 30 min at 4700 rpm. The pellet was resuspended in 100 mM Tris/HCl buffer pH 8.5, whereas the supernatant was decanted back to the beaker and 3.8 M ammonium sulfate solution was added again. The activity of the fractions was determined via biotransformation.

3.5.10 Ion exchange chromatography

For purification of the transaminase from *Burkholderia phytofirmans* strain BS115, ion exchange chromatography was conducted, after prepurification via ammonium sulfate precipitation. The most common anion exchangers are diethylaminoethyl (DEAE) and quaternary amino ethyl (QAE) substituents which are attached to hydroxyl groups on the matrix. The adsorbants have a single positive charge on a nitrogen atom and, in the case of QAE-adsorbants it is nondissociable, whereas with DEAE-adsorbants, the proton of the nitrogen dissociates at high pH and leaves the material uncharged above pH 9.5. In this work, a QAE adsorbant was used (Q-Sepharose HiTrap column). For AEX an ÄKTAEplorer Chromatographic System (GE Healthcare Bio-Sciences AB, Upsalla, S) and as a stationary phase a Q-Sepharose HP column (5 ml) was used. The controlling software is Unicorn 5.31. During the experiment a flow rate of 2.5 ml/min was used. The column was equilibrated with 5 times column volume with 50 mM Tris/HCl buffer, pH 6.8 and subsequently with 1 M NaCl (in 50 mM Tris/HCl, pH 6.8). Afterwards 600 µl of the desalted ammonium sulfate fractions

(pooled fraction 30 %-35 % saturation) were injected with a loop and the column was washed with Tris/HCl again. For elution a linear gradient was chosen with 0.4 M NaCl dissolved in 50 mM Tris/HCl, pH 6.8 for 32 min. Furthermore, elution was conducted with 0.4 M NaCl for 4 min and with 1 M NaCl for 6 min, to eluate the remaining protein from the column. The detection of the eluted proteins was performed via UV at a wavelength of 280 nm. During elution the fraction were collected in 1 ml volume. All fractions of one peak were pooled and buffer exchange was conducted for 3 h to 50 mM Tris/HCl buffer, pH 8 with Slide-a Lyzer™ Mini Dialyse Device (Thermofisher Scientific, Waltham, US).

3.6 BIOTRANSFORMATION

3.6.1 Kinetic resolution

The biotransformation was performed to determine the activity of the enzyme and to verify if the enzyme was purified and immobilized effectively. For a standard biotransformation with immobilized enzymes on 20 mg/ml magnetic beads, the mixture was incubated at 30° C for at least 2 h and 950 rpm (ThermoShaker, Eppendorf AG, Hamburg, DE), as well as 70 µl of the reaction mixture were frequently taken as samples after 0 h, 5 min, 10 min, 20 min, 30 min, 60 min and 120 min for the immobilized aminotransferase. For the aminotransferase from *Burkholderia phytofirmans*, samples were taken between 0 h and 24 h, at differing times. The standard substrates are shown in table 3.15. To stop the biotransformation the samples were incubated at 95° C for 10 min and centrifuged at 13200 rpm for 5 min.

Table 3.15: Standard substrates for biotransformation.

Substances	Concentration / mM
<i>rac</i> -β-phenylalanine (amino donor)	10
α-ketoglutarate (amino acceptor)	5
Pyridoxal-5'-phosphate	0.2
NaCO ₃ buffer pH 9	100

3.6.1.1 Testing of optimal temperature and temperature stability

To investigate the optimal temperature of the immobilized aminotransferase (using 20 mg/ml magnetic beads), biotransformations (triplicates) were performed at 30° C, 40° C, 50° C, 60° C, 70° C and 80° C. The substrates in the same concentration as in table 3.15. were utilized and incubated at certain temperatures for 2 h and at 950 rpm. Samples were frequently taken at 0 min, 5 min, 10 min, 20 min, 30 min, 60 min and 120 min. The biotransformation was stopped by incubating the samples for 10 min at 95° C. Subsequently the samples were centrifuged for 5 min at 13.200 rpm.

The immobilized aminotransferase was also examined in terms of their stability at different temperatures. Therefore, the immobilized enzyme was incubated for 2 h at certain temperatures (30° C, 40° C, 50° C, 60° C, 70° C and 80° C) and every biotransformation was performed as triplicate. After incubation the immobilized enzymes were cooled down to room temperature and subsequently used for the biotransformation at standard conditions (30° C biotransformation temperature, 950 rpm and substrate concentrations as shown in table 3.15.). Samples were taken as well in the same time intervals, as described above.

3.6.1.2 Testing of different pH values for pH optimum and stability

To find the optimal pH for the immobilized enzyme (20 mg/ml magnetic beads) and to investigate if the immobilized enzyme is more stable to harsher conditions, buffers were used for biotransformation with a pH range between 4 and 11. Every experiment was carried out as a triplicate. The composition of these buffers is shown in chapter 3.1.6.1. The conditions of the biotransformation were the same as shown in table 3.15 except that the buffer had changed. The protein concentration of the enzyme immobilized on the beads was determined after biotransformation by incubation in 1 % SDS for 20 min at 90° C.

3.6.1.3 Substrate scope (β -amino acids)

The substrate range of the immobilized aminotransferase was compared with the substrate range of the crude cell extract. A variety of *rac*- β -amino acids (see table 3.2.) were utilized as amino donors with the same composition of reaction mixture and the same reaction conditions as described above, incubation at 30° C for 120 min and 950 rpm. For the immobilized enzyme 20 mg/ml magnet beads were used, the protein concentration of the enzyme immobilized on the beads was determined after biotransformation by incubation in 1 % SDS for 20 min at 90° C. To investigate the substrate range of the free enzyme in crude cell extract, a protein concentration of 1 mg/ml was used for every biotransformation. Every reaction with immobilized enzyme and crude cell extract was performed in a triplicate.

3.6.1.4 Amino acceptors

The reaction mechanism of a transaminase reaction consists of an amino donor, PLP as a cofactor, the enzyme and an amino acceptor. To find the amino acceptor with which the transaminase has the highest activity, α -ketoglutarate, pyruvate, oxaloacetate and acetophenone were utilized for the biotransformation with immobilized aminotransferase (20 mg/ml beads in a triplicate) and with the enzyme crude cell extract from *Burkholderia phytofirmans* (protein concentration 0.2 mg/ml in a triplicate). The reaction conditions were the same as shown in table 3.15 except of the different amino acceptors.

3.6.1.5 Different concentrations of magnetic M-PVA beads

To determine the binding efficiency of the enzyme in crude cell extract, magnetic M-PVA beads were incubated in different concentrations with 30 mg/ml protein of the crude cell extract containing the aminotransferase (~1 %). The magnetic beads were diluted to 10 mg/ml beads, 20 mg/ml beads (the usual concentration for all other experiments with magnetic beads), 40 mg/ml beads and 60 mg/ml beads as a triplicate. The incubation and immobilization was performed as described in chapter 3.5.6. The activity of the immobilized enzyme as well as the protein concentration after immobilization was determined directly after incubation of the crude cell extract with the magnetic beads. The biotransformation was conducted as described in chapter 3.6.1.

3.6.1.6 Incubation of magnetic M-PVA beads with various protein concentrations

The binding efficiency of the enzyme from crude cell extract to magnetic M-PVA beads was investigated as well by incubation of 20 mg/ml M-PVA beads with various protein concentrations of the crude cell extract (2.5 mg/ml, 5 mg/ml, 10 mg/ml, 20 mg/ml and 26 mg/ml), every concentration in a triplicate. The immobilization was carried out as described in section 3.5.6. The protein concentration was determined after incubation of the beads with the crude cell extract, as well as after immobilization by incubation of the immobilized enzyme in 1 % SDS and at 90° C. Furthermore the activity of the immobilized enzymes with different bead concentrations was analyzed via biotransformation with standard conditions described in chapter 3.6.1 and table 3.15.

3.6.1.7 Long-term stability

Immobilized enzymes offer the advantage of long-term stability, due to the stabilizing effects of the immobilization matrix. To investigate the long-term stability of the immobilized aminotransferase, the activity was determined over 38 days. The bead concentration was 20 mg/ml incubated with 30 mg/ml crude cell extract (triplicate), as described in section 3.5.6. At 12 time periods within 38 days, biotransformations were conducted with the standard conditions as described in chapter 3.6.1 and table 3.15. After the biotransformation the immobilized enzymes were stored in biotransformation buffer (100 mM NaCO₃ buffer, pH 9) and 1 mM PLP at 4° C until the next biotransformation. The long-term stability of the immobilized enzyme was compared to the long-term stability of the free enzyme in the crude cell extract. Biotransformations were performed at the same time as for the immobilized enzyme and the same reaction conditions and sample time periods were used as well. For these biotransformations, the same crude cell extract was used as for incubation with the beads for the immobilization. The protein concentration for the biotransformation was 1 mg/ml.

The crude cell was stored at 4° C during the experiment and only the needed amount of protein was taken and added to the biotransformation mixture.

3.6.1.8 Recyclability of immobilized aminotransferase

Another advantage of immobilized enzymes is the recyclability of the biocatalyst and the easy removability, especially for immobilization on magnetic beads. The recyclability of the immobilized aminotransferase was tested for 7 recycling steps within two days. At day one, three biotransformations with freshly immobilized enzymes (20 mg/ml beads and 30 mg/ml crude cell extract, described in chapter 3.5.6.) were conducted with the standard conditions described in chapter 3.6.1 and table 3.15. Every biotransformation took 120 min, after that time the reaction mixtures were removed, the beads were washed with biotransformation buffer (100 mM NaCO₃ buffer, pH 9) and the new reaction mixture was added again for 120 min. At day two, four biotransformations were performed. The immobilized enzyme was stored overnight at 4° C in 100 mM NaCO₃ buffer, pH 9 and 1 mM PLP.

3.6.2 Asymmetric synthesis

The asymmetric synthesis was performed to synthesize enantiopure β -amino acids. Due to the instable spontaneously carboxylating substrate (β -keto acid) the substrate has to be prepared freshly. Hence, an enzyme cascade is necessary.

3.6.2.1 Hydrolysis of β -keto acid esters via lipases

The lipases of table 3.8 were used to hydrolyze β -keto acid esters (table 3.7). The lipases were utilized with an activity of 100 U, 70 U and 1.2 U and the concentration of the β -keto acid ester varied between 2 mM, 5 mM, 10 mM, 50 mM and 100 mM. The lipase, the substrate (β -keto acid ester), PLP and DMSO (10 %) were mixed and incubated 30° C for 24 h. The substrate was dissolved in biotransformation buffer (NaCO₃, pH 9, Tris/HCl, pH 8) Samples were taken frequently. The substrate was analyzed via HPLC and the resulting ethanol was analyzed by GC.

3.6.2.2 Cascaded enzyme reaction

The cascaded enzyme reaction was conducted with 1.2 U lipase, 1 U immobilized β -amino acid aminotransferase/free enzyme in crude cell extract, PLP, the substrate ethyl benzoylacetate (concentrations of 2.5 mM and 5 mM) and 125 mM amino donor (table 3.4) in biotransformation buffer (Tris HCl, pH 8) for 24 h at 30° C with frequent sample taking.

3.6.2.3 Asymmetric synthesis with 3-oxo-3-phenyl propionate as substrate

Sodium 3-oxo-3-phenyl propionate was purchased to investigate its stability and if the immobilized β -amino acid aminotransferase/crude cell extract is able to convert it. A wavelength scan of the substrate was taken for 24 h, with scans every 10 min in the first hour. The substrate was as well frozen and thawed and cooked at 99° C. Furthermore, 3-oxo-3-phenyl propionate was used in a biotransformation with immobilized aminotransferase and crude cell extract, with PLP and an amino donor (table 3.4) in biotransformation buffer (Tris/HCl, pH 8) for 24 h at 20° C and 950 rpm. Samples were taken frequently.

4 RESULTS

4.1 KINETIC RESOLUTION OF β -AMINO ACIDS

Kinetic resolution catalyzed by a β -amino acid aminotransferase starts with a racemic substrates and an amino acceptor (see figure 4.1). A production yield of 50 % can be achieved and a high ee is only possible when the reaction rate is 50 %. The equilibrium of this reaction lies totally on the product side, due to spontaneous decarboxylation of the emerging β -keto acid. Therefore, kinetic resolution with aminotransferase as a biocatalyst is a rewarding method for enrichment of enantiopure amines and α - and β -amino acids [8, 122, 123].

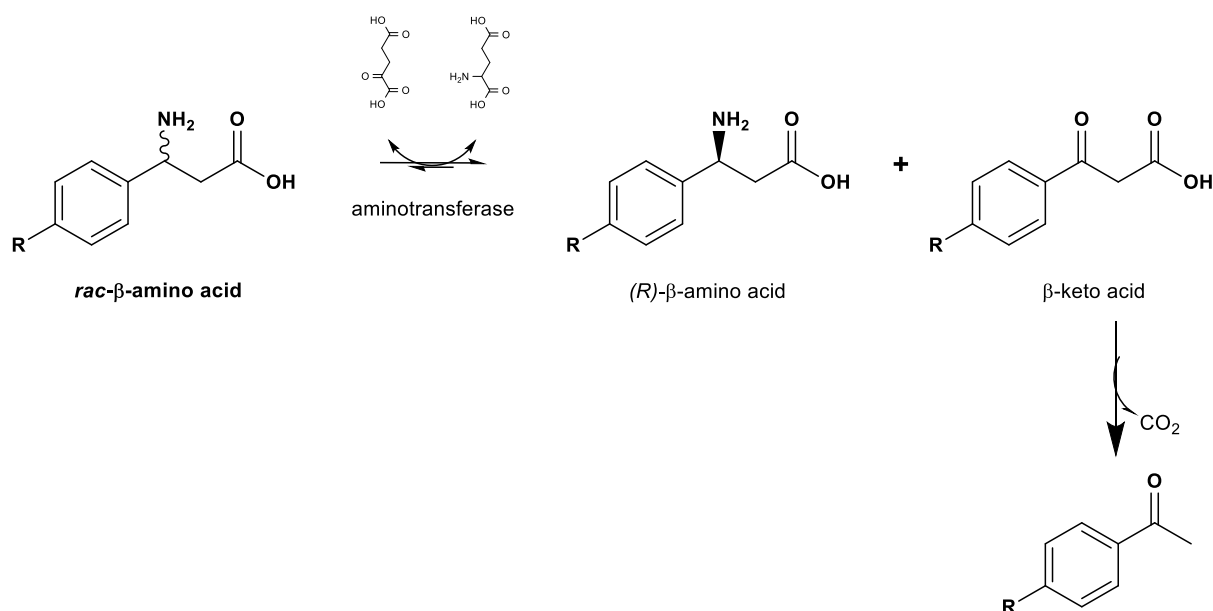


Figure 4.1: Kinetic resolution to synthesize enantiopure β -amino acids.

4.1.1 Introduction of a polyhistidin tag

For the synthesis of β -amino acids with aminotransferases the β -amino acid aminotransferase gene from *Variovorax paradoxus* (characterized by Crismaru and coworkers [116]) was synthesized by ThermoScientific and a sequence coding for a His₆-tag was added. The gene was introduced in the pET21b and pET11a plasmids. These plasmids contain ampicillin resistance genes for selection. To control the size of the plasmid and the gene, the plasmid was digested with restriction enzymes (the plasmid card with the suitable restriction enzymes are shown in appendix 7.2, figure 7.1). The size of the empty plasmid pET21b is ~5.442 kb and the size of encoding gene with the coding sequence for a His₆-tag is ~1.311 kb. The size of the empty plasmid pET11a is 5.677 kb and the size of the encoding gene without His₆-tag is ~1.314 kb.

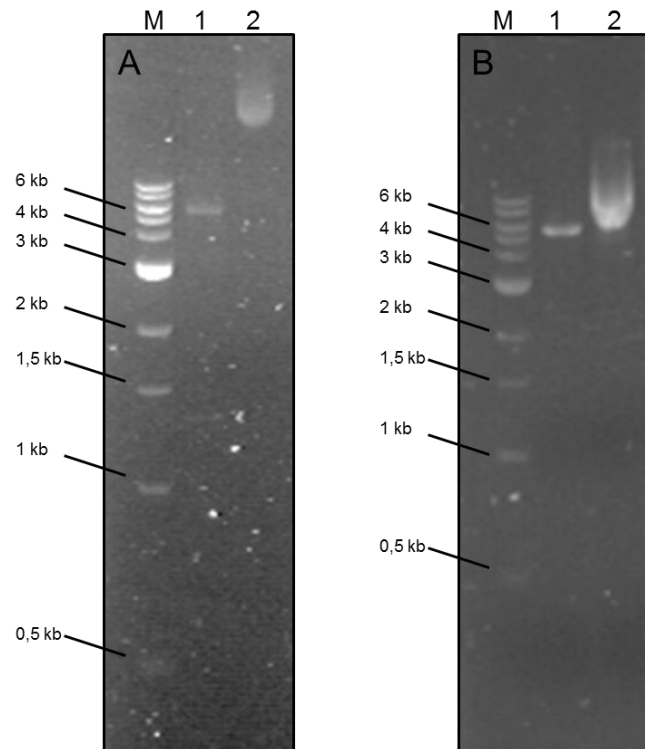


Figure 4.2: Agarose gel electrophoresis of plasmid pET21b and pET11a. A: pET21b after digestion with restriction enzymes Ndh I and Xho I (lane 1) and without digestion (lane 2) and B: pET11a after digestion with restriction enzymes Ndh I and BamH I (lane 1) and without digestion of the plasmid (lane 2). Lanes marked with M shows the marker.

In figure 4.2 A, the gel electrophoresis of the plasmid pET21b is shown. In lane 1, the plasmid was digested with the restriction enzymes Ndh I and Xho I, lane 2 shows the undigested plasmid. Two bands are visible in lane 1 with the size between 5 and 6 kb and between 1 and 1.5 kb. The first band is the empty plasmid, with an expected size of ~ 5.442 kb, the second band is the encoding gene with a size of ~1.311 kb. In lane 2 the undigested plasmid is shown, due to the cyclic form of the undigested plasmid the band is not clear. In figure 4.2 B, the gel electrophoresis of plasmid pET11a is shown. In line 1 the plasmid was digested by the restriction enzymes Ndh I and BamH I and shows a size between 5 and 6 kb, which corresponds to the size of the empty plasmid pET11a with 5.677 kb. A second band for the encoding gene does not appear (even after digestion of pET11a + encoding gene for several times). This means, that either the amount of encoding gene in the agarose gel was too low or the encoding gene was not incorporated. Further investigations were made to prove that the gene was included to the plasmid pET11a (see next chapter).

4.1.2 Expression and activity of the His-tagged aminotransferase

The first expression of the β -amino acid aminotransferase gene from *Variovorax paradoxus* ligated to the plasmid pET21b (with His-tag) and pET11a (without His-tag) in *E.coli* strain BL21DE was performed to investigate if the enzyme was correctly folded and catalytically active. Various approaches were performed to examine the basal activity of the strain and the

expression of the enzyme, followed by occurring activity without induction, due to the T7 promotor: Transformation of both plasmids with and without the encoding genes was performed into strain BL21DE and the expression was induced by adding IPTG. Furthermore, the gene was expressed without induction by IPTG. A description of all investigated plasmids and expression combinations are shown in table 4.1.

Table 4.1: Description of entries shown in Figure 4.3.

Entry	Plasmid	Gene yes/no	IPTG induction yes/no
1	pET11a	no	yes
2	pET11a	no	no
3	pET21b	no	yes
4	pET21b	no	no
5	pET11a	yes	yes
6	pET11a	yes	no
7	pET21b	yes	yes
8	pET21b	yes	no
9	no	no	-

The experiments consist of the cultivation of the strain BL21DE, the expression of the aminotransferase gene and a biotransformation with the crude cell extract of the cultures with the different combinations of plasmids and with or without induction, displayed in Table 4.1. The biotransformation was performed as described in chapter 3.6.1 and table 3.15. As the free β -amino acid aminotransferase only catalyzes the conversion of the (*S*)-enantiomer, in all further figures merely the activity towards this enantiomer is shown. The (*R*)-enantiomer was never converted at all (figure 7.3; appendix 7.4).

In figure 4.3, relative conversion of (*S*)- β -phenylalanine is pictured after 7 h for all entries, which are precisely described in table 4.1. The biotransformation for the negative control (nc) was performed without enzyme.

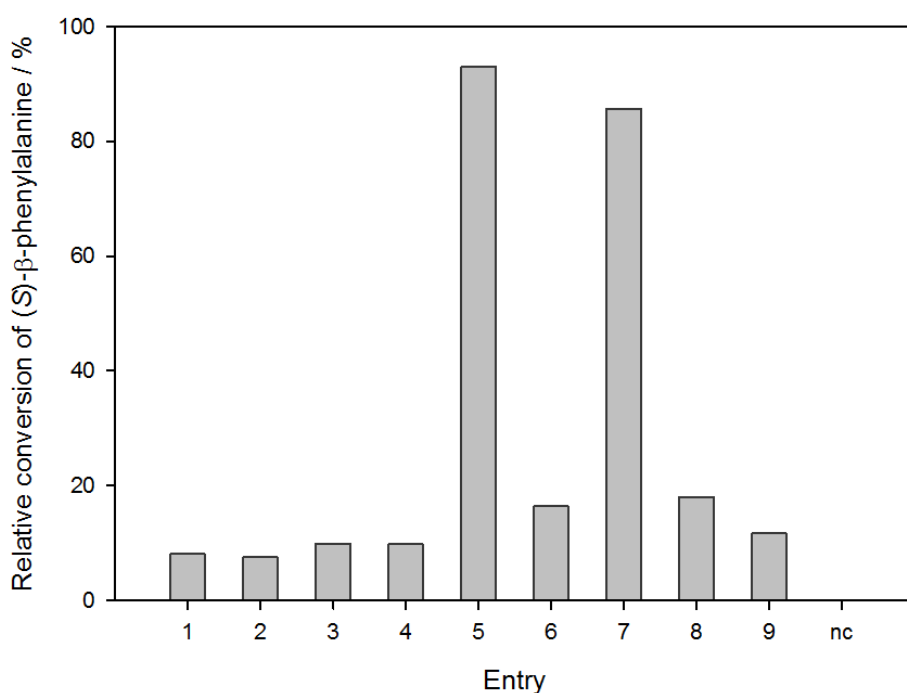


Figure 4.3: Relative conversion of (S)-β-phenylalanine catalyzed by the β-amino acid aminotransferase from *Variovorax paradoxus* for different expression conditions. The gene was expressed in *E.coli* strain BL21DE, activity toward β-phenylalanine was tested for a variety of different combinations. Transformation of the two plasmids pET21b and pET11a were performed into BL21DE with (entry 5, 6, 7 and 8) and without (entry 1, 2, 3 and 4) the gene for the aminotransferase and the expression was performed with (entry 1, 3, 5 and 7) and without (entry 2, 4, 6 and 8) the induction substrate IPTG. The strain BL21DE was investigated without the plasmids (entry 9) as well. For the negative control (nc) the biotransformation was performed without the enzyme. Biotransformation conditions: 10 mM *rac*-β-phenylalanine, 5 mM α-ketoglutarate, 0.2 mM PLP and 0.2 mg/ml crude cell extract, incubated at 30 °C.

Entry 1, 2, 3 and 4 reveal no significant conversion of (S)-β-phenylalanine which correlates to the results of entry 9. More precisely, the introduction of empty plasmids reveals no increase in the conversion of the substrate, compared to the strain without the plasmids. Entry 6 and 8 indicate an increased conversion of the substrate with ~ 20 % conversion compared to ~8-10 % of entry 1-4 and 9. Higher conversion rates of 93 % and 86 % could be achieved by entry 5 and 7, respectively. The specific activity is calculated for the gene expressed in plasmid pET11a and pET21b to illustrate the differences in activity for the enzyme with and without a His-tag. For the conversion of (S)-β-phenylalanine with the expressed genes in plasmid pET11a, the specific activity is 0.36 U/mg and the specific activity after expressing the gene with plasmid pET21b is 0.27 U/mg.

The stability of the enzyme in crude cell extract was tested for storing at 4° C for 38 days and for freezing and thawing. After 18 days at 4° C the crude cell extract lost its activity (figure 4.15). Three freezing and thawing cycles were performed which resulted in a loss of activity of 40 % (figure 7.2).

For further characterization the His-tagged enzyme was purified via an affinity chromatography (IMAC), described in the following section.

4.1.3 Purification via immobilized metal ion affinity chromatography

The purification of the β -amino acid aminotransferase (AT) was conducted via immobilized metal ion affinity chromatography (IMAC), due to the His-tag attached to the enzyme. The strain BL21DE containing the plasmid pET21b with the encoding gene and a His-tag coding element was cultivated and the expression was induced by adding IPTG. The elution of the enzyme, the activity toward the (S)-enantiomer of β -phenylalanine of the fraction and the crude cell extract (the lysate after cell disruption), SDS-PAGE of the fractions and an overview of the recovery and purification fold is illustrated in the next section.

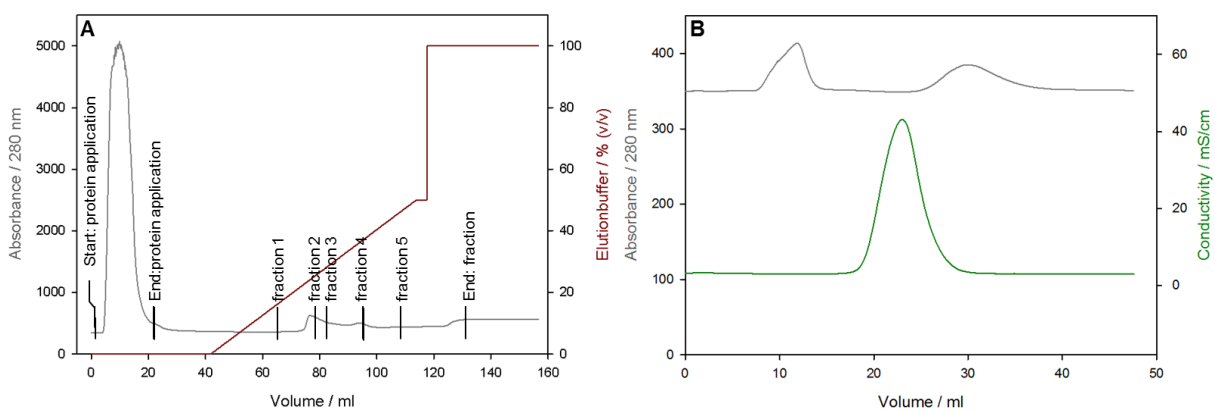


Figure 4.4: Chromatogram of the protein purification via IMAC. In A the absorbance of proteins at 280 nm is shown and the fraction collected after starting the elution of the His-tagged β -amino acid aminotransferase with elution buffer containing imidazole. The peak between start and end of protein application is the fraction of the unbound protein. Part B shows the desalting of fraction 3 as an example. The absorbance of the protein at 280 nm is shown as well as the conductivity.

For the purification via IMAC (see figure 4.4 A), the crude cell extract was applied to the column with a flow rate of 0 ml/min to 20 ml/min (Start: protein application to End: protein application, named below as unbound protein). Subsequently, the elution of the His-tagged aminotransferase started with 0 % elution buffer to 50 % elution buffer containing 500 mM imidazole in 75 min. During that time 5 fractions (F1-F5) were collected. After 75 min the gradient of the elution buffer was raised to 100 % elution buffer, but no protein was eluted after that. The enzymes were dissolved in a fraction containing a high concentration of imidazole. For this reason the fraction was subsequently desalted. In figure 4.4 B, the absorbance at 280 nm is shown (grey line). The first peak illustrates the enzyme fraction and the second peak may be induced by the imidazole, since no protein was determined in this fraction. The conductivity peak (dark green line) shows the elution of the sodium chloride, which is included in the buffer. The crude cell extract, the unbound protein and fractions 1-3 were chosen for

determination of activity toward (S)- β -phenylalanine, see figure 4.5. In fraction 4 and 5, no protein could be detected. Hence both fractions were not tested toward activity.

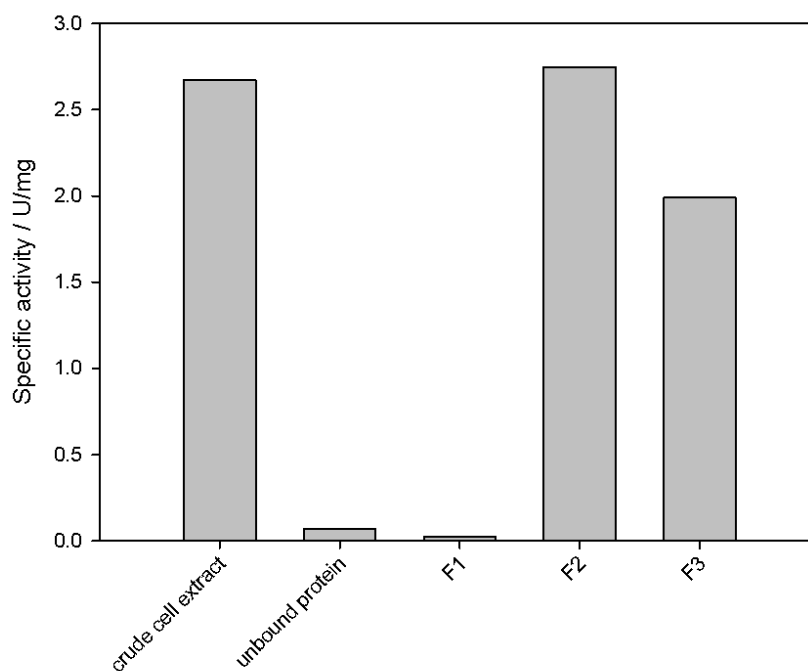


Figure 4.5: Specific activity of the fractions after IMAC purification. Crude cell extract is the lysate of the cultivated cells after cell disruption, unbound protein is the fraction after the lysate was applied to the column and the desired His-tagged aminotransferase was bound to the matrix. F1-F3- are the collected fractions after starting the elution with elution buffer.

A specific activity of 2.6 U/mg was determined for the crude cell extract (lysate of the cultivated cells after cell disruption), after application to the column almost no activity (0.07 U/mg, see table 4.2) could be shown for the unbound protein. Hence, the column was not overloaded during the experiment and all His-tagged enzymes were able to bind. In fraction 1, no activity (0.02 U/mg, see table 4.2) could be detected. The highest activity with 2.75 U/mg and 1.99 U/mg could be identified for the fractions 2 and 3, respectively (see table 4.2). The activity for fraction 2 and 3 shows that, in this fraction, the desired His-tagged β -amino acid aminotransferase was eluted.

For the identified fractions a SDS-PAGE (see figure 4.6) was conducted to display the protein concentration. Moreover, the SDS-PAGE served to verify if the purified enzyme is the desired β -amino acid aminotransferase with a molecular weight of 46 kDa for the monomer.

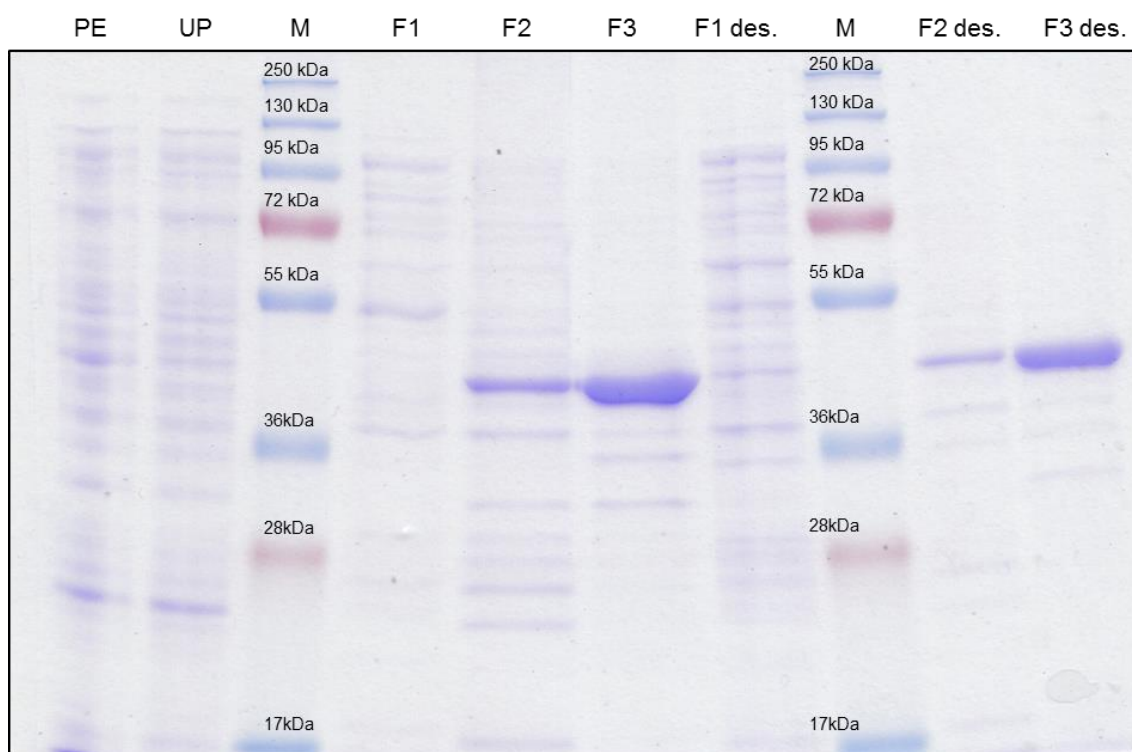


Figure 4.6: SDS-PAGE gel for the fractions of the IMAC purification. PE is the lane for the crude cell extract (lysate of the cultivation after cell disruption), UP is the lane for the unbound protein fraction, F1-F3 are the collected fractions after starting the elution of the His-tagged β -amino acid aminotransferase. F1 des., F2 des. and F3 des. are the lanes for the fractions 1, 2 and 3 after desalting. M is the marker.

The first lane of the SDS-PAGE gel in figure 4.6 shows the crude cell extract, various bands can be seen. The same amount of bands is shown in lane UP for the unbound protein. In the lane for fraction 1, no band emerges at 46 kDa, compared to lane F2 and F3, where distinct bands show up at the right molecular weight. For the lanes F2 des and F3 des the bands appear thinner compared to the fractions before the desalting step.

For the quantification of the enzyme purification the total activity, the protein content, the specific activity (correspond to figure 4.5), recovery and the purification factor are summarized in table 4.2. The formula to calculate the specific activity, recovery and purification factor is given in chapter 3.2.4.

Table 4.2: Quantification of enzyme purification via IMAC of the His-tagged β -amino acid aminotransferase.

	Total activity / U	Protein content / mg	Specific activity / U/mg	Recovery / %	purification fold
Crude cell extract	219.15	81.97	2.67	100.00	1.00
unbound protein	4.39	65.51	0.07	2.00	0.03
F1	0.13	5.48	0.02	0.06	0.01
F2	2.86	1.04	2.75	1.30	1.03
F3	4.93	2.48	1.99	2.25	0.74

The best recovery is achieved in fraction 3 with 2.25 % and with a purification factor of 0.74. The highest purification factor was reached in fraction 2 with 1.03, but with a lower recovery of 1.3 %. In fraction 2 the specific activity is 2.75 U/mg and higher compared to the specific activity of fraction 3 with 1.99 U/mg.

4.1.4 Purification via magnetic M-PVA beads

The purification of the His-tagged β -amino acid aminotransferase via magnetic functionalized M-PVA beads is based on the same binding mechanism as purification via IMAC. The crude cell extract (cell lysate of the cultivation broth) was added to the magnetic beads functionalized with IDA and Ni^{2+} . After binding of the enzyme the supernatant was removed (fraction after incubation) and the beads (20 mg) were washed three times. The supernatant of the first wash fraction contained a low concentration of protein (~ 1 mg/ml), compared to the second and third wash fraction without protein. After washing the beads, the elution was started by incubating the beads with elution buffer for 5 min (fraction E). For all of these fractions, biotransformation was carried out. Furthermore, the residual activity was determined for the enzymes remaining on the magnetic beads after elution (IE).

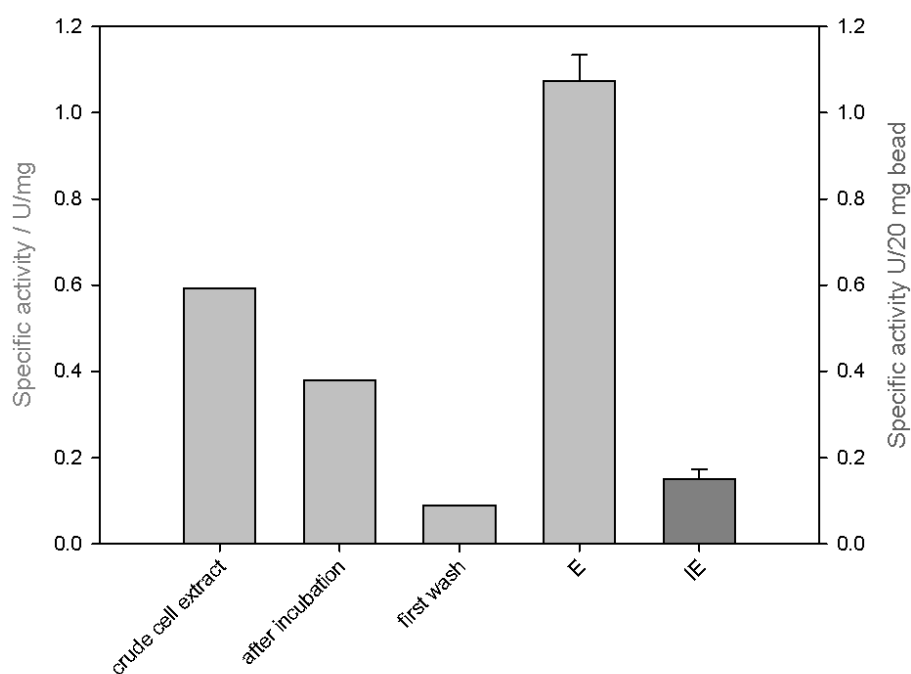


Figure 4.7: Specific activity (U/mg and U/20 mg beads) of the fractions after elution of the β -amino acid aminotransferase off the magnetic M-PVA beads. Crude cell extract is the lysate of the cultivation after cell disruption, after incubation means the crude cell extract after incubation with magnetic beads, the beads were washed with buffer and the activity of this fraction is shown. E shows the activity of the purified β -amino acid aminotransferase and IE the residual activity on the beads after elution with elution buffer. Statistical error of $n=3$ experiments.

Figure 4.7 shows the specific activity of the fraction of the aminotransferase purification via magnetic M-PVA beads. The crude cell extract displays an activity of 0.59 U/mg. After incubation of the magnetic beads with crude cell extract, the fraction still shows a specific activity of 0.38 U/mg. Even the first wash fraction exhibits a slight activity of 0.09 U/mg. The specific activity of the free purified enzyme is 1.1 U/mg. After elution of the beads with elution buffer, the magnetic beads still have bound aminotransferase, which is illustrated in the residual activity of 0.15 U/20 mg magnetic beads.

A SDS-PAGE of the fractions is shown in figure 4.8. It was conducted to display the protein concentrations and shows if the fractions contain the desired aminotransferase with a molecular weight of 46 kDa for the monomer.

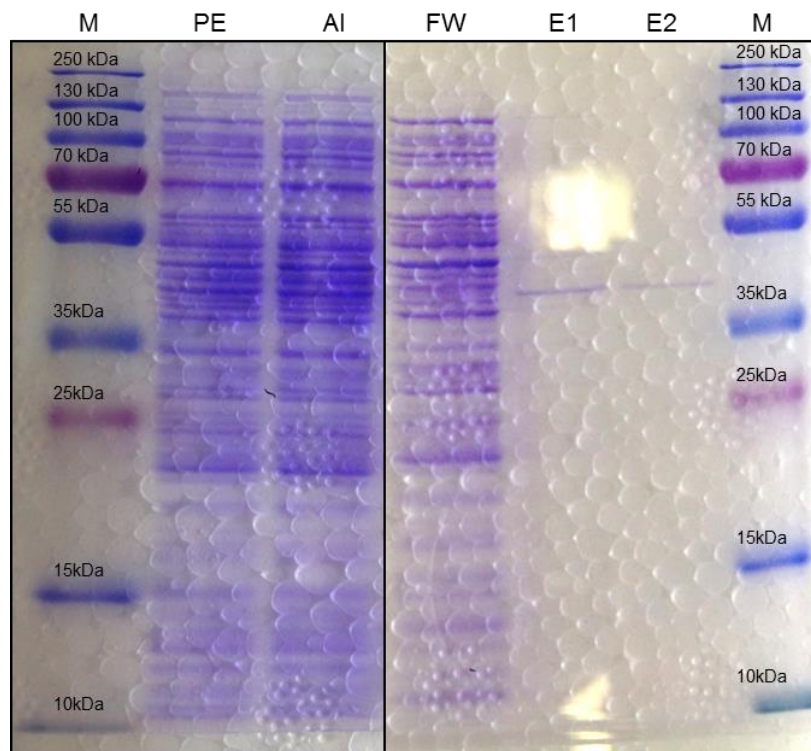


Figure 4.8: SDS-PAGE gel for the fractions after elution of the β -amino acid aminotransferase off magnetic M-PVA beads. PE is the fraction of the crude cell extract; AI is the fraction after incubation; FW is the fraction after with first washing of the magnetic beads. E1 and E2 display the free enzyme purified using magnetic beads. M is the lane for the marker. The aminotransferase has a weight of 46 kDa for the monomer.

A distinct band at 46 kDa is shown in the lanes E1 and E2 which display the free enzyme after purification via magnetic beads. In the lane PE, which displays the crude cell extract no distinct band at 46 kDa can be defined.

For the quantification of the aminotransferase, purified using magnetic M-PVA beads the total activity, the protein content, the specific activity, the recovery and purification factor are shown in table 4.3.

Table 4.3: Quantification of the His-tagged β -amino acid aminotransferase purification using magnetic M-PVA beads.

Sample	Total Activity / U	Protein Content / mg	Specific Activity / U/mg	Recovery / %	Purification fold
crude cell extract	25,82	44,1	0,59	100,0	1,0
after incubation	14,84	39	0,38	57,5	0,6
first wash	0,13	1,4	0,09	0,5	0,2
E 1 + 2	0,57	0,5181	1,10	2,2	1,9

The recovery of the free enzyme after elution is 2.2 % and was purified 1.9 fold. After incubation, the recovery of the aminotransferase is 57.5 %, but with a low purification with the factor 0.6. The highest specific activity shows the free aminotransferase after purification with 1.1 U/mg. After the first washing step almost no protein was found. Hence, only a recovery of 0.5 % was achieved, as well as a purification factor of 0.2 and a specific activity of 0.09 U/mg.

The residual activity of the enzymes remaining on the magnetic beads (fraction IE) after elution is 0.15 U/20 mg beads. The recovery could not be calculated.

For further characterization of the immobilized β -amino acid aminotransferase using M-PVA beads several experiments were conducted and described in the following chapter.

4.1.5 One-step purification and immobilization using magnetic M-PVA beads

His-tagged β -amino acid aminotransferase from *Variovorax paradoxus*, cultivated and expressed in *E. coli* strain BL21DE, was purified and immobilized in one step using magnetic M-PVA beads. The immobilized aminotransferase was characterized regarding influence on temperature and pH spectrum, substrate scope (different amino donors), activity toward a variety of amino acceptors and long-term storage stability and its recyclability. Furthermore, examinations were performed to find a suitable ratio of magnetic beads and crude cell extract for immobilization. After every experiment, the beads were incubated in 1 % SDS at 90° C for 20 min and the protein concentration was determined to know the overall concentration of immobilized enzyme on the beads during the experiment. The beads were then washed and used for further experiments. No activity could be detected after incubation at 90° C and no aminotransferase remained on the beads (ensured by a second incubation with 1 % SDS at 90° C). For *rac*- β -phenylalanine as a substrate it is known that only the (*S*)-enantiomer is converted by this β -amino acid aminotransferase [116]. Hence, in further experiments only the activity toward the (*S*)-enantiomer is pictured (see figure 7.3). Biotransformation with only the magnetic beads (without previous incubation with crude cell extract) showed no activity as well. The biotransformations were performed as described in section 3.6.1. With this immobilization technique the aminotransferase was found to be stable for at least 38 days and is recyclable

for 7 cycles without significant loss of activity. Additionally, the immobilized enzyme shows increased pH and temperature stability.

4.1.5.1 Influence of bivalent metal ions

During immobilization on magnetic beads bivalent metal ions have affinity to the His-tagged β -amino acid aminotransferase and form chelate complexes with the IDA functionalized beads. Various metal ions be possible for using as metal ion, like Co^{2+} , Ni^{2+} , Cu^{2+} , Fe^{2+} and Fe^{3+} . In this work Co^{2+} , Ni^{2+} and Cu^{2+} were used and the binding capacity of the aminotransferase is illustrated by means of activity toward the substrate β -phenylalanine. The beads were prepared with buffers containing bivalent metal ions (section 3.1.6.3). For the experiment 20 mg beads were incubated with crude cell extract and subsequently the biotransformation was performed at standard conditions: *rac*- β -phenylalanine, α -ketoglutarate, PLP and NaCO_3 buffer pH 9 at 30° C and 950 rpm.

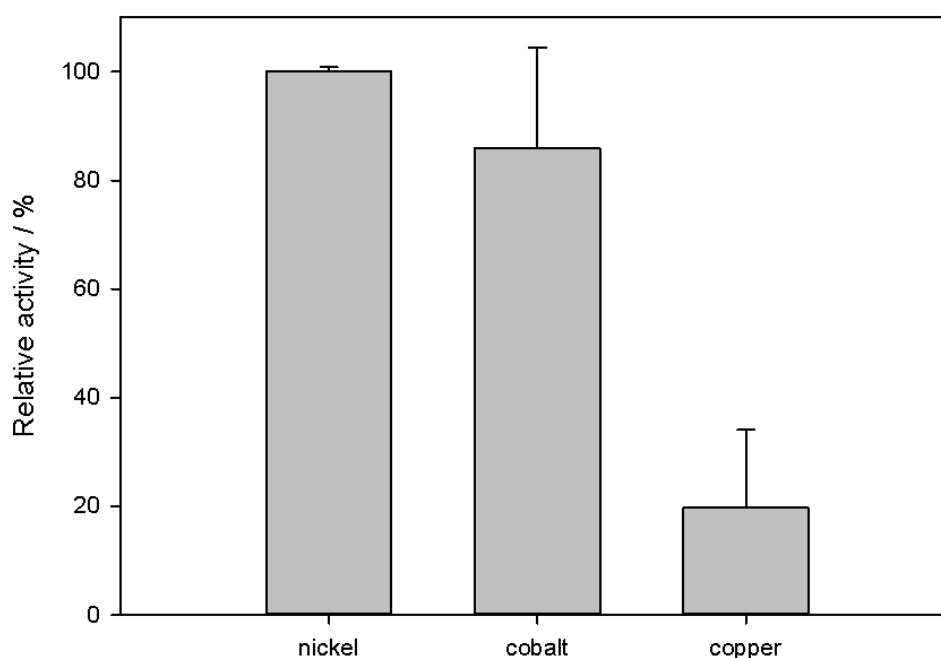


Figure 4.9: Relative activity of the immobilized His-tagged β -amino acid aminotransferase. Immobilized by its affinity toward bivalent metal ions (Ni^{2+} , Co^{2+} , Cu^{2+}). 100 % refers to the activity of 0.81 U toward (*S*)- β -phenylalanine. Statistical error of n=3 experiments.

In figure 4.9, the relative activity of the aminotransferase is pictured. It is based on the binding efficiency of the enzyme to the metal ion building a complex with the IDA functionalized magnetic beads. Immobilization with nickel showed a relative activity of 100 % which refers to the activity of 0.81 U toward (*S*)- β -phenylalanine. Cobalt (Co^{2+}) as a bivalent metal ion for immobilization exhibits a relative activity of 85 % compared to immobilization with Ni^{2+} . The relative activity of 21 % with copper as affinity metal ion ligand is five times lower compared to

100 % relative activity for immobilization with nickel. The relative activity of 21 % was determined for the first biotransformation with immobilized aminotransferase with copper. For the second and third time of biotransformation almost no activity can be detected, in contrast to the immobilization of the aminotransferase with nickel and cobalt as affinity ligand (results of recyclability of immobilized aminotransferase with nickel, cobalt and copper is shown in section 4.1.5.7 and figure 4. 16).

For the further work described herein, Ni^{2+} was used as metal ion for the immobilization.

4.1.5.2 Influence of the temperature

Temperature has an influence on enzyme activity. Immobilized aminotransferase was compared to free enzyme in crude cell extract considering the effect of temperature on activity. The temperature optimum was determined by performing the biotransformation at 30° C, 40° C, 50° C, 60° C, 70° C and 80° C (with *rac*- β -phenylalanine, α -ketoglutarate, PLP and NaCO_3 buffer, pH 9 and at 950 rpm). Besides, the stability of the immobilized aminotransferase and the free enzyme in crude cell extract was examined by incubation of the (immobilized) enzyme at the above mentioned temperatures for 2 h. After incubation, the aminotransferase was cooled down to room temperature before biotransformation was carried out at 30° C.

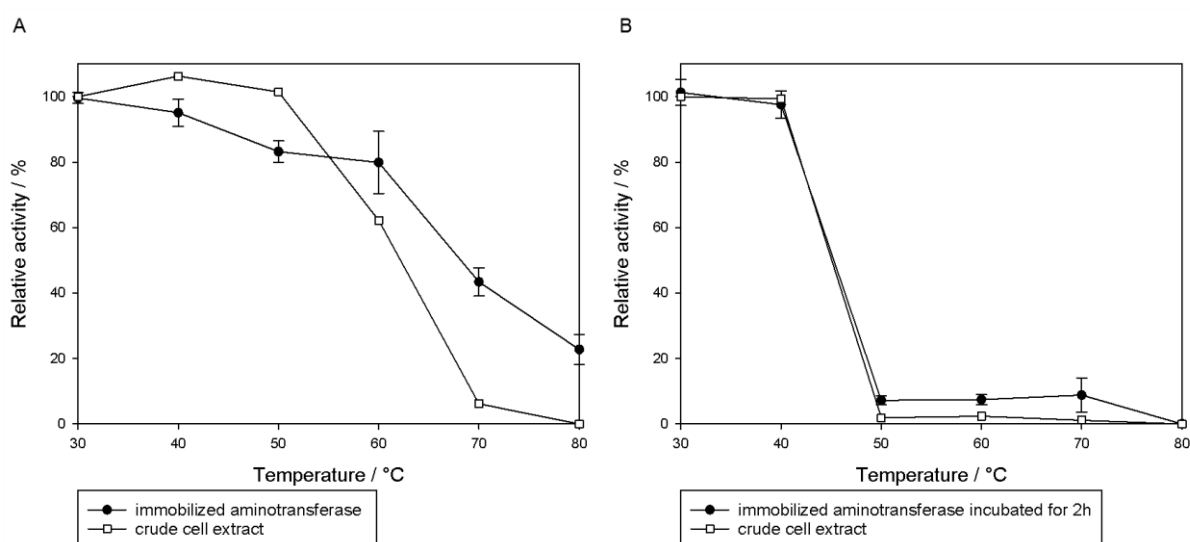


Figure 4.10: Relative activity of immobilized aminotransferase and crude cell extract toward the substrate (S)- β -phenylalanine at different temperatures: A shows the activity at different temperatures (100 % refers to 0.95 U for the immobilized aminotransferase and 0.57 U for the crude cell extract). B shows the activity after incubation at different temperatures for 2 h (100 % refers to 0.84 U for the immobilized aminotransferase and 0.68 U for the free enzyme in crude cell extract). After incubation, the immobilized enzyme and the crude cell extract were cooled down to room temperature and biotransformation was performed at 30° C. Statistical error of n=3 experiments.

The relative activity of the crude cell extract is shown in figure 4.10 A (white squares). The optimal temperature is 40° C with 106 % and 0.6 U, but the specific activity is still high at 50° C with 100 % and 0.58 U. The activity rapidly decreases at 60° C and almost all activity is lost at

70° C. At 80° C, the crude cell extract shows no activity toward the substrate (*S*)- β -phenylalanine. The immobilized aminotransferase shows activities over a wider range of temperatures, with the best activity at 30° C of 100 % and 0.84 U (figure 4.10 A; black dots). Over time, the activity decreases as well, but the activity at 60° C is still high with ~ 80 % and 0.62 U at 80° C the immobilized aminotransferase shows 22 % of its activity of 0.22 U at 30° C. After incubation for 2 h and subsequent cool down to room temperature, the relative activity remains the best at 30° C with 0.84 U and 0.68 U for the immobilized aminotransferase (figure 4.10 B black dots) and the crude cell extract (white squares), respectively. Incubation at 40° C shows no significant influence on enzyme activity neither for the immobilized enzyme nor the crude cell extract. A rapid decrease at 50° C is illustrated for immobilized and free enzyme, whereas the immobilized enzyme still has a remaining activity of 7 % of the activity at 30° C with 0.1 U. The crude cell extract loses its activity after incubation at 50° C. The immobilized enzyme loses its activity only after incubating for 2 h at 80° C. The temperature stability of the enzyme has improved after immobilization, even after incubation at high temperatures for 2 h. Furthermore, the immobilized enzyme shows activity over a wider range of temperatures.

4.1.5.3 Influence of the pH

A variety of different buffers with pH of 4, 7, 9 and 11 were used for the biotransformation with the immobilized β -amino acid aminotransferase and the free aminotransferase in crude cell extract and the activity was determined toward the model substrate (*S*)- β -phenylalanine. To determine the activity at different pH values, several buffer systems were used. For pH 4, citric acid buffer was used, for pH 7 NaPP buffer and for pH 9 and 11 a NaCO₃ buffer. The biotransformation was performed with immobilized enzyme (20 mg beads incubated with crude cell extract) and crude cell extract (1.5 mg protein) with *rac*- β -phenylalanine, α -ketoglutarate, PLP at 30° C and 950 rpm.

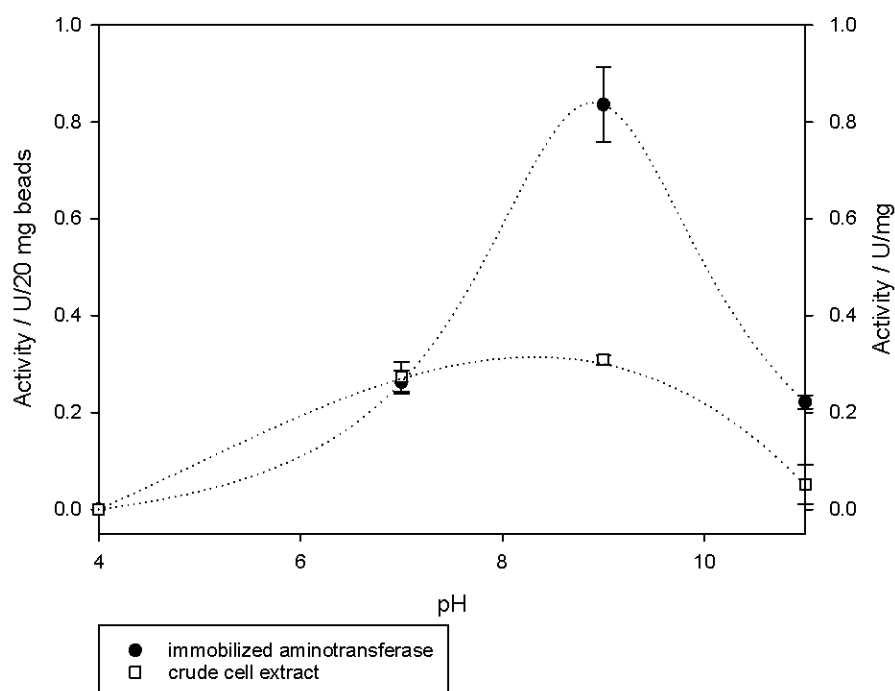


Figure 4.11: Specific activity of the immobilized β -amino acid aminotransferase and crude cell extract at different pH. Biotransformation with immobilized enzyme using 20 mg magnetic M-PVA beads at 30 °C with *rac*- β -phenylalanine, α -ketoglutarate, PLP and 950 rpm. For biotransformation with crude cell extract 1 mg protein was utilized. Statistical error of n=3 experiments.

The effect of pH on the immobilized aminotransferase and the free aminotransferase in crude cell extract is illustrated in figure 4.11. It is shown, that the crude cell extract and immobilized enzyme exhibit a different pH optimum. The enzyme in crude cell extract shows almost no difference in activity for pH 7 and 9, with a specific activity of 0.27 U/mg and 0.3 U/mg, respectively. The immobilized enzyme, on the other hand, has a significantly higher specific activity of 0.89 U/20 mg beads at pH 9 compared to 0.26 U/20 mg beads at pH 7. Furthermore, the enzyme in the crude cell extract shows nearly no activity at pH 11 (0.05 U/mg) compared to the immobilized aminotransferase (0.22 U/20 mg beads). Stability at high pH and a broader pH spectrum can be achieved by immobilization.

4.1.5.4 Influence of different amino acceptors

For transferring the amino group in a kinetic resolution of *rac*- β -phenylalanine with a β -amino acid aminotransferase, an amino acceptor is necessary. There is a wide range of amino acceptors which is accepted by the aminotransferase, but the best combination of amino donor and amino acceptor has to be found. This biotransformation was conducted with the immobilized aminotransferase using 20 mg beads and the crude cell extract (1 mg) to investigate with which of the four tested substrates (α -ketoglutarate, pyruvate, oxaloacetate and acetophenone) the best activities can be achieved. The biotransformation was performed at 30° C with *rac*- β -phenylalanine as amino donor, PLP in NaCO₃ buffer pH 9 and 950 rpm.

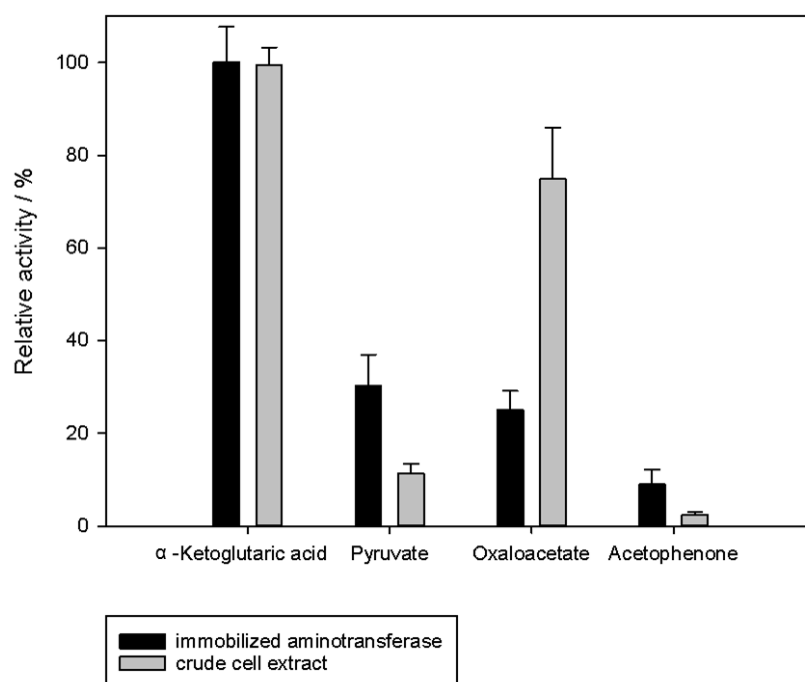


Figure 4.12: Relative activity of the immobilized β -amino acid aminotransferase (using 20 mg beads) and crude cell extract for the biotransformation with different amino acceptors. The biotransformation was performed with *rac*- β -phenylalanine as amino donor, PLP in NaCO_3 buffer pH 9 at 30 °C and 950 rpm. For biotransformation with crude cell extract, 1 mg protein was utilized. Statistical error of $n=3$ experiments.

For the immobilized aminotransferase and the enzyme in crude cell extract the highest activity is achieved with α -ketoglutarate as amino acceptor, with activities of 0.77 U and 0.44 U, respectively (see figure 4.12). The immobilized aminotransferase shows an activity of 35 % with pyruvate (0.28 U), whereas the enzyme in crude cell extract has an activity of ~10 % (0.06 U). Using oxaloacetate as an amino acceptor an activity of 80 % compared to α -ketoglutarate (0.4 U) is shown for the free enzyme, but only 25 % activity compared to α -ketoglutarate (0.24 U) is found for the immobilized enzyme. Acetophenone is the least accepted amino acceptor for immobilized and enzyme in crude cell extract with 9 % and 3 % remaining activity, respectively. Since α -ketoglutarate is the most suitable amino acceptor for the immobilized aminotransferase and the enzyme in crude cell extract, this amino acceptor was utilized in all further experiments.

4.1.5.5 Substrate scope

The immobilized aminotransferase and the crude cell extract were tested for their ability to convert various β -amino acids. Conversion, relative activity and ee are shown in table 4.4 for the immobilized enzyme (^a) and the crude cell extract (^d). The immobilized aminotransferase and enzyme in the crude cell extract show clear preferences for the conversion of certain enantiomers. For all tested substrates, the (*S*)-enantiomer is the preferred one and is completely converted at least after 24 h, whereby the (*R*)-enantiomer is enriched. The

experiment was conducted with immobilized enzyme using 20 mg magnetic M-PVA beads with several β -amino acids as amino donors and α -ketoglutarate as amino acceptor and crude cell extract with 1 mg utilized protein. The buffer for the biotransformation was NaCO_3 buffer, pH 9 and PLP was included in the reaction mixture.

The relative activity of 100 % refers to 0.35 U activity toward entry 1 for the immobilized enzyme and 100 % of activity refers to 0.17 U for the crude cell extract. For the immobilized aminotransferase, the conversion rate is 48 % and it is shown that the (*R*)-enantiomer is not converted at all. The crude cell extract and the immobilized enzyme show similar activities, except for entry 5. No activity was determined for entry 5 for the crude cell extract, compared to a high activity (130 %) for the immobilized enzyme. Furthermore, the crude cell extract shows enhanced activity for entry 9 and 11. The ee of the enzyme in crude cell extract is higher for entry 9, 10 and 11. The immobilized enzyme shows activity towards both enantiomers for entry 10 and 11, whereas the crude cell extract is selective for the (*S*)-enantiomers for all tested substrates.

Table 4.4: Substrate scope of the immobilized enzyme (^a) and crude cell extract (^d).

Entry	Amino acid	Rel. activity / % ^a	Conv. / % ^a	ee / % ^a	Rel. activity / % ^d	Conv. / % ^d	ee / % ^d
1	<i>rac</i> - β -PA	100 ^a	48	>90 (<i>R</i>)	100	52	>88 (<i>R</i>)
2	(<i>S</i>)- β -PA	100	98		-	-	
3	(<i>R</i>)- β -PA	NA ^b	-		-	-	
4	<i>rac</i> - β -hPA	45	27	>69 (ND)	42	13	>60 (ND)
5	<i>rac</i> - β -(OCH ₃)PA	130	50	>85 (ND)	-	-	-
6	<i>rac</i> - β -(F)PA	96	54	>92 (<i>R</i>)	100	23	>99 (<i>R</i>)
7	<i>rac</i> - β -(NO ₂)PA	58	33	>75 (ND)	62	12	>72 (ND)
8	<i>rac</i> - β -(OH)PA	105	50	>85 (ND)	103	48	>96 (ND)
9	<i>rac</i> - β -(Cl)PA	88	31	>69 (<i>R</i>)	121	27	>99 (<i>R</i>)
10	<i>rac</i> - β -(Br)PA	100	55	>58 (ND)	113	28	>76 (ND)
11	<i>rac</i> - β -(<i>iso</i> propyl)PA	97	64	>57 (ND)	195	49	>99 (ND)

^a) Initial rates were measured, conversion and ee were determined after 10 min at 30°C. The activity toward β -PA, corresponding to 0.35, was taken as 100 % for immobilized aminotransferase. 2.5 mM amino donor and 5 mM α -ketoglutaric acid were utilized.

^b) NA, no activity.

^c) Initial rates were measured; conversion and ee were determined after 10 min at 30°C. The activity toward β -PA, corresponding to 0.17 U, was taken as 100% for the crude cell extract.

ND not determined

4.1.5.6 Influence of various bead and crude cell extract concentrations

To characterize the binding efficiency for immobilization of the β -amino acid aminotransferase various bead and crude cell extract concentrations were examined. For this experiment, various concentrations of beads were incubated with 45 mg protein in crude cell extract. Quantities of 10 mg, 20 mg, 40 mg and 60 mg of magnetic beads were utilized and 0.5 mg, 0.99 mg, 1.3 mg and 1.9 mg bound protein were determined after incubation with crude cell extract, respectively (via BCA after incubation with 1 % SDS at 90° C). Furthermore, varying amounts of crude cell extract were used for immobilization of 20 mg beads. Protein quantities of the crude cell extract of 3.75 mg, 7.5 mg, 15 mg, 30 mg and 39 mg were utilized, but after incubation 0.26 mg, 0.4 mg, 0.65 mg, 0.91 mg and 1.05 mg of protein have bound to the beads, respectively (determined via BCA after incubation with 1 % SDS at 90° C). The activity and specific activity/mg bead of the immobilized β -amino acid aminotransferase toward (S)- β -phenylalanine is illustrated in figure 4.13 and 4.14.

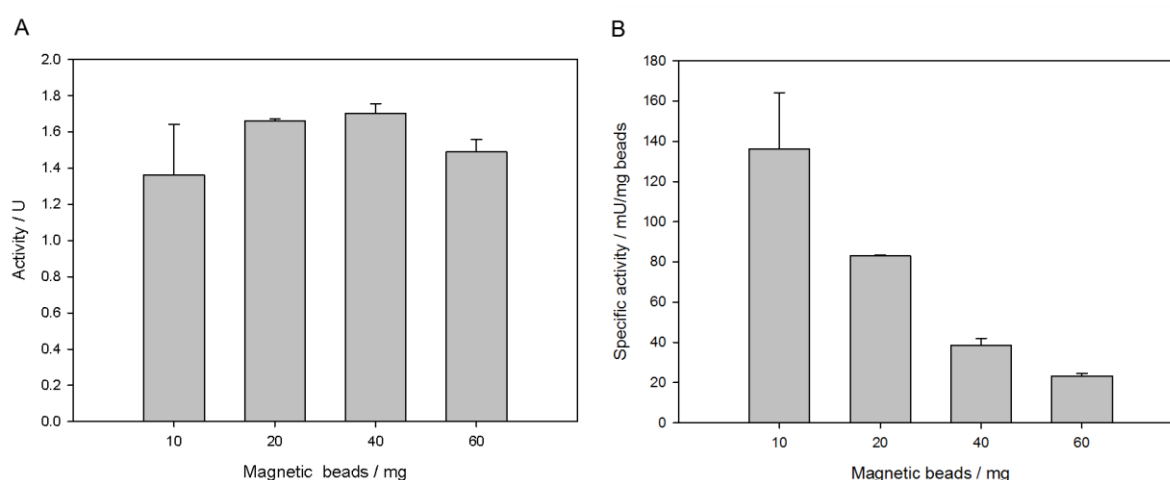


Figure 4.13: Activity of immobilized β -amino acid aminotransferase after incubation of different bead concentrations with crude cell extract. A crude cell extract incubated with various concentrations of magnetic beads (10 mg, 20 mg, 40 mg and 60 mg). The amount of protein in crude cell extract was kept at 45 mg. B Specific activity in mU/mg beads (detected after 20 min). Biotransformation conditions: *rac*- β -phenylalanine, α -ketoglutarate, PLP at 30 °C in NaCO₃ buffer pH 9 and 950 rpm. Statistical error of n=3 experiments.

The activity of the immobilized β -amino acid aminotransferase after incubating the crude cell extract with increasing amounts of magnetic beads is illustrated in figure 4.13 A. An increase in activity was observed for utilizing 10 mg beads with 1.34 U and 20 mg beads with 1.66 U. A slightly further increase in activity is shown for immobilization with 40 mg beads with 1.7 U compared to 20 mg beads. The activity of the immobilized aminotransferase using 60 mg beads, on the other hand, shows a decrease to 1.5 U. Referring the activity to the magnetic bead concentration, the specific activity decreases over increasing bead concentrations (figure 4.13 B).

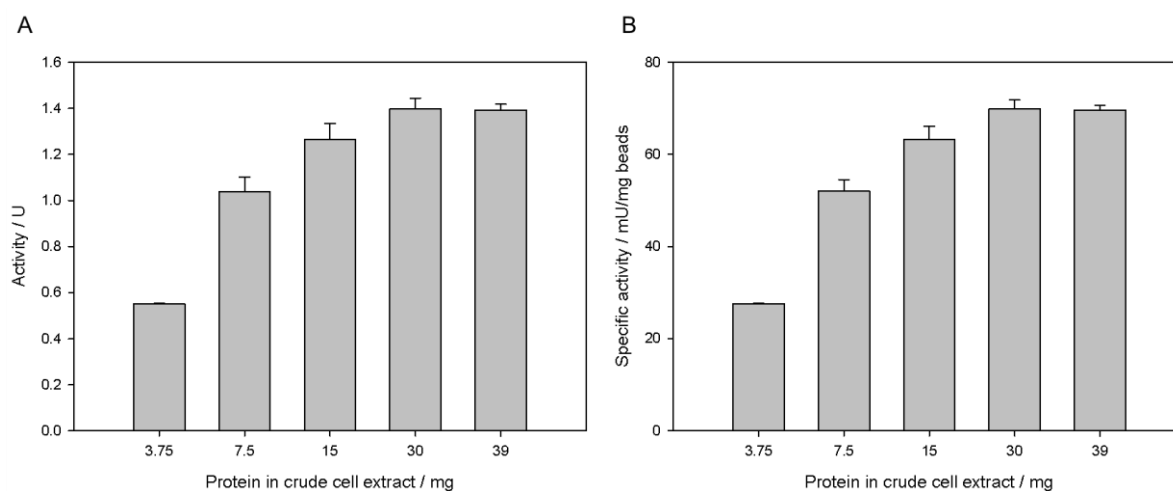


Figure 4.14: Activity of immobilized β -amino acid aminotransferase after incubation of 20 mg magnetic beads with a variety of concentrations of crude cell extract containing (3.75 mg, 7.5 mg, 15 mg, 30 mg and 39 mg). The amount of magnetic beads was kept at 20 mg. A Activity of immobilized β -amino acid aminotransferase after incubation of 20 mg magnetic beads with a variety of concentrations of crude cell extract containing B Specific activity in mU/mg beads (determined after 10 min). Biotransformation conditions: *rac*- β -phenylalanine, α -ketoglutarate, PLP at 30° C in NaCO₃ buffer pH 9 and 950 rpm. Statistical error of n=3 experiments.

After immobilization of the β -amino acid aminotransferase by incubating 20 mg magnetic beads with different amounts of crude cell extract, the protein content of the actually bound protein was determined via BCA. The activity of the enzyme immobilized with various amounts of protein is illustrated in figure 4.14 A. With increasing amount of protein, the activity increases, but no different activity is detected for immobilization with 30 mg and 39 mg protein. The specific activity referring to 20 mg beads is pictured in figure 4.14 B. An increase in activity is observed for increasing protein amounts. The peak of activity with 70 mU/mg bead specific activity is shown for 30 mg and 39 mg protein in crude cell extract.

When comparing the two experiments, it is observed that the specific activity for immobilization using 20 mg beads and immobilization with 39 mg protein are in the same range. Hence, the two experiments provide information about the concentration of actually bound β -amino acid aminotransferase and demonstrate which concentration of beads is suitable for immobilization of the aminotransferase out of crude cell extract with an overall protein amount of 45 mg.

4.1.5.7 Storage stability and recyclability

The storage stability of the immobilized β -amino acid aminotransferase in contrast to crude cell extract was investigated for 38 days. During the experiment the enzyme was stored at 4° C in biotransformation buffer (NaCO₃ buffer, pH 9) and extra PLP. The biotransformations were conducted with *rac*- β -phenylalanine as amino donor, α -ketoglutarate as amino acceptor, PLP at 30° C and 950 rpm in NaCO₃ buffer, pH 9.

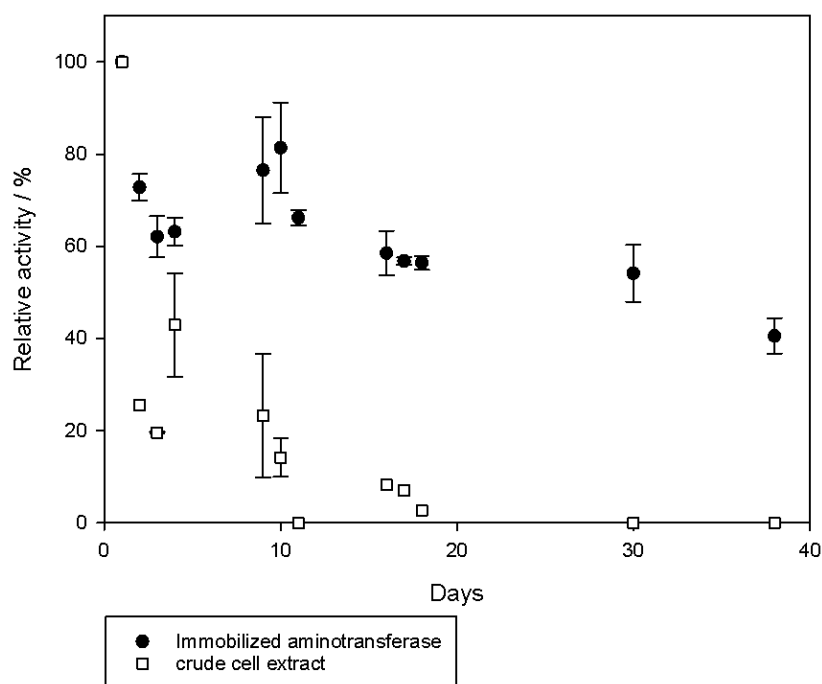


Figure 4.15: Relative activity of the immobilized β -amino acid aminotransferase and the crude cell extract toward (*S*)- β -phenylalanine for storage at 4° for a time period of 38 days using 20 mg magnetic M-PVA beads. The enzymes were stored at 4 °C in NaCO₃ buffer pH 9, which included PLP. 100 % relative activity refers to 1 U for the immobilized enzyme and 0.3 U for the crude cell extract. Biotransformation conditions: *rac*- β -phenylalanine, α -ketoglutarate, PLP at 30° C in NaCO₃ buffer pH 9 and 950 rpm. Statistical error of n=3 experiments.

The relative activity of the crude cell extract rapidly decreases in the first 10 days (figure 4.15, white squares). A slight increase during day 16 and 17 is illustrated, as well as a decrease after 18 days. After day 18, no residual activity is determined. The immobilized β -amino acid aminotransferase shows a loss in activity in the first day to ~80 % relative activity (figure 4.15, black dots). However, the activity remains constantly between 60 % - 70 % relative activity for the next 30 days. After 38 days, the immobilized enzyme is still active with 40 % relative activity.

The immobilized enzyme was also tested for its storage stability at -20° C by freezing with liquid nitrogen, storage at -20° C over night and subsequent thawing. The results are shown in figure 7.2. After three freezing and thawing cycles the conversion of (*S*)- β -phenylalanine was still 80 % of the starting 96 %.

The recyclability of the immobilized β -amino acid was examined for 7 cycles after immobilization of the enzyme with three bivalent metal ions. The experiment was conducted within 2 days, three successive recycling steps at day one and four successive cycles on the next day. In between the experiments the immobilized enzyme was stored at 4° C in biotransformation buffer (NaCO₃ buffer, pH 9) which included PLP. The biotransformation conditions were the same as described above.

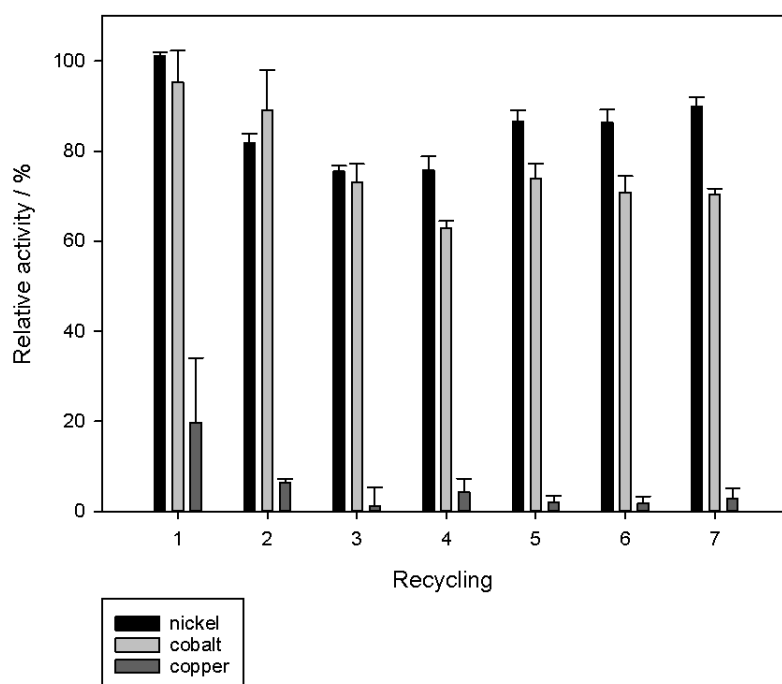


Figure 4.16: Relative activity of the immobilized β -amino acid aminotransferase, immobilized with nickel, cobalt and copper as affinity metal ions using 20 mg magnetic M-PVA beads for 7 recycling steps. 100 % relative activity refers to 0.81 U activity of the nickel immobilized aminotransferase. Biotransformation conditions: *rac*- β -phenylalanine, α -ketoglutarate, PLP at 30 °C in NaCO₃ buffer pH 9 and 950 rpm. Statistical error of n=3 experiments.

In figure 4.16, the relative activity is pictured for the recyclability of the immobilized β -amino acid aminotransferase with three different bivalent metal ions forming the chelate complex to immobilize via affinity to the enzyme. In section 4.1.5.1, it was mentioned that almost no activity remained after the second and third recycling step for the immobilized enzyme with copper. Activities between 0.05 and 0.02 U are shown for the second and third recycling step. In contrast, the immobilized aminotransferase with nickel and copper shows high activity even after 7 recycling steps. The activity of the nickel immobilized enzyme is 0.81 U at 100 % for the first step. After seven recycling cycles the activity remains at 0.72 U (85 %). After immobilization with cobalt, the enzyme shows an activity of 0.76 U for the first cycle, which correlates to 95 % relative activity corresponding to the highest activity reached for the immobilization with nickel ions. After seven recycling steps, the activity of enzyme immobilized with cobalt is 0.56 U and 70 % relative activity.

4.2 ASYMMETRIC SYNTHESIS OF β -AMINO ACIDS

Asymmetric synthesis catalyzed by a β -amino acid aminotransferase starts with a prochiral ketone and an amino donor (see figure 1.3 (a)). It is possible to achieve a yield of 100 %, but high enantiomeric selectivity is necessary for a high ee value. The equilibrium of this reaction is often completely on the substrate side. Hence, the choice of a suitable amino donor and

acceptor is important to shift the equilibrium toward the side of the product. The amino donor could convert to the ketone byproduct which is volatile or the ketone byproduct could be removed from the reaction, leading to a shift of the equilibrium. Furthermore, immediate removal of the product could be a possibility to increase the yield. One major challenge in asymmetric synthesis of β -amino acids is the instable, spontaneously decarboxylating prochiral ketone as a substrate.

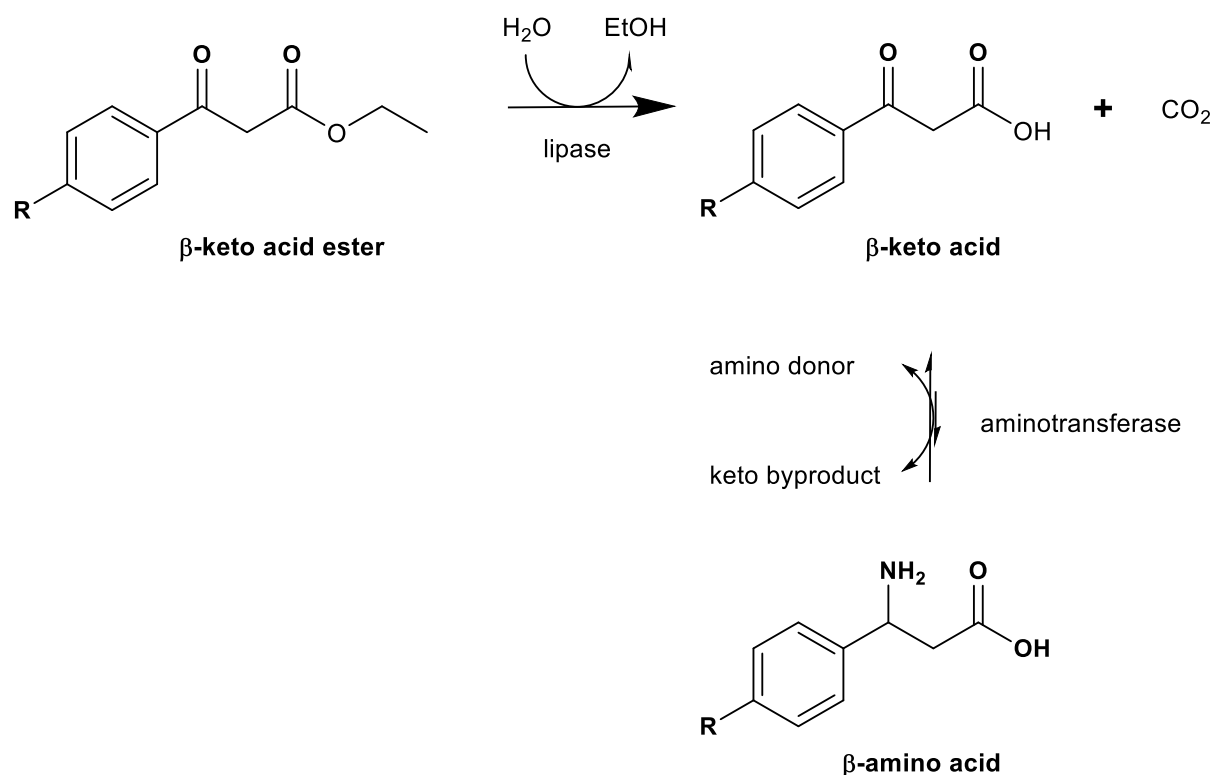


Figure 4.17: Enzyme cascade for the asymmetric synthesis of β -amino acids.

Therefore, an enzyme cascade needs to be established: starting with a β -keto acid ester hydrolyzed by a lipase (figure 4.17). The freshly prepared intermediate, the β -keto acid, acts as the substrate for the aminotransferase, to produce β -amino acids.

4.2.1.1 Hydrolysis of β -keto acid esters

As a first attempt, β -keto acid esters with different residues were catalyzed by a lipase from *Thermomyces lanuginosus*, *Rhizomucor miehei* and *Candida rugosa*. The β -keto acid esters with F, Cl, NO_2 and CH_3 as a residue next to the phenyl ring were converted.

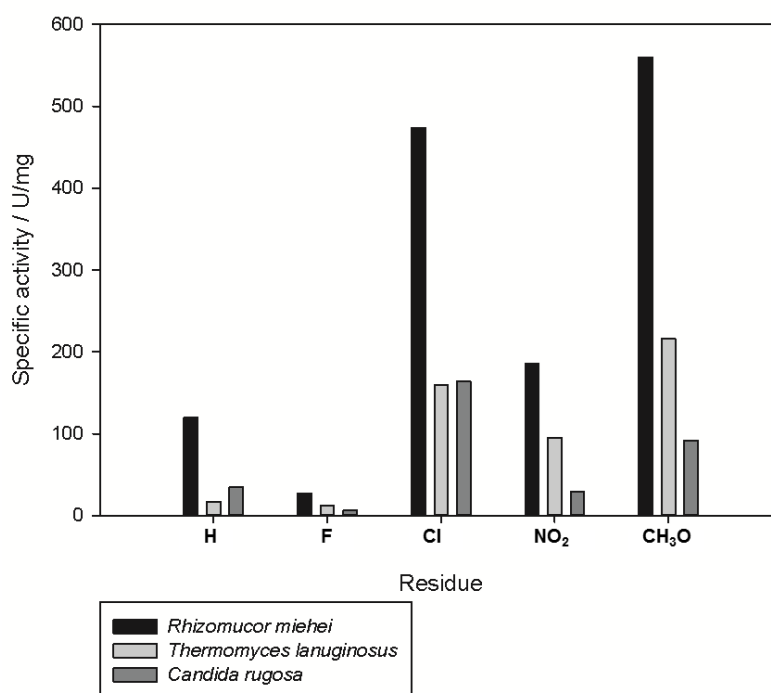


Figure 4.18: Specific activity of the lipase from *Rhizomucor miehei*, *Thermomyces lanuginosus* and *Candida rugosa* toward various β -keto acid esters with different moieties. The lipase was dissolved in 2.5 mM NaPP buffer, pH 7, with 2 mM β -keto acid ester (for the ester with residue NO₂ and Cl. 5%/10% DMSO was added) at 30 °C.

The three lipases showed activity toward the β -keto acid esters with different moieties at the phenyl ring, shown in figure 4.18. The lipase from *Rhizomucor miehei* hydrolyses all β -keto acid esters. The highest specific activity of ~ 500 U/mg and 550 U/mg was determined with Cl and CH₃ as a moiety at the phenyl ring, respectively. The lipase from *Thermomyces lanuginosus* shows a low activity toward β -keto acid ester without a residue and for the ester with F as a residue. The lipase from *Candida rugosa* is active for the β -keto acid esters with no residue, with Cl as a residue, NO₂ and CH₃ as a residue, with activities of 36 U, 164 U, 29 U and 92 U respectively. For the other β -keto acid ester with F as a residue at the phenyl ring, only a low activity of 6 U was observed.

For hydrolysis of ethyl benzoylacetate (no residue) catalyzed by a lipase from *Candida rugosa*, the decrease in concentration, the increase in ethanol and the negative control (without lipase) was examined. The activity of the utilized enzyme was 1.2 U with 6 mM ethyl benzoylacetate. In this experiment, the biotransformation buffer was 100 mM NaCO₃ buffer pH 9, to stabilize the emerging 3-oxo-3-phenyl propionate (the β -keto acid ester) and to decelerate the decarboxylation. Furthermore, the immobilized aminotransferase shows high activity at pH 9. The reaction temperature was 30° C.

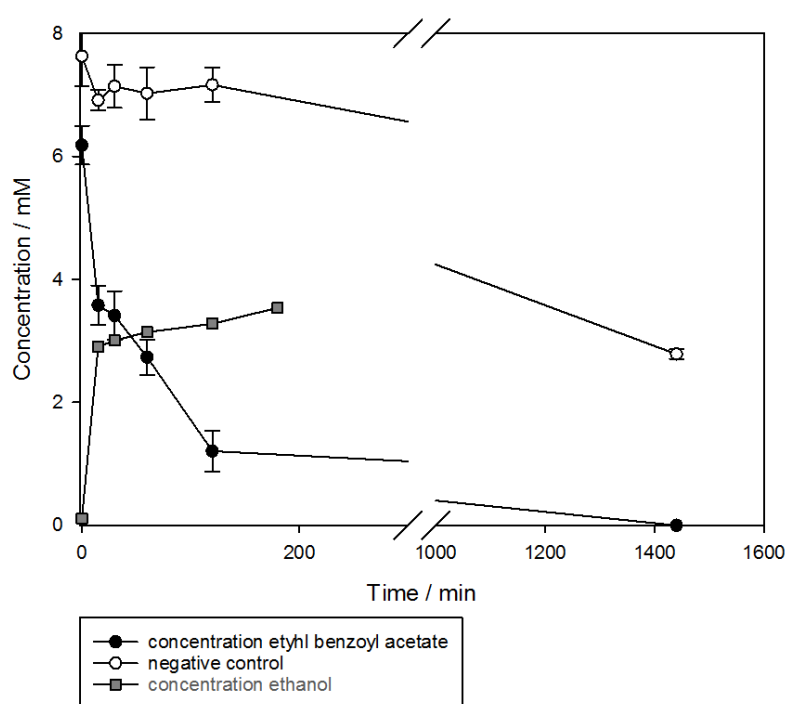


Figure 4.19: Conversion of ethyl benzoylacetate by a lipase from *Candida rugosa* (1.2 U) and the concentration of ethanol during the reaction. The biotransformation buffer was NaCO₃ buffer pH 9 and the reaction was performed at 30 °C. Statistical error of n=3 experiments.

The decrease of ethyl benzoylacetate through hydrolysis by a lipase from *Candida rugosa* is shown in figure 4.19. With utilization of 1.2 U of the lipase, ~2.5 mM of the substrate was converted after 15 min, whereas the concentration of ethanol increases to ~2.8 mM. After 120 min, the concentration of ethyl benzoylacetate decreases to ~1 mM, but the concentration of ethanol increases only to ~4 mM after 180 min. The negative control (without lipase) shows no conversion of ethyl benzoylacetate for the first 120 min, but it is shown that, after 24 h, the concentration significantly decreases to ~3 mM.

4.2.1.2 Asymmetric synthesis of β -amino acids via enzyme cascade

As illustrated in figure 4.17, the asymmetric synthesis of β -amino acids via an enzyme cascade was conducted with two different lipases (lipase from *Rhizomucor miehei* and from *Candida rugosa*) and two amino donors (3-aminobutanoic acid and (S)/(R)-methylbenzylamine). These two amino donors were chosen because 3-aminobutyric acid converts to an intermediate after amino group transfer and the intermediate decarboxylates to acetone. Methylbenzylamine converts to acetophenone (see figure 4.20).

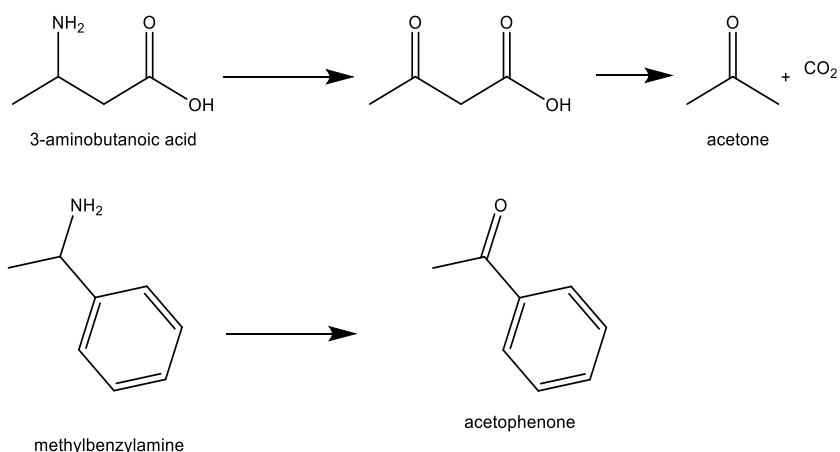


Figure 4.20: Amino donors for asymmetric synthesis of β -amino acids.

Acetone is a volatile ketone and acetophenone could not be utilized as amino donor because it is not able to bind to the active site of the enzyme (described in section 5.1.3.3 and 5.2.2), this favors the shift of the equilibrium toward product side. The next reaction step the transamination is catalyzed by the β -amino acid aminotransferase (immobilized on magnetic M-PVA beads using 20 mg beads with an activity of 1 U and crude cell extract with 1 mg protein). The lipase (RML) had an activity of 1.2 U and the reaction was conducted in NaCO_3 buffer, pH 9, which included PLP. The crude cell extract was utilized in a protein concentration of 1 mg/ml.

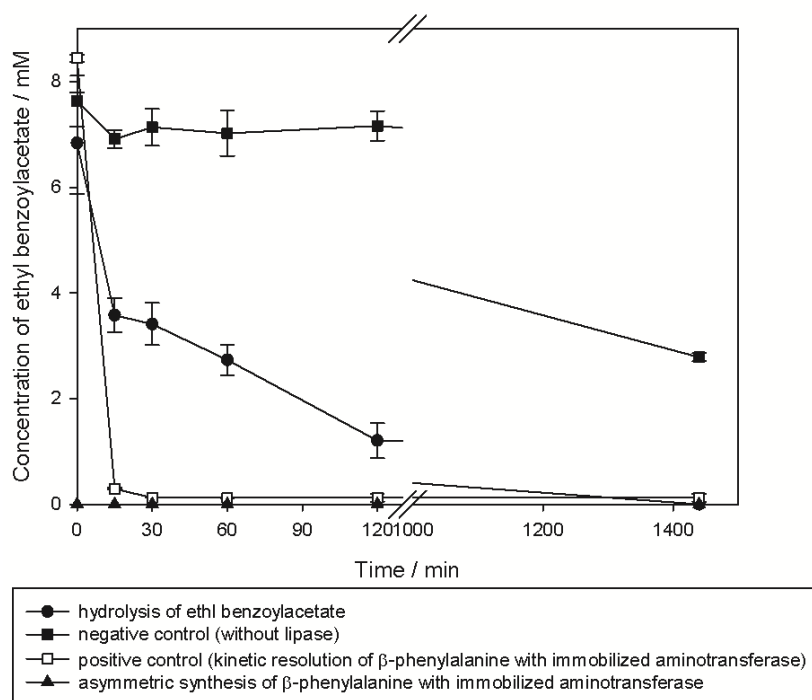


Figure 4.21: Concentration of ethyl benzoylacetate and β -phenylalanine synthesized via asymmetric synthesis, in an enzyme cascade with a lipase from *Rhizomucor miehei* and a β -amino acid aminotransferase. A negative control is shown without lipase and a positive control to test whether the aminotransferase is active. The biotransformation was conducted in NaCO_3 buffer, pH 9, with (*R*)/(*S*)-methylbenzyl amine amino donors and extra PLP at 30 °C and 950 rpm. The crude cell extract was utilized in a protein concentration of 1 mg/ml. Statistical error of n=3 experiments.

The asymmetric synthesis in an enzyme cascade was conducted in several experiments. In the first half of the reaction, the hydrolysis of the β -keto acid ester is successfully performed as described in section 4.2.1.1. In the second half of the reaction, the transamination of the freshly prepared β -keto acid intermediate was performed with several amino donors and with immobilized aminotransferase and crude cell extract. Figure 4.21 illustrates the asymmetric synthesis of β -amino acids via an enzyme cascade. The synthesis was conducted with 1.2 U lipase, 6 mM ethyl benzoylacetate in 10 % DMSO, 125 mM of amino donor ((*R*)/(*S*)-methylbenzylamine), 1 U immobilized transaminase, 1 mM PLP in 100 mM Tris/HCl buffer, pH 8, at 30° C and 950 rpm. The conversion of ethyl benzoylacetate hydrolyzed with the lipase is pictured with a black circle. No synthesis of β -amino acids is demonstrated for asymmetric synthesis with the immobilized aminotransferase (black triangle). The conversion of (*S*)- β -phenylalanine was tested via kinetic resolution with the utilized immobilized aminotransferase to confirm its activity (white squares). Hence, the ethyl benzoylacetate is converted to the intermediate β -keto acid, but no further conversion to β -amino acid is shown for the active immobilized aminotransferase. Furthermore, asymmetric synthesis with the reaction conditions was conducted with the crude cell extract for the transamination of the keto acid with no synthesis of β -phenylalanine as well.

Furthermore, 3-aminobutanoic acid was utilized as amino donor and still no synthesis of β -amino acids was observed. The aminotransferase was used either in the immobilized or in crude cell extract. The activity of the aminotransferase in the presence of DMSO was investigated as well and no loss in activity is shown for DMSO concentrations up to 20 % (figure 7.4 in Appendix 7.5). The reaction was also conducted in Tris/HCl buffer, pH 8 which exhibited the results as shown in figure 4.21.

4.2.1.3 Asymmetric synthesis of β -amino acids with 3-oxo-3-phenyl propionate

The asymmetric synthesis of β -amino acid is challenging due to the unstable substrate, namely the β -keto acid (3-oxo-3-phenyl propionate). To gain further understanding of the stability of this unstable substrate, a wavelengths scan was conducted after 0 h, 1 h and 24 h. The substrate depicted in figure 4.17 (without a residue) will convert to acetophenone after decarboxylation.

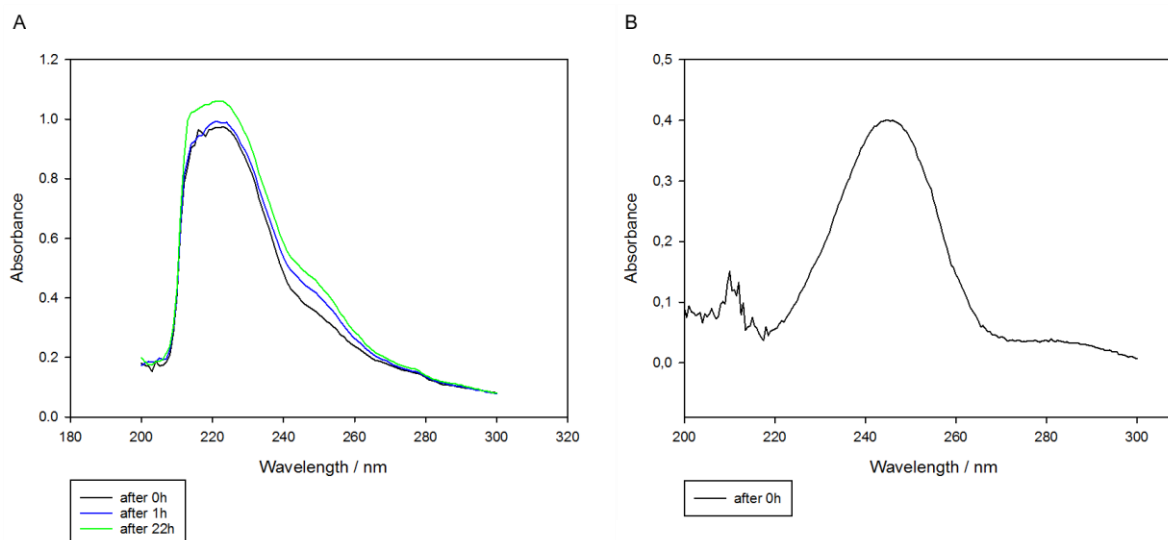


Figure 4.22: Wavelengths scan of 3-oxo-3-phenyl propionate A and acetophenone B.

The wavelengths scans of 3-oxo-3-phenylpropionate (A) and acetophenone (B) are shown in figure 4.22. At 0 h, the β -keto acid shows a peak at \sim 221 nm, after 1 h, another slight peak at \sim 250 nm emerges (figure A). This peak at 250 nm may correlate to the absorption peak of acetophenone which has its absorption peak at 250 nm (see figure 4.22 B). The same shift of absorption maximum illustrated for 3-oxo-3-phenylpropionate after 22 h, is shown after incubating at 90° C for 10 min and after freezing and thawing. This is leading to the assumption that no significant change in absorption can be determined for 3-oxo-3-phenylpropionate.

The asymmetric synthesis starting with the prochiral ketone 3-oxo-3-phenyl propionate was not successful (figure 7.5, Appendix 7.6). No conversion of the substrate was observed after 2 h and no β -phenylalanine is produced with the immobilized aminotransferase. A positive control via kinetic resolution of β -phenylalanine with the immobilized enzyme was carried out

for every experiment. The substrate was utilized in a concentration of ~10 mM with 20 mM 3-aminobutyric acid as amino donor, 1 U of the immobilized aminotransferase and 1 mM PLP. The asymmetric synthesis starting with 3-oxo-3-phenyl propionate was conducted as well with isopropylamine, glutamate and alanine as amino donors, but neither conversion of the substrate nor the production of the product was observed.

4.3 CHARACTERIZATION OF TRANSAMINASE ACTIVITY OF *BURKHOLDERIA PHYTOFIRMANS* SPEC.

Several bacterial strains for their activity to convert β -amino acids were examined in 2011 [67]. The strain BS115 showed activity exclusively toward the (S)-enantiomer of *rac*- β -phenylalanine. The enzyme which is responsible for the conversion of (S)- β -phenylalanine is assumed to be a transaminase due to its dependency on PLP as a cofactor and α -ketoglutaric acid as amino acceptor. The strain BS115 showed a 99 % homology to the β -proteobacterium *Burkholderia phytofirmans* strain PsJN. Furthermore, the genome of the latter strain was completely sequenced by Weilharter in 2011 [109]. The aim of this work is to characterize the transaminase activity of the strain BS115 and to purify the corresponding enzyme. The enzyme can be utilized in biotechnological processes for the production of β -amino acids as compounds in peptidomimetics or other drug components. Furthermore, no details are known so far about the consumption of β -amino acids in bacterial strains and the expression of the enzymes which are able to metabolize them. Regarding these aspects, the strain BS115 was cultivated in shaking flask and via fermentation with *rac*- β -phenylalanine as sole nitrogen source and glucose as carbon source. Fermentation is also necessary to gain more protein for the purification of the transaminase out of the crude cell extract. Furthermore, the substrate scope and the accepted amino acceptors for kinetic resolution were investigated. Additionally, first steps were conducted to purify the transaminase, via enrichment of the enzyme by ammonium sulfate precipitation and ion exchange chromatography.

For all experiments conducted in this work the transaminase activity had to be induced by adding β -phenylalanine to the preculture. If no β -phenylalanine was added, neither growth of the strain BS115 (with β -phenylalanine as sole nitrogen source) nor activity toward β -amino acids was observed.

4.3.1 Cultivation of *Burkholderia phytofirmans spec.* with β -amino acid as nitrogen source

The cultivation of the *Burkholderia phytofirmans* strain BS115 was conducted in shaking flasks with minimal medium (composition as described in section 3.4.3.2). *Rac*- β -phenylalanine was utilized as sole nitrogen source while glucose served as carbon source. As amino donor for the conversion of β -amino acids α -ketoglutarate was added, as well as PLP serving as a cofactor. The shaking flasks were incubated at 30° C and 120 rpm and samples were taken at given times (see figure 4.23). Several concentrations of *rac*- β -phenylalanine and glucose were investigated and the specific growth rate (μ /h), the consumption rate (R) for (*R*)- and (*S*)- β -phenylalanine (R_R , R_S and R_{Glc}) and glucose were calculated.

In shaking flask experiments it was shown that acetophenone and *rac*- β -phenylalanine could serve as a carbon source as well. This is depicted in figure 7.7. The strain BS115 was cultivated with ammonium sulfate as nitrogen and acetophenone (2.5 mM) as carbon source whereby an OD₆₀₀ of 0.5 was reached. With 5 mM *rac*- β -phenylalanine an OD₆₀₀ of 1 was achieved. Hence, not only glucose serves as a carbon source for the cultivations, of the cultivations shown in this chapter.

Figure 4.23 illustrates the shaking flask experiments with different concentrations of *rac*- β -phenylalanine (β -Phe) and glucose (Glc). For the experiment with 5 mM *rac*- β -phenylalanine and 20 mM glucose (figure 4.23 A) the exponential growth phase is between 5 h and 20 h. After ~20 h the (*S*)-enantiomer is completely consumed and the (*R*)-enantiomer is utilized as nitrogen source. The glucose is completely consumed at ~30 h and limits further growth. The concentration of acetophenone is increasing in the first ~30 h to 1.5 mM, after 30 h its concentration decreases rapidly to 1 mM. Acetophenone is a product for the conversion of (*S*)- β -phenylalanine (reaction is illustrated in figure 4.1).

As the concentration of *rac*- β -phenylalanine was increased to 10 mM, the exponential growth of strain BS115 ended after complete consumption of the (*S*)-enantiomer (figure 4.23 B). At this time, the glucose is completely consumed as well and no conversion of the (*R*)-enantiomer is observed. The starting glucose concentration in this experiment stayed the same, but it is illustrated that the glucose is consumed faster during this cultivation compared to cultivation with 5 mM *rac*- β -phenylalanine (figure 4.23 A). The concentration of acetophenone increases to 2 mM during the exponential growth. After the stationary phase is reached, the concentration decreases to ~1 mM.

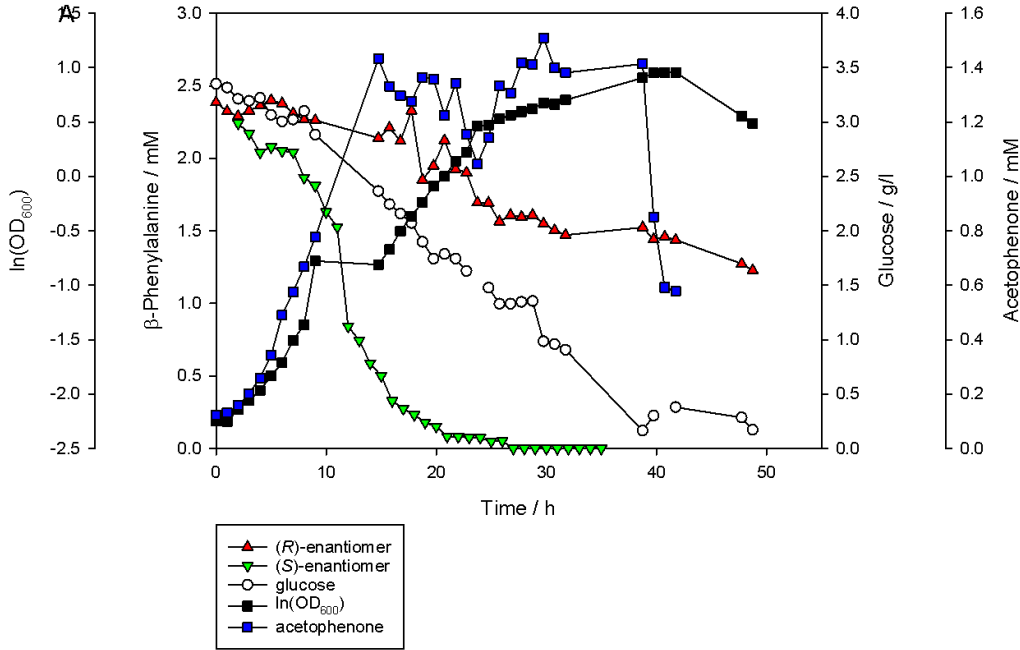
Another raise of *rac*- β -phenylalanine concentration to 20 mM is illustrated in figure 4.23 C. The (*S*)-enantiomer is completely consumed after 21 h, however no decrease of the concentration of the (*R*)-enantiomer is illustrated, since the glucose is completely consumed after 25 h and

(*S*)- β -phenylalanine is still available in the culture medium. Acetophenone concentration increases to 3 mM in 20 h and decreases to 1 mM after the growth is limited.

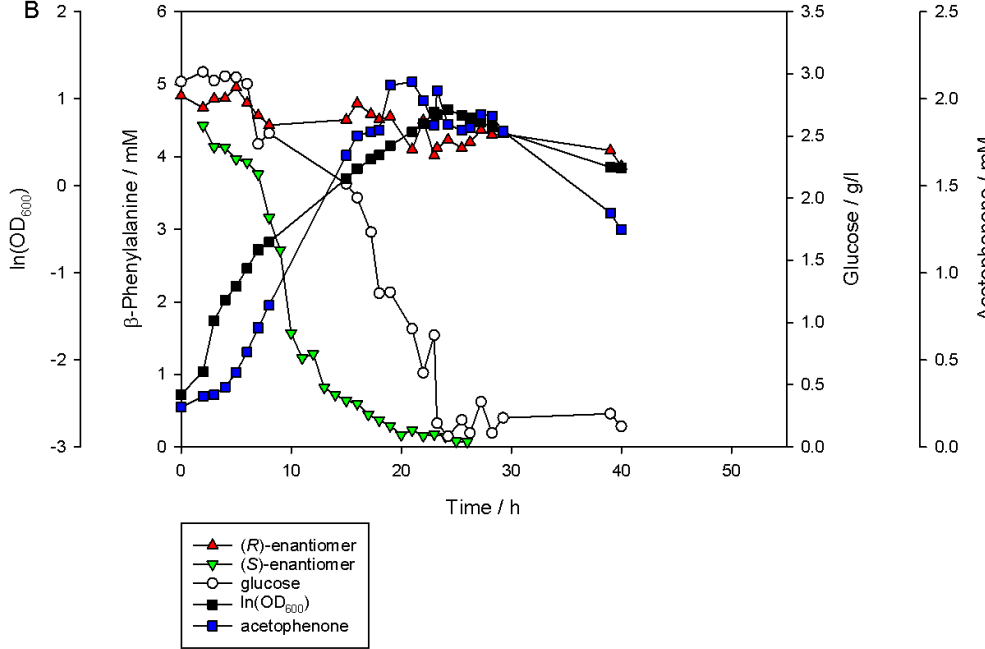
To elongate the growth phase by preventing lack of carbon and to determine the conversion of the (*R*)-enantiomer after complete consumption of the (*S*)-enantiomer, the glucose concentration was increased to 100 mM, whereas the *rac*- β -phenylalanine concentrations stayed at 10 mM (illustrated in figure 4.23 D). Exponential growth is observed between 5 h and ~30 h. After 30 h the (*S*)-enantiomer is completely converted and the concentration of the (*R*)-enantiomer decreases from 5 mM to 3.5 mM. The growth is not limited by the glucose. Corresponding acetophenone increases to 2 mM after 30 h and decreases afterwards to 1.5 mM. The stationary phase is reached at ~30 h, even though glucose is still in the medium and the (*R*)-enantiomer is not completely consumed as well.

The maximal growth rate (μ_{max}), overall consumption rate of (*R*)- and (*S*)- β -phenylalanine and glucose, as well as the maximal OD₆₀₀ and the doubling time (t_d) for all shaking flask experiments and fermentation are shown in table 4.4 in chapter 4.3.2.

M1 (5 mM *rac*- β -phe + 20 mM Glc)



M1 (10 mM *rac*- β -Phe+20 mM Glc)



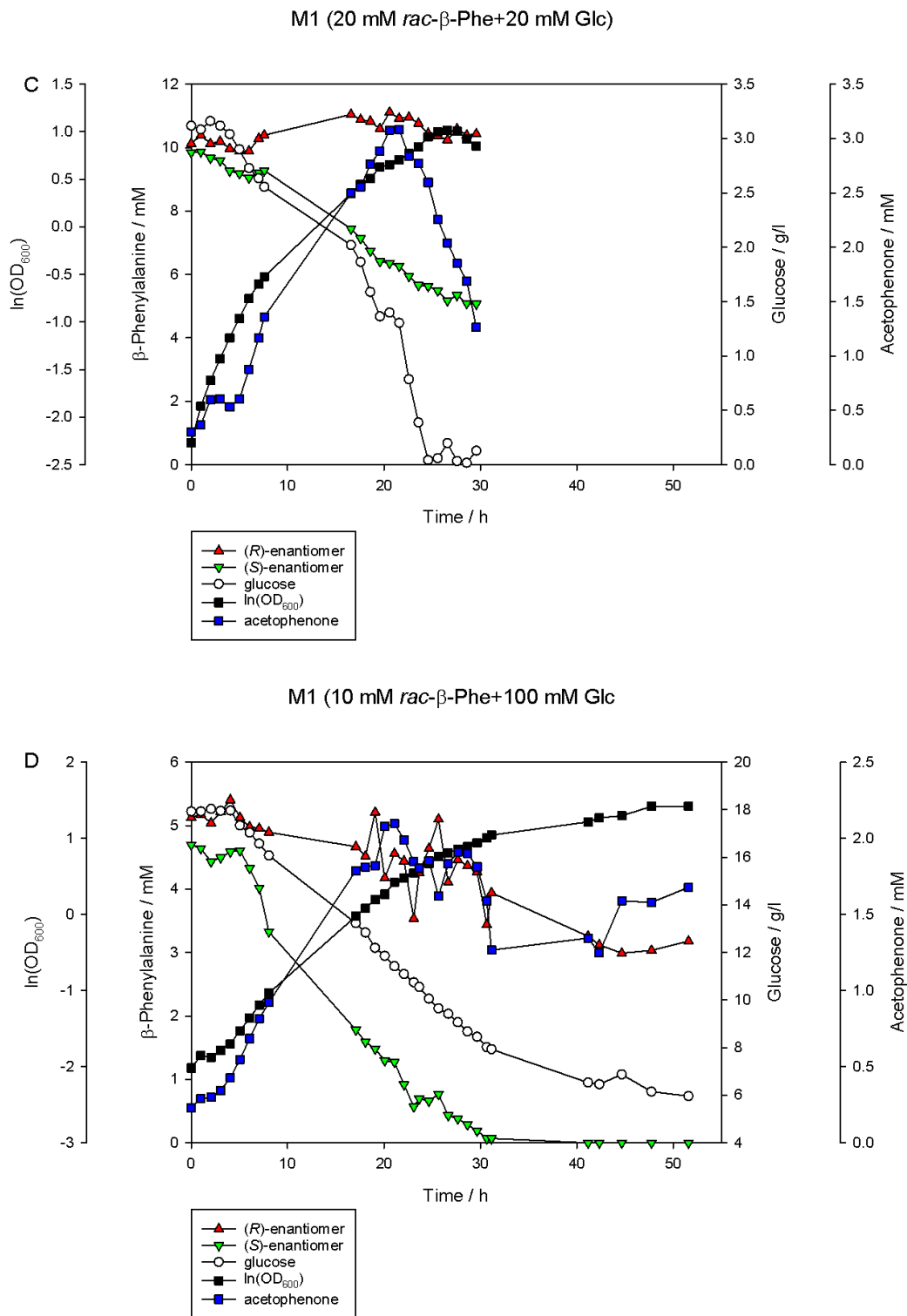


Figure 4.23: Shaking flask experiments with *rac*- β -phenylalanine as sole nitrogen and glucose as the carbon source. The experiments were conducted at 30 °C and 120 rpm. The concentration of β -phenylalanine was determined via HPLC, the glucose concentration with a glucose assay kit, acetophenone was determined via photometer measurements at 250 nm. Several concentrations of the *rac*- β -phenylalanine and glucose were utilized.

4.3.2 Fermentation of *Burkholderia phytofirmans spec.*

The fermentation of the *Burkholderia phytofirmans* strain BS115 was performed in a benchtop reactor (Minifors, Infors) with a total volume of 1 l in minimal medium containing 10 mM *rac*- β -phenylalanine, 5 mM α -ketoglutarate, 100 mM glucose and extra PLP. The preculture was prepared in minimal medium and the expression of the transaminase able to convert β -amino acids is induced with *rac*- β -phenylalanine. The temperature was set to 30° C, air flow was 1 lpm and the stirrer was set to 120 rpm. The pH and pO_2 were not controlled during the reaction. The experiment was conducted in a triplicate.

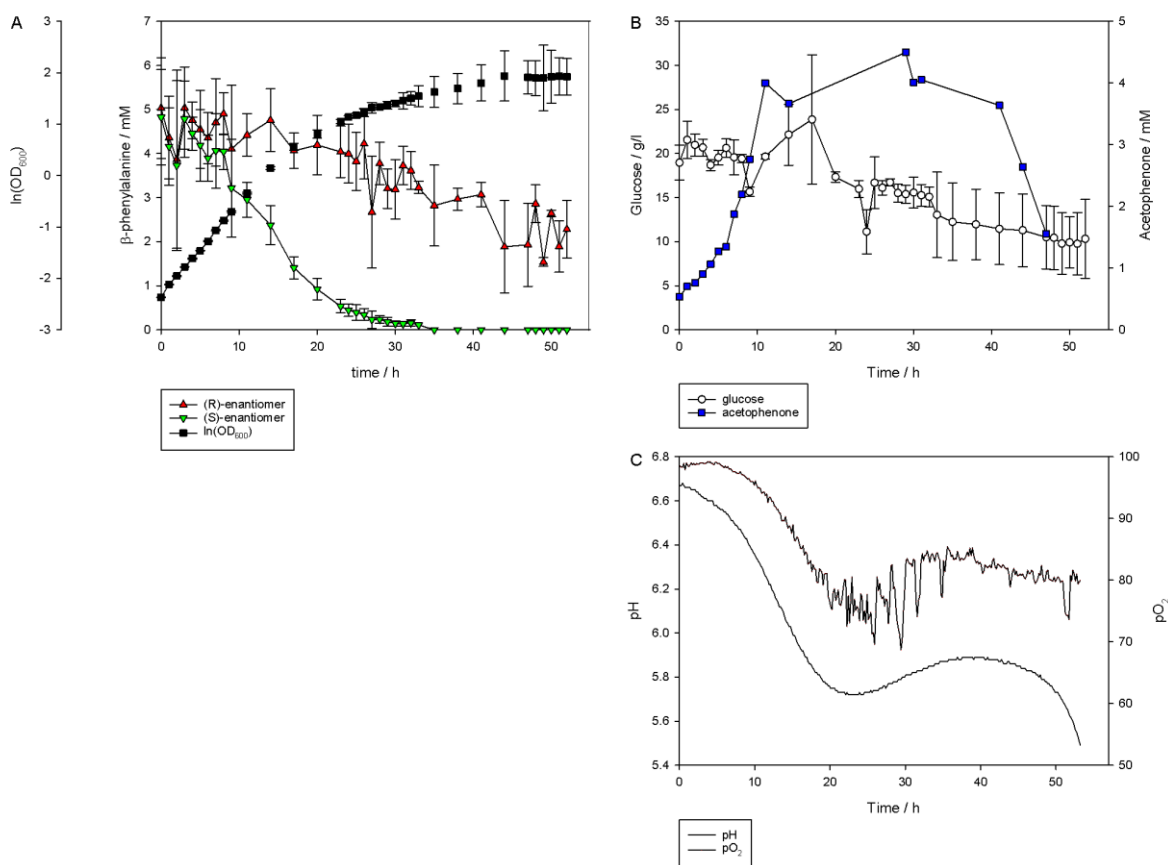


Figure 4.24: Fermentation of *Burkholderia phytofirmans* strain BS115 in minimal media containing 10 mM *rac*- β -phenylalanine, 5 mM α -ketoglutarate, 100 mM glucose and PLP. The temperature was set to 30° C and the stirrer to 120 rpm. The air flow was 1 lpm during the reaction time. A shows the $\ln(OD_{600})$, concentration of (R)- and (S)- β -phenylalanine, concentration of glucose and acetophenone are shown in B. In C, pH and pO_2 are pictured. Statistical error of $n=3$ experiments.

The fermentation is illustrated in figure 4.24. Exponential growth is observed between 0 h and 21 h, the growth is not limited since (S)- β -phenylalanine serves as a nitrogen source. The (S)- β -phenylalanine is completely consumed after 21 h and the (R)-enantiomer serves as the nitrogen source. But only 3 mM is consumed, until the stationary phase is reached at ~55 h. Concentrations of acetophenone and glucose are pictured in figure 4.24 B. Glucose decreases over time, but 5-10 g/l are still remaining in the medium after the stationary phase is reached. Acetophenone concentration increases to 4.5 mM in the first 30 h of fermentation, hereafter

the concentration decreases to 1.5 mM. In figure 4.24 C, the pH and pO₂ are illustrated over time. The pH decreases, starting from pH 7 to pH 5.8 in the first 21 h. Between 21 h and 45 h, the pH increased to 5.8. The pO₂ decreases from 100 % to 75 % in the first 21 h and increases to 85 % in the next 19 h.

In the following table 4.5, the maximal specific growth rate (μ_{\max}), the doubling time (t_d), the consumption rate of (*R*)- β -phenylalanine (R_R), (*S*)- β -phenylalanine (R_S) and of glucose (R_{Glc}) and the maximal OD at 600 nm are shown for the shaking flask experiments and the fermentation. All data were calculated with the formula shown in chapter 3.2.4.

Table 4.5: Comparison of μ_{\max} / h, t_d / h, the consumption rates of (*R*)- β -phenylalanine / g/h (R_R), (*S*)- β -phenylalanine / g/h (R_S) and of glucose / g/h (R_{Glc}) and the maximal OD at 600 nm for shaking flask experiments (SF) and fermentation (Fer) of *Burkholderia phytofirmans* strain BS115.

		μ_{\max} / h	t_d / h	R_R / g/h	R_S / g/h	R_{Glc} / g/h	OD _{600 max}
SF 1	5 mM β -Phe + 20 mM Glc	0.10	6.61	0.00	0.01	0.07	1.74
SF 2	10 mM β -Phe + 20 mM Glc	0.13	5.33	0.00	0.02	0.07	2.34
SF 3	20 mM β -Phe + 20 mM Glc	0.14	5.15	0.00	0.02	0.10	2.76
SF 4	10 mM β -Phe + 100 mM Glc	0.11	6.49	0.01	0.02	0.23	4.14
Fer ^{a)}	10 mM β -Phe + 100 mM Glc	0.17	4.23	0.01	0.02	0.15	8.35

^{a)} conducted in a triplicate, mean value derived out of three experiments

Comparing the shaking flask experiments (SF) and the fermentation (Fer) (table 4.5), it is shown that the highest growth rate of 0.17 / h and a doubling time of 4.23 / h were achieved via fermentation with the maximal OD₆₀₀ of 8.35. For the fermentation the consumption rate of (*R*)- β -phenylalanine is 0.01 g/h and 0.02 g/h of the (*S*)-enantiomer are consumed. The highest consumption rate of glucose is shown for SF 4 with 0.23 g/h. In the experiment SF 1, SF 2 and SF 3 the consumption rate of (*R*)- β -phenylalanine is 0. Furthermore, the consumption rate of glucose increases with higher *rac*- β -phenylalanine and higher glucose concentrations. For the shaking flask experiments SF 2, SF 3 and SF 4 and for the fermentation, the same consumption rate for (*S*)- β -phenylalanine of 0.02 g/h is observed. For the experiment with 5 mM *rac*- β -phenylalanine the consumption rate of (*S*)- β -phenylalanine is 0.01 g/h.

Centrifugation of the samples revealed a white viscous phase for every sample which was taken after the (*S*)- β -phenylalanine was completely consumed. Furthermore, this viscous phase increased in all further samples that were taken. To characterize this viscous phase, the bacteria culture was stained with ink after 72 h cultivation time and investigated using phase-contrast microscope.



Figure 4.25: Negative contrast of an ink-stained bacteria cell culture (*Burkholderia phytofirmans* strain BS115) under phase-contrast microscope. The bright spot is the encapsulated bacterial cell.

The negative contrast of a bacteria cell after ink-staining is shown in figure 4.25. An encapsulated *Burkholderia phytofirmans* cell (bright spot) is shown with a length of ~6.5 μm .

4.3.3 Substrate scope and choice of amino acceptor to characterize the transaminase activity of *Burkholderia phytofirmans spec.*

Various amino donors (β -amino acids) were utilized to investigate the substrate scope of the *Burkholderia phytofirmans* strain BS 115. The cells were disrupted and the experiments were performed with crude cell extract (0.2 mg/ml). For investigating the substrate scope, α -ketoglutarate (5 mM) was used as amino donor. The reaction was conducted at 30° C in 50 mM Tris buffer (pH 8) for 24 h. The concentration of amino donor was 10 mM of the racemate, except for *rac*- β -(Cl)PA, *rac*- β -(F)PA, *rac*- β -(Br)PA, 2 mM were utilized due to the low solubility in aqueous solutions. As a control experiment, the reaction was conducted without crude cell extract and no change of amino donor concentration was observed (data not shown).

Table 4.6: Transaminase substrate scope (amino donor) of the *Burkholderia phytofirmans* strain BS115.

Entry	Amino donor	Rel. activity / % ^{a)}	Conversion / % ^{b)}	ee / % ^{b)}
1	<i>rac</i> - β -PA	100.0	46.3	>99 (R)
2	<i>rac</i> - β -hPA	-	-	-
3	<i>rac</i> - β -(Cl)PA	19.0	47.2	>99 (R)
4	<i>rac</i> - β -(F)PA	61.3	48.0	>99 (R)
5	<i>rac</i> - β -(Br)PA	28.0	53.2	>99 (ND)
6	<i>rac</i> - β -(NO ₂)PA	34.6	51.3	>91 (ND)
7	<i>rac</i> - β -(COH)PA	46.3	50.8	>96 (ND)
8	(S)- β -(OH)PA	69	100	>99 (R)

^{a)} relative activity was determined after 30 min of reaction

^{b)} conversion rates and ee were determined after 24 h of reaction

ND not determined

The activity toward *rac*- β -phenylalanine (entry 1) refers to 100 % with 0.23 U/mg, shown in table 4.6. Conversion rate of the racemate is ~50 % for all investigated amino donors and ~100 % for entry 8 after 24 h, except for entry 2, where no conversion can be observed at all. Best relative activities are shown for entry 4, entry 7 and entry 8 with 61.3 %, 46.3 % and 69 %, respectively. The enantioselectivity of the enzyme is determined for all amino donors and strict conversion of the (*S*)-enantiomer is observed. High *ee* values for all converted amino donors are achieved with >99 % for entry 1, entry 3, entry 4, entry 5 and entry 8. Slightly lower *ee*'s are shown for entry 6 and entry 7 with 91 % and 96 %, respectively. The specific activity was determined after 30 min to guarantee the conversion with substrate saturation. The conversion rate was calculated after 24 h.

Additionally, several amino acceptors were tested for kinetic resolution of *rac*- β -phenylalanine as amino donor. The acceptance of the transaminase from the *Burkholderia phytofirmans* strain BS115 for the amino acceptors may give information to classify the enzyme. Five keto acids were chosen: α -ketoglutarate, pyruvate, oxaloacetate, acetone and acetophenone. The biotransformation was conducted in 50 mM Tris buffer, pH 8, with 0.2 mg/ml crude cell extract at 30° C for 24 h. As a negative control, biotransformation without crude cell extract was conducted and no concentration change is observed after 24 h (data not shown).

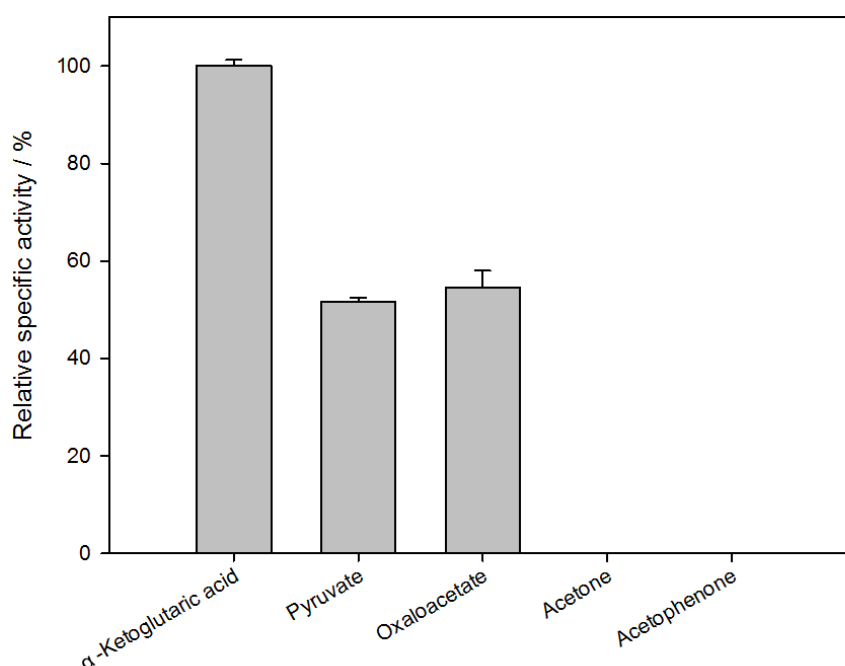


Figure 4.26: Relative activity of transaminase from the *Burkholderia phytofirmans* strain BS115 with *rac*- β -phenylalanine as amino donor and α -ketoglutarate, pyruvate, oxaloacetate, acetone and acetophenone. 100 % activity refers to 0.2 U/mg for α -ketoglutarate as amino acceptor. The biotransformation was performed with 10 mM *rac*- β -phenylalanine and 5 mM amino acceptor at 30° C in 50 mM Tris buffer pH 8 for 24 h. Errors bars of n=2 experiments.

The relative activity of the transaminase from *Burkholderia phytofirmans* strain BS115 with *rac*- β -phenylalanine as amino donor and α -ketoglutarate, pyruvate, oxaloacetate, acetone and acetophenone is shown in figure 4.26. Relative activity of 100 % refers to 0.2 U/mg for kinetic resolution with α -ketoglutarate. Relative activities of ~ 50 % are illustrated for pyruvate and oxaloacetate as amino acceptors. Acetone and acetophenone are not accepted as amino acceptors for this transaminase which shows no activity at all.

The enzyme exhibiting transaminase activity was purified for further characterization. This was conducted via ammonium sulfate precipitation and anion exchange chromatography, described in the following section.

4.3.4 Protein enrichment via ammonium sulfate precipitation

The first step for enzyme purification is enrichment via ammonium sulfate precipitation. Ammonium sulfate solution (3.8 M) was kept at 4° C during the precipitation and titrated by using a burette. The crude cell extract was stored on ice for the experiment and stirred for 10 min for every state of ammonium sulfate saturation. Subsequently, the pellet was centrifuged and dissolved in 50 mM Tris/HCl buffer, pH 8 with PLP added. The cultivation of the strain BS115 was performed via shaking flask or fermentation and the cultivation broth was disrupted by sonication. The specific activity was determined via biotransformation with 10 mM *rac*- β -phenylalanine, 5 mM α -ketoglutarate, extra PLP and 0.2 mg/ml crude cell extract at 30° C for 24 h. The first ammonium sulfate precipitation was conducted with 25 %, 50 %, 75 % and 95 % saturation (data not shown). For further investigations the saturation range was widened to 25 %, 35 %, 45 %, 55 %, 75 % and 95 %.

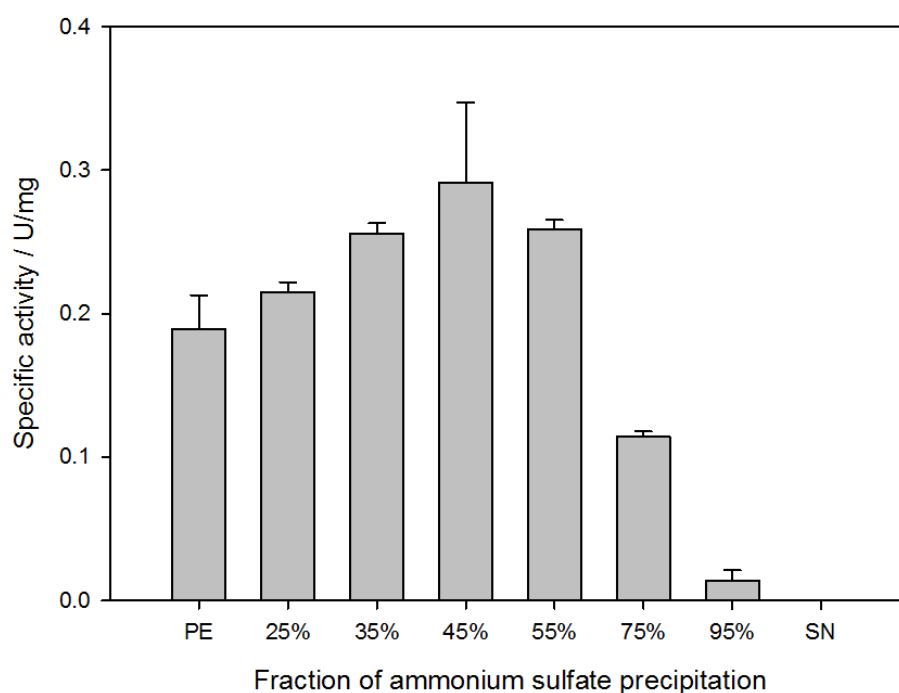


Figure 4.27: Specific activity of the fractions of ammonium sulfate precipitation. The saturations of 25 %, 35 %, 45 %, 55 %, 75 % and 95 % of ammonium sulfate solution were titrated. Furthermore, the activities of the crude cell extract (PE) and the supernatant (SN) after precipitation with 95 % saturation was determined. Biotransformation conditions: 10 mM rac- β -phenylalanine, 5 mM α -ketoglutarate, 0.2 mM PLP, 0.2 mg/ml protein in 50 mM Tris/HCl buffer pH 8 at 30° C. Specific activity was determined after 30 min reaction time. Statistical errors of n=2 experiments.

The specific activity of the dissolved pellets after ammonium sulfate precipitation is illustrated in figure 4.27. The crude cell extract shows a specific activity of 0.19 U/mg. With 25 % saturation, the specific activity is slightly higher with 0.215 U/mg. The highest specific activity was determined with 35 %-55 % saturation, of 0.25 U/mg, 0.291 U/mg and 0.265 U/mg, respectively. With 75 % saturation, the specific activity decreases to 0.13 U/mg and at 95 % saturation a specific activity of 0.014 U/mg is shown. The supernatant with 95 % saturation shows no activity at all.

For quantification of enzyme purification, the total activity, protein content, specific activity recovery and purification factor are illustrated in table 4.7.

Table 4.7: Quantification of enzyme purification via ammonium sulfate precipitation. Ammonium sulfate saturation is shown in %. PE is the crude cell extract without ammonium sulfate.

	Total activity / U	Protein content / mg	Specific activity / U/mg	Recovery / %	Purification fold
PE	21.38	113.13	0.189	100	1
25 %	0.21	0.99	0.215	1	1.14
35 %	4.11	16.05	0.256	19.22	1.35
45 %	3.64	12.51	0.291	17.03	1.54
55 %	3.1	11.97	0.259	14.5	1.37
75 %	2	17.56	0.114	9.36	0.6
95 %	0.01	0.67	0.014	0.04	0.07

The highest specific activity of 0.256 U/mg, 0.291 U/mg and 0.259 U/mg is shown with 35 %-55 % ammonium sulfate saturation. The highest recovery of 19.22 %, 17.03 % and 14.5 % is achieved for the fractions with 35 %-55 % ammonium sulfate saturation, respectively. Moreover, the highest purification with 1.35, 1.54 and 1.37 is also achieved with 35 %-55 % ammonium sulfate saturation. For further purification of the enzyme with transaminase activity from the *Burkholderia phytofirmans* strain BS115, the fractions with 35 %-55 % ammonium sulfate saturation were combined and anion exchange chromatography was conducted using an ÄKTAEplorer.

4.3.5 Protein enrichment via anion exchange chromatography

For purification of transaminases anion exchange chromatography (AEX) is described as a standard method like the ammonium sulfate precipitation. The pooled fractions with 35 %-55 % ammonium sulfate saturation were dialyzed with a Slight-a Lyzer™ Mini Dialysis Device with 50 mM Tris/HCl buffer pH 6.8 containing 0.2 mM PLP. Subsequently, the transaminase was purified via anion exchange chromatography. Elution of the enzyme was performed with a linear gradient from 0–0.4 M NaCl (1 M NaCl dissolved in 50 mM Tris/HCl buffer, pH 6.8).

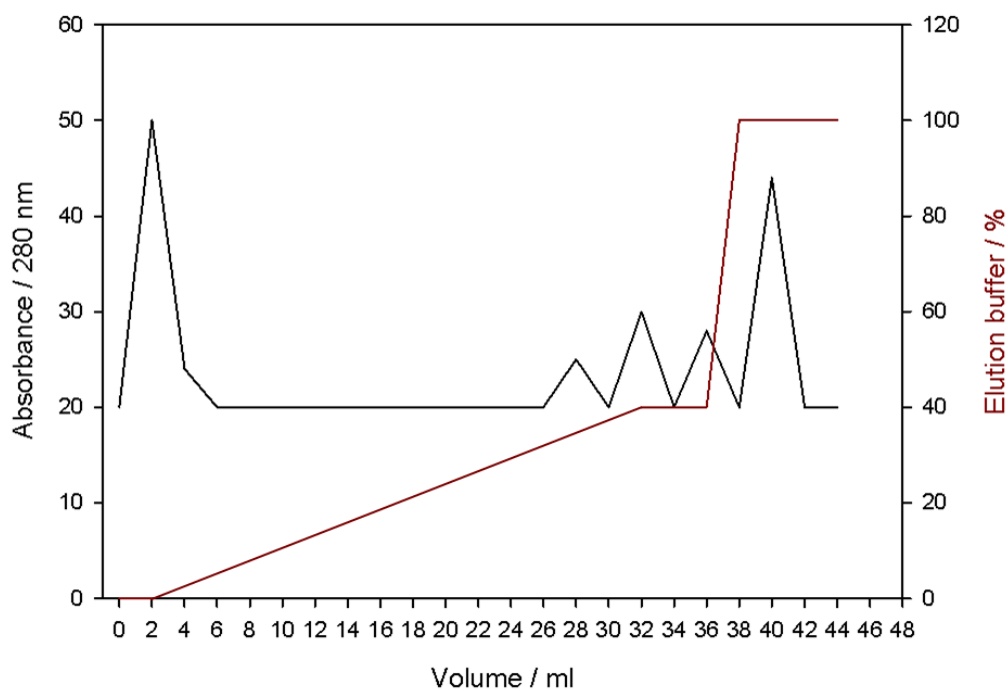


Figure 4.28: Chromatogram of the protein purification via anion exchange chromatography (AEX). The absorbance of proteins at 280 nm is shown. Fractions were collected every 1 ml. Elution was conducted with a linear gradient 0-0.4 M NaCl (1 M NaCl dissolved in 50 mM Tris/HCl buffer pH 6.8).

The chromatogram of protein purification via anion exchange chromatography is pictured in figure 4.28. The absorbance at 280 nm is shown as well as concentration of elution buffer in %. Several peaks are pictured at 0 % elution buffer, at 35 % elution buffer, at 40 % elution buffer and at 100 % elution buffer. Fractions were collected every 1 ml and the fractions for the same peak were pooled and subsequently dialyzed with 50 mM Tris/HCl buffer pH 8 and 0.2 mM PLP. Table 4.8 illustrates the loss of protein after dialysis and after several purifications steps. For ammonium sulfate precipitation, 76.84 mg protein was utilized, after ammonium sulfate precipitation 12.8 mg was left and 2.87 mg of protein was lost during dialysis (see table 4.8). After AEX, 8.64 mg protein remained for all fractions. The activities for the pooled fractions for the peak at 0 %, 35 %, 40 % and 100 % were examined. However, only for the fraction with the peak at 35 % elution buffer, activity is determined. To determine the activity of the active fraction for biotransformation an amount of 0.084 mg protein was used after anion chromatography.

Table 4.8: Protein content before and after purification of a transaminase from the *Burkholderia phytofirmans* strain BS115.

	Protein content / mg
starting crude cell extract	76.84
pooled fraction after (NH ₄) ₂ SO ₄ precipitation	12.8
dialyzed fraction after (NH ₄) ₂ SO ₄ precipitation	9.93
all pooled fractions after AEX	8.64

For a quantitative summarization of the purification of a transaminase from *Burkholderia phytofirmans* BS115 total activity, protein content, specific activity, recovery and purification fold are shown in table 4.9. The specific activity was determined after 30 min.

Table 4.9: Quantification of purification with ammonium sulfate and subsequent purification via anion exchange chromatography of a transaminase from *Burkholderia phytofirmans* strain BS115.

	Total activity / U	Protein content / mg	Specific activity / U/mg	Recovery / %	Purification fold
PE	14.91	76.84	0.194	100	1
(NH ₄) ₂ SO ₄	2.59	9.93	0.261	17.37	1.35
Q-sepharose HP	0.32	0.17	1.84	2.14	9.48

A purification factor of 1.35 and 9.48 for ammonium sulfate precipitation and purification with AEX was determined, respectively. A recovery of 17.37 % is shown for ammonium sulfate precipitation and 2.14 % for AEX. An activity loss of ~83 % is registered by comparing the crude cell extract and the fraction after ammonium sulfate precipitation and an activity loss of ~15 % for the fraction after ammonium sulfate precipitation and AEX. Furthermore, the total protein content decreases about 87 % after ammonium sulfate precipitation and about 99 % after AEX referring to the protein content utilized in the beginning.

5 DISCUSSION

5.1 KINETIC RESOLUTION OF β -AMINO ACIDS

5.1.1 Expression and activity of the His-tagged aminotransferase

The gene encoding for the β -amino acid aminotransferase from *Variovorax paradoxus* was synthesized and ligated to two plasmids. The gene ligated to pET21b obtains a polyhistidine tail, for the gene ligated to pET11a, in which no histidine-tag was introduced. To examine if the β -amino acid aminotransferase is ligated to the plasmids pET11a (without His-tag) and pET21b (with His-tag) and if it is correctly expressed, folded and active several experiments were performed. The combinations for cultivation, induction and expression with the two plasmids are shown in Table 4.1. After cultivation of the strain BL21DE, containing empty plasmids with (entry 1 and 3) and without IPTG (entry 2 and 4), and expression of the enzyme with BL21DE and plasmids containing the encoding gene with (entry 5 and 7) and without (entry 6 and 8) induction, biotransformation has been performed and the relative conversion of (S)- β -phenylalanine was detected, which is shown in Figure 4.3. Entry 1-4 illustrate the relative conversion of the substrate with the crude cell extract after cultivation of the strain BL21DE containing the empty plasmids. Entry 9 shows the conversion of the substrate with the crude cell extract after cultivation of the strain BL21DE. Only ~10 % of the substrate was converted after 7 h. This experiment was conducted only one time, thus the conversion rate of 10 % could be influenced by fluctuations of the HPLC analysis of (S)- β -phenylalanine. Hence, the enzyme was not expressed and no basal activity was shown. Conversion rates of about 20 % could be determined for entry 6 and 8. This increase of nearly 10 % is attributed to the T7 promotor which is included in the plasmid to induce the expression of the enzyme. It is known to show low basal transcriptional activity without induction [124, 125]. The T7 promotor is the starting point for the expression of the gene of interest induced by T7 RNA polymerase. The strain BL21DE contains the gene *lacI*, which repress the transcription and translation of the T7 RNA polymerase. Hence, the basal expression of the T7 RNA polymerase is lower compared to *E.coli* strains without this gene [126]. As expected, the highest conversion rates of 85 %– 95 % could be achieved with strain BL21DE containing the plasmids pET11a and pET21b ligated to the encoding β -amino acid aminotransferase gene after inducing the expression with IPTG, shown in Figure 4.3, entries 5 and 7. The specific activity of the latter combinations was determined and a slightly higher negligible activity for the gene expressed in pET11a occurred. In most cases, in which histidine-tagged enzymes were used, no influence on enzyme activity was observed. However, for a few enzymes, the His-tag may interfere with the enzyme activity [127, 128]. Lowered enzyme activity is mostly caused by inclusion bodies or misfolded conformations when expressed in *E. coli* [129]. But formation of inclusion bodies was not

observed for the expression of the His-tagged β -amino acid aminotransferase used in this work.

The β -amino acid aminotransferase shows high enantioselectivity for conversion of *rac*- β -phenylalanine, it is strictly (*S*)-selective for this substrate (shown in figure 7.3). Crismaru and coworkers showed (*S*)- preference for *para*- substituted analogous of β -phenylalanine of this enzyme [116]. (*R*)-selective aminotransferases have not been widely studied, but in the last years the counterpart to (*S*)-selective aminotransferases gained more attention. The (*R*)-selective aminotransferase homolog of an enzyme from *Arthrobacter spec* [130] was used for mutation studies for the synthesis of sitagliptin [13]. Furthermore it was shown that a single point mutation can change the enantiopreference of an ω -transaminase [131]. Some examples of (*R*)-selective ω -transaminases isolated from wild-type strains are given in section 5.3.3. The difference in enantiopreference of aminotransferases is attributable to their classification. Aminotransferases with (*S*)-enantiomer preference usually belong to the PLP fold class I, whereas for aminotransferases with (*R*)-enantiomer preference similarities were found to resemble enzymes in PLP fold class IV, like D-amino acid transaminases or branch-chain L-amino acid transaminases [132, 133].

Purification of the His-tagged enzyme is facilitated due to the utilization of metal affinity chromatography, which is described in the following section.

5.1.2 Purification of the β -amino acid aminotransferase

The purification of the desired β -amino acid aminotransferase was carried out in two ways. First, the purification via IMAC was conducted with an ÄKTAExplorer and a HisTrap column, whereas the second way for the purification of the enzyme was performed using magnetic M-PVA beads. The beads are functionalized with IDA and Ni^{2+} and the enzyme is able to bind to the beads via the introduced His-tag.

Purification via IMAC is a common method to obtain purified aminotransferases [133, 134]. In this study a linear gradient from 0 % to 50 % elution buffer and a sharp increase to 100 % elution buffer was found to be the best approach in regard to enzyme yield and activity. For the purification via IMAC the best recovery could be achieved in fraction 3 with 2.25 % and a purification fold of 0.74 (see table 4.2). The highest purification factor is determined for fraction 2 with 1.03. These results are inconsistent with results of Crismaru [116], his group showed for the same enzyme and purification via IMAC a recovery of 56 % and a purification factor of 2.5. The reason for the poor overall recovery of 5.61 % may be ascribed to the stressful purification conditions. Imidazole was used for the elution, in a high concentration. Furthermore, the enzyme was not stored at 4° C during the purification and desalting process, since the refrigerator was opened during purification process. Another reason may be that

Crismaru used β -mercaptoethanol which is commonly used to stabilize proteins. Besides, there is a possibility of remaining enzyme on the column, which was not investigated. To overcome the instability of the enzyme, immobilization is a useful technique to achieve long term stability and to prevent stressful purification conditions. For higher recovery, purification factors and yield of the β -amino acid aminotransferase after purification it is necessary to improve the overexpression of the enzyme. As shown in figure 4.6, no distinct band appears at 46 kDa in the lane for the crude cell extract (the weight of the monomer of the aminotransferase), in contrast to Crismarus work in which a distinct band was shown even in the crude cell extract. That indicates a low level of overexpression of the desired enzyme. Furthermore, the elution conditions can be improved to obtain a better elution of the enzyme off the column. Crismaru used a linear gradient with 0-0.5 M imidazole and a flow rate of 1 ml/min. Reproducing these elution conditions within this work, a poor recovery, purification factor and activity was obtained compared to the linear gradient used instead (data not shown). After all, the purification via IMAC was successful. The desired enzyme was enriched as shown in figure 4.6 lane F2 and F3.

Purification using magnetic M-PVA beads is a method for enzyme purification without expensive columns and with minimum time expenditure, under mild conditions. Immobilization was accomplished as described in chapter 3.5.7, followed by elution with elution buffer for 5 min. Subsequently, the period of time from cell disruption to the purified enzyme is minimal and the contact with imidazole is really short. As shown in table 4.3 the enzyme recovery was only 2.2 % but with purification factor of 1.9. In the fraction after incubation of the beads, 58 % of the activity was recovered. This means that more than half of the enzyme activity was found in this fraction. Hence, the crude cell extract contained more enzyme than available binding places on the beads. Furthermore, after investigating the incubated eluted beads, a residual activity of 0.15 U/20 mg beads (20 mg beads were utilized for purification) was determined. This means the elution of the enzyme off the magnetic beads is insufficient and a more efficient elution method has to be established. Despite all these facts, the purification of enzymes in a simple and time efficient way was established with a high purity as shown in figure 4.8, lane E1 and E2. The purification using His Mag Sepharose magnetic beads was performed for *Bacillus licheniformis* aldehyde dehydrogenase [135]. For efficient elution, a 20 mM sodium phosphate buffer was used with 500 mM NaCl and 500 mM Imidazole. One step purification and immobilization was as well conducted by Ha and coworkers [136]. A his-tagged aminopeptidase was immobilized using poly(2-acetamidoacrylic acid)hydrogel and was purified with 20 mM Tris/HCl elution buffer containing 500 mM NaCl and 250 mM imidazole. Taking a closer look at the SDS-gels of Ha's work and the SDS-gel shown in this work (figure 4.8), the purification efficiency seems comparable. However, no information was given about elution time for the latter work. In this work, elution was performed with elution buffer containing

200 mM imidazole for 5 min and 2 h and no difference in protein content or change in activity was observed (data not shown). The immobilized, extracted enzyme out of the crude cell extract showed the same advantages as described for the immobilized, free enzyme, like recyclability and higher stability at higher temperatures. The same M-PVA beads were used for immobilization and purification in one-step. Further characterization of the immobilized enzyme is reported in the following section.

5.1.3 One-step purification and immobilization using magnetic M-PVA beads

The immobilization of β -amino acid aminotransferase was performed via one-step purification and immobilization using magnetic M-PVA beads. With this immobilization technique, a reusable and long-term stable biocatalyst was produced. This is a rewarding and an efficient way to utilize an immobilized aminotransferase in kinetic resolution of *rac*- β -amino acids to synthesize enantiopure β -amino acids. To investigate its applicability, various experiments were conducted.

5.1.3.1 Influence of bivalent metal ions

For immobilization of the His-tagged β -amino acid aminotransferase with magnetic beads, the IMAC principle is used and the IDA- functionalized magnetic beads are treated with bivalent metal ions forming chelating complexes. Copper, nickel and cobalt were investigated as bivalent metal ions. Copper (Cu^{2+}) has the strongest binding capacity to His-tagged enzymes, but the poorest specificity. Cobalt (Co^{2+}) exhibits a specific interaction to His-tagged enzymes, as well as nickel (Ni^{2+}) which has good binding efficiency [82]. Due to the high metal-binding capacity for the IDA- functionalized M-PVA beads and the high affinity of imidazole, Cu^{2+} has been described previously as the best choice [71].

As shown in figure 4.9, the best activity is achieved with Ni^{2+} and Co^{2+} ; Cu^{2+} shows low activity in the first recycle step and no detectable activity (< 0.02 U) after the second step (figure 4.16). This leads to the assumption that the His-tagged enzyme is not able to bind to the copper complex or the enzyme is inactive in the presence of copper. The first explanation can be excluded, since the binding of His-tagged enzymes to a copper complex has been described for affinity chromatography using Cu^{2+} as bivalent metal ions. A possible reason may be the formation of a Cu^{2+} -pyridoxal-5'-phosphate complex, which prevents further binding of the substrate to the Schiff base formed by the enzyme and PLP [137]. The reaction mechanism of aminotransferases is known [138] and shown in figure 1.2. In the first half reaction of the amine group transfer, an internal aldimine, consisting of PLP, forming a schiff-base with ϵ -group of the lysine in the active site of the enzyme, reacts with the amino donor to an external aldimine (PLP and amino donor). Stepuro and coworkers showed the stabilizing effect of copper to aldimine bonds. Furthermore, copper increases the binding of PLP to the enzyme [139]. This

stabilizing effect could prevent further binding of the amino donor to the internal aldimine prevents conversion of the amino donor. Therefore, for all immobilization experiments conducted in this work nickel was used as bivalent metal ion forming complexes with the His-tagged enzyme.

5.1.3.2 Influence of temperature and pH on immobilized aminotransferase

The performance of the immobilized β -amino acid aminotransferase was examined at different temperatures (figure 4.10). The temperature optimum of the immobilized enzyme and the crude cell extract were examined for temperatures between 30° C and 80° C (figure 4.10 A). The temperature optimum of the crude cell extract is 40° C (0.6 U), but the crude cell extract still has high activity at 50° C (0.58 U). The immobilized enzyme has its optimum at 30° C with an activity of 0.84 U (100 %). At 60° C the activity decreases for the immobilized enzyme and the crude cell extract. The immobilized enzyme still has a remaining activity of 20 % at 80° C, whereas the crude cell extract shows no activity. This indicates that the immobilized aminotransferase operates in a wider range of temperatures, in contrast to the crude cell extract. Crismaru showed the highest activity at 55 °C and no activity at 65 °C for the free aminotransferase from *Variovorax paradoxus* [116]. The environment of the enzyme may be important in order to investigate the influence of temperature on activity. Hence, the crude cell extract may show stabilizing effects on the aminotransferase due to other cell components. It is known that proteins have stabilizing effects on adjacent proteins which is given in crude cell extract which contains all soluble proteins or enzymes of bacterial cells. Furthermore, hydration of enzyme and protein structure induced by osmolytes is also showing effects on enzyme stability [140].

For the examination of the thermal stability, the immobilized and free enzyme were incubated for 2 h at different temperatures, cooled to room temperature and the biotransformation was performed at 30° C (figure 4.10 B). The incubation of the immobilized enzyme and crude cell extract at 50° C - 80° C revealed a significant decrease in activity. Yet, the immobilized enzyme remained with a residual activity after incubation at 50° C, 60° C and 70° C, whereas the crude cell extract loses its activity already after incubation for 2 h at 50 °C. The shift in temperature optimum and higher thermal stability for high temperatures was reported before for immobilized enzymes [141–143]. Koszelewski for example, immobilized a commercially available ω -transaminase 117 via encapsulation and the temperature optimum was shifted from 30° C to 40° C. For immobilization of (*R*)- and (*S*)-transaminases on chitosan beads, a higher stability of the immobilized enzymes, compared to the free enzyme, was shown at higher temperatures. A possible explanation may be that, during inactivation at high temperatures enzymes were characterized by a specific site, where the unfolding process begins. The free fraction of the immobilized enzyme behaves like a free enzyme and denatures

at higher temperatures, whereas the immobilized fraction of the enzyme is protected by the immobilization matrix and its stabilizing effects [144]. This phenomenon explains the increase in enzyme stability at higher temperatures after immobilization.

The improved stability at higher pH of the immobilized aminotransferase is shown in figure 4.11. The optimum of the immobilized enzyme is pH 9, with a significant higher activity of 0.89 U. Furthermore, the immobilized aminotransferase is still active at pH 11. In contrast the crude cell extract shows activity between pH 7 and 9 (0.27 U and 0.3 U), but is completely inactivated at pH 11. The free, native enzyme investigated by Crismaru and coworkers exhibited a broad pH stability range, ranging from 4 to 11.2 [116]. Maybe the pH related effects, like protein-protein interactions or increasing activity of some enzymes (like proteinases) within the crude cell extract, denature the aminotransferase in the cell extract and therefore, no activity is shown at pH 11. The shifts of pH optimum and the broadening of the pH stability are observed for several immobilized aminotransferases. For example, for aminotransferases entrapped in sol-gel matrices a slight shift in pH optimum was observed [142]. Covalently immobilized aminotransferase on chitosan support showed the same pH optimum as the free enzyme, however, the immobilized enzyme showed higher activity at elevated pH [145]. The ω -transaminase immobilized on PVA Fe_3O_4 beads and the free enzyme exhibit their pH optimum at pH 7. However, the immobilized enzyme showed higher activity at pH 10 compared to the free enzyme [91]. The reason may be the change of the H^+ concentration by the microenvironment (the magnetic matrix of the beads) of the immobilized enzyme. The H^+ concentration in the immobilized enzyme may be higher as compared to the H^+ concentration around the immobilized enzyme. The H^+ ion from the inside may be released to the outside of the enzyme, which leads to a pH shift to alkaline pH [146, 147]. No activity at pH 4 is detected for the crude cell extract and the immobilized aminotransferase. Before starting the biotransformation it was observed that the yellow PLP solution added to the buffer (citrate buffer, pH 4) immediately lost its color. Hence, it can be assumed that PLP is degraded. This may be induced by increasing hydrolysis of the PLP due to the low pH of the buffer, which is described for PLP [148]. Therefore, PLP is not able to function as a cofactor for transamination which is indispensable for transamination reactions. Additionally, it was necessary to choose four different buffer systems, a sodium phosphate buffer for pH 7, a citric acid buffer for pH 4 and a NaCO_3 buffer for pH 9 and 11. Different buffer systems are known to influence conformation stability of proteins [149], which may have an effect on enzyme activity as well. An effect of citrate buffer on PLP can be excluded, as PLP dependent enzymes show activity in citrate buffer [150].

Nevertheless, the immobilized aminotransferase still shows activity at elevated pH and temperature, which makes it suitable for application in biotechnological processes.

5.1.3.3 Influence of amino acceptors

For transamination reaction an amino acceptor and an amino donor are needed. Every aminotransferase has its specific preference of a combination of amino acceptor and amino donor. In this work, 10 mM of *rac*- β -phenylalanine was converted with 5 mM of amino donor at 30° C. The immobilized β -amino acid aminotransferase and the crude cell extract show high activity with α -ketoglutarate and only 30 % of the activity with α -ketoglutarate for pyruvate and oxaloacetate as amino donors (shown in figure 4.12). With acetophenone as amino donor the enzyme exhibits no activity, neither with the immobilized enzyme nor the crude cell extract.

Aminotransferases belong to different fold types based on B6 database of PLP dependent enzymes. The enzyme used in this work is fold type I. Another classification based on substrate scope assigns this aminotransferase to subgroup II like other aminotransferases which are able to convert β -amino acids [116]. Looking at the influence of amino acceptors, this enzyme shows similarity to the β -transaminase from *Mesorhizobium spec* strain LUK [68]. This β -transaminase shows the same high activity for reactions with pyruvate and α -ketoglutarate and a slightly lower activity for oxaloacetate. Crismaru showed activity for the β -amino acid aminotransferase with pyruvate and α -ketoglutarate [116]. This is special for this kind of aminotransferases, because aminotransferases usually show a clear preference for either of the amino acceptors [22, 151]. Almost no activity is observed for the reaction with acetophenone as amino acceptor, both for the immobilized enzyme and for the crude cell extract. Product inhibition for ketone byproducts has often been observed for reactions with transaminases [152, 153]. The reason for the negligible activity with acetophenone may be that acetophenone hardly binds to the active site of the enzyme. This suggestion is supported by the work of Seo and coworkers [154]. They tested the two half reactions of an aminotransferase reaction with acetophenone as amino acceptor and alanine as amino donor to increase the yield of (*S*)- α -methylbenzylamine, which was synthesized via asymmetric synthesis using an ω -transaminase from the *Vibrio fluvialis* strain JS17. Furthermore, they showed that the right choice of amino donor and acceptor pairs can overcome kinetic hindrance and even acetophenone can be used as amino acceptor. A more precise discussion of the kinetic hindrances with acetophenone as amino acceptor is found in chapter 5.2.2.

5.1.3.4 Substrate scope

β -amino acid derivatives were used as amino donors for a kinetic resolution toward enantiopure (*R*)- β -amino acids (table 4.4). The immobilized enzyme and the crude cell extract were utilized to catalyze this reaction and were compared regarding activity, conversion and *ee*. The *rac*- β -amino acids utilized in this experiment have a concentration of 5 mM, due to the low solubility of *para* substituted analogues of β -phenylalanine with F, Cl, NO₂ and *iso*-propyl

as a moiety on the phenyl ring. Moreover, 5 mM of the α -ketoglutarate were utilized (triplicate approach). For the β -amino acids with F, Br and Cl as a residue at the phenyl ring the immobilized aminotransferase shows activities of 96 %, 88 % and 100 %, respectively (activity toward the *rac*- β -phenylalanine refers to 100 %). For the same β -amino acids, the crude cell extract shows comparable activities of 100 %, 121 % and 113 %. But the immobilized enzyme shows higher conversion rates. For entry 5, no activity is determined for the crude cell extract in contrast to the immobilized enzyme which shows an activity of 130 % and a conversion rate of 50 %. An explanation for this phenomenon cannot be given, because sterically hindrances of the methoxy group can be excluded since residues with bigger sizes are converted by the crude cell extract. No influence of the activity induced by the size of the residues connected to the phenyl ring is observed for immobilized aminotransferase and crude cell extract. The immobilized enzyme shows activity towards both enantiomers of entry 10 and 11, whereas the crude cell extract only converts one enantiomer selectively. These changes of activity and enantioselectivity may be induced by distortion of the active site and reduced overall mobility of the immobilized enzyme. Conformational changes of the immobilized enzyme and the modulation of immobilization support, leading to different rigidity and microenvironment, which were reported to influence the catalytic properties of the enzyme [90, 155, 156]. Another possible explanation for the differences in activity and conversion rate is based on the influence of the metal ions used for immobilization of the aminotransferase on the enzyme, leading to changes in activity [157]. This has to be investigated in further experiments by adding nickel to the reaction mixture.

In literature, the K_M of the free β -amino acid aminotransferase used in this work is stated as 0.3 mM for the conversion of 10 mM (*S*)- β -phenylalanine [116]. Other aminotransferases show much higher K_M values, like the ω -transaminase from the *Mesorhizobium* strain LUK of 1.2 mM for (*S*)- β -phenylalanine [24]. No information on K_M values of enzyme in crude cell extract could be found. However, immobilization of enzymes has been described to have an influence on the K_M . A catalase immobilized on chitosan beads was compared to the free, native catalase with regard to the K_M and a significant higher K_M was observed for the immobilized enzyme [158]. This may be induced by structural changes of the enzyme after immobilization. The increased K_M indicates that the affinity of the substrate toward the immobilized enzyme is lower than to the free one. This could be caused by steric hindrance of the active site by the immobilization matrix or a loss of enzyme flexibility which is necessary for substrate binding. Jia and coworkers observed the same influence of immobilization on the K_M value after immobilization of an ω -transaminase on magnetic PVA-Fe₃O₄ beads (K_M 4.4 mM) [91]. The reason for the increase of the K_M in the case of magnetic PVA beads may be the high hydrophilicity of PVA which reduces the local concentration of the substrate in the

microenvironment surrounding the enzyme [159]. To compare the K_M of the immobilized aminotransferase and the free one, kinetic studies have to be performed.

5.1.3.5 Influence of various beads and crude cell extract concentrations

Two experiments were conducted to determine which amount of His-tagged β -amino acid aminotransferase binds to the magnetic M-PVA beads. In figure 4.13, the activity of the aminotransferase immobilized using four amounts of magnetic beads is illustrated. As expected, the activity increases with rising amount of magnetic beads, except for the immobilization with 60 mg beads, where the activity was not higher as immobilization on 40 mg beads. This indicates that, at 40 mg beads, the His-tagged β -amino acid aminotransferase which is suspended in crude cell extract has completely bound to all binding sites of the M-PVA beads. After determination of the protein effectively bound to the beads (10 mg beads/0.5 mg bound protein; 20 mg beads/0.99 mg bound protein; 40 mg beads/1.3 mg bound protein; 60 mg beads/1.9 mg bound protein), it can be assumed that about 1 mg β -amino acid aminotransferase is suspended in the crude cell extract which effectively binds to the beads. The higher quantity of protein bound to 40 mg and 60 mg beads indicates that, after the His-tagged aminotransferase has specifically bound, unspecific binding occurs. The activity does not increase by utilizing more than 40 mg beads with the same amount of crude cell extract which is supporting this thesis.

In figure 4.14 20 mg beads were incubated with various amounts of protein out of crude cell extract. The activity of the His-tagged β -amino acid aminotransferase increases with higher amounts of protein. But no further increase of activity is observed for incubation with 39 mg protein out of crude cell extract. The concentration of the bound protein (3.75 mg protein /0.25 mg bound protein; 7.5 mg protein /0.4 mg bound protein; 15 mg protein/0.65 mg bound protein; 30 mg protein /0.91 mg bound protein; 39 mg protein /1.05 mg bound protein) indicates that 30 mg is the highest amount of crude cell extract which can be utilized for immobilization of aminotransferases using 20 mg beads.

Comparing the specific activity of the aminotransferase in relation to the amount of magnetic beads, incubation with crude cell extract using 20 mg beads results in about 70 mU pro mg bead. This is comparable with the highest specific activity of ~ 80 mU/mg bead after incubation with different amounts of magnetic beads and 45 mg crude cell extract. The small difference in specific activity may be related to the utilization of different batches of crude cell extract for the two experiments: 45 mg and 39 mg protein.

After comparing the experiments and determining the residual activity of the supernatant of the crude cell extract after incubation, it can be observed that for up to 15 mg utilized protein the complete activity was found on the beads, with 3 % and 7 % residual activity in the supernatant

(shown in table 5.1). That means that all aminotransferases suspended in the crude cell extract can be found on the magnetic beads, for immobilization using 20 mg beads and 3.75 mg, 7.5 mg and 15 mg protein in the crude cell extract. For this protein amounts, 0.25 mg, 0.4 mg and 0.62 mg protein could be determined as efficiently bound aminotransferase to 20 mg magnetic beads (determined by incubating the beads with 1 % SDS at 90° C). Hence, it is supported that only 0.4 mg -0.65 mg of His-tagged β -amino acid aminotransferase are able to bind to the beads which is the amount of aminotransferase included in 39 mg crude cell extract. Assessing these results, it can be calculated that ~25 mg aminotransferase is able to be immobilized using 1 g magnetic M-PVA beads. Summarizing the results, 20 mg beads efficiently bind 0.4-0.62 mg of aminotransferase, which can be achieved by diluting the crude cell extract to 7.5 mg-15 mg protein. Therefore, lower amounts of magnetic beads resulted in higher activity (using 10 mg magnetic beads for immobilization exhibited the highest activity, figure 4.13). Higher amounts of protein in crude cell extract or magnetic beads are not efficient, since unspecific binding of proteins to the magnetic beads occurs.

The aminotransferase immobilized on 20 mg magnetic beads (using 39 mg protein out of crude cell extract) was removed by incubating in 1 % SDS at 90° C for 20 min. Subsequently a SDS-PAGE was conducted where a distinctive band at ~46 kDa can be observed, which represents the molecular weight of the aminotransferase monomer (figure 7.6). However, not only the aminotransferase band is shown but other unspecific bands. This is correlating with the results that unspecific binding occurs by using 20 mg beads with about 39 mg of the crude cell extract. Nevertheless, the band of aminotransferase indicates that about 60 % aminotransferase was bound to 20 mg magnetic M-PVA beads, like illustrated in table 5.1.

Table 5.1: Residual activity after incubating the beads with crude cell extract.

	Activity/ U	Residual Activity [%^{a)}	Residual Activity [%^{b)}
Crude cell extract	0.52		
39 mg	0.19	37.2	268.9
30 mg	0.2	37.75	269.88
15 mg	0.04	6.99	243.97
7.5 mg	0.03	5.19	200.73
3.75 mg	0.02	3.49	106.34

^{a)} Residual activity in % of the crude cell extract after incubation

^{b)} Residual activity in % of the immobilized enzyme on the beads

Motejadded immobilized a lipase out of the crude cell extract via a HaloTag™ and tested several enzyme:bead ratios [92]. For the ratio 0.025 mg crude cell extract:8 mg beads an activity of 1200 mU was achieved, whereas the activity of the lipase in the crude cell extract was 200 mU. However, saturation of the beads with enzyme was not given at 8 mg beads. Hence, a residual activity of ~200 % was accomplished for 8 mg beads. For the β -amino acid

aminotransferase used in this work, a residual activity of ~200 % is observed with the protein:bead ratio of 7.5 mg protein:20 mg bead (table 5.1). Furthermore, Motejadded investigated the activity of the lipase immobilized out of the crude extract and for immobilization of purified enzyme. A slight increase in activity could be observed for the lipase immobilized after purification. In literature, the immobilization yield was detected by dividing the initial concentration of a free enzyme solution by the concentration of the enzyme after immobilization. Ni and coworkers used different adhesive composites for immobilization of an ω -transaminase and observed that 195 mg enzyme can be bound per g iron oxide nanoparticles [160]. Martin tested various enzyme concentration of an (S)-aminotransferase per g bead (calcium alginate) and showed a loss of enzyme of about 30 % for every enzyme concentration tested [161]. Morhardt and coworkers demonstrated a possibility to detect the enzyme loading capacity on non-porous magnetic M-PVA beads via FTIR ATR by quantification of the emerging amide after adsorptive binding of α -chymotrypsin [162]. The immobilization efficiency of α -chymotrypsin was 95 %-100 %.

5.1.3.6 Storage stability and recyclability

The activity of the immobilized β -amino acid aminotransferase was investigated for 38 days and compared to the crude cell extract (figure 4.15). The crude cell extract shows already no activity after ~10 days, in contrast to the immobilized enzyme which is stable for 38 days and maintain 50 % of its starting activity. Moreover, the immobilized aminotransferase is even stable after three freezing and thawing cycles (figure 7.2). The enhanced storage stability is one huge advantage of enzyme immobilization. This is observed for most of the immobilized enzymes. (R)- and (S)-amine transaminases from *Aspergillus fumigatus*, *Ruegeria pomeroyi* and *Rhodobacter sphaeroides* were immobilized on chitosan with glutaraldehyde or divinylsulfone as linkers and show a high activity after 35 days [143]. For immobilization of an ω -transaminase on catechol iron oxide nanoparticles a relative activity of 70 % was determined after 15 days [160]. For an ω -transaminase immobilized on PVA-Fe₃O₄ beads, the relative activity remained 90 % of its former activity after 45 days [91]. Immobilization of an ω -transaminase from *Vibrio fluvialis* JS17 on chitosan exhibited a residual activity of 30 % after 24 days and 2.5 % residual activity after 24 days for immobilization on Eupergit® C [145]. The lipase immobilized out of the crude cell extract via HaloTag™ showed the same activity at day 1 and day 38 [92]. These examples confirm that the β -amino acid aminotransferase from *Variovorax paradoxus* immobilized on magnetic M-PVA beads shows the same and even improved storage stability over a time period of 38 days.

Another benefit for immobilization of enzymes is the recyclability. The downstream process for magnetic beads is particularly easy, due to the easy removal of the immobilized enzyme via magnetism. The β -amino acid aminotransferase immobilized on magnetic M-PVA beads is

recyclable for at least 7 successive cycles, with a relative residual activity of 90 % using nickel as bivalent metal ion (figure 4.16). For immobilization with cobalt, a relative activity of 70 % was observed after 7 cycles. Only copper as bivalent metal ion showed almost no activity after the second cycle (discussed in chapter 5.1.3.1). An ω -transaminase immobilized on chitosan catechol beads was reused 15 times and exhibited a relative activity of 50 % after cycle 15, after 7 cycles the relative activity was 80 % [160]. The ω -transaminase immobilized on PVA-Fe₃O₄ beads was reused 19 times and still showed 50 % activity after the 19th cycle [91]. Immobilization of ω -transaminase on chitosan and Eupergit® C showed 77 % and 19 % of their initial activity after the 5th cycle, respectively [145]. Hence, with a relative activity of 90 % after 7 cycles the immobilized aminotransferase in this work exhibits comparable recyclability and long-term stability like other aminotransferase immobilized on different supports.

The immobilized aminotransferase characterized in this study shows the advantages attributable to a successful immobilization: extant activity after incubation at 50° C- 70° C, high activity at pH 11, high remaining activity after storage at 4 °C for 38 days, recyclability for seven consecutive cycles and easy removal of the biocatalyst out of the reaction due to the magnetic properties of the carrier.

5.2 ASYMMETRIC SYNTHESIS OF β -AMINO ACIDS VIA ENZYMATIC CASCADE

5.2.1 Hydrolysis of β -keto acid esters

Lipases catalyze the hydrolysis of triglycerides and insoluble esters with varying chain length. Lipases belong to the α/β hydrolase fold family. After the substrate is binding a tetrahedral intermediate is formed by nucleophilic attack of the catalytic serine and stabilized by the oxyanion hole. The ester bond is cleaved and the alcohol leaves the enzyme. Then, the acyl enzyme is hydrolyzed and the nucleophilic attack by the catalytic serine is mediated by the catalytic histidine and the aspartic or glutamic acid (catalytic triade). A lid, consisting of one or two α -helices, is linked to the rest of the lipase. If the enzyme is in its active form, the lid is moving away from the active site and gives access to the substrate. [163, 164]

Three lipases were tested to hydrolyze five β -keto acid esters with several residues (figure 4.18 and for ethyl benzoylacetate 4.19). The best activity is achieved with the lipase from *Rhizomucor miehei* (RML) which shows activity toward all keto acid esters. The lipase from *Candida rugosa* (CRL) shows low activity for the β -keto acid esters with F and NO₂ as moieties on the phenyl ring. The lipase from *Thermomyces lanuginosus* (TLL) shows activity toward all keto esters. The substrate binding pocket of RML is a bowl with a long axis of 18 Å and a width of 4.5 Å. Hence, even substrates with bigger side chains can be bound and converted, which explains the high activities with all tested β -keto acid esters, even of those with big moieties. In contrast to that, the CRL has a completely different and exceptional substrate binding

pocket. The binding site is located inside a L-shaped tunnel with a right hand side entrance. This may explain the low activities of CRL for keto acid esters with big residues (NO_2 and F) which are not able to enter the binding pocket [163, 165, 166].

Figure 4.19 illustrates the hydrolysis of ethyl benzoylacetate catalyzed by the CRL. The emerging ethanol was determined via gas chromatography. The concentration of ethanol is shown from 0 min to 180 min. At 60 min the ethyl benzoylacetate decreases from 6 mM to 3 mM and the ethanol concentration increases to 3 mM. After 60 min, the ethanol concentration is increasing to 4 mM whereas the ethyl benzoylacetate decreases from 6 mM to ~1 mM. The difference of emerging ethanol and decreasing ethyl benzoylacetate may be ascribed to fluctuation of the ethanol concentration. The analysis of the ethanol was performed as single value and only the first 180 min were determined.

A decrease of ethyl benzoylacetate for the negative control without lipase was determined after 24 h. This could be induced by base catalyzed hydrolysis due to the NaCO_3 buffer with a pH of 9 [167]. Furthermore, the concentration of ethyl benzoylacetate may be decreasing due to evaporation from the reaction mixture. Since, ethyl benzoylacetate is not soluble in aqueous solutions, in this experiment DMSO was used to dissolve the substrate in NaCO_3 buffer, pH 9. After 24 h DMSO may have evaporated. Since, the substrate was no longer dissolved in buffer and a lower concentration of the substrate was detected at 24 h.

5.2.2 Asymmetric synthesis via enzyme cascade

Several challenges have been encountered for the asymmetric synthesis via an enzyme cascade. First, the equilibrium of substrate and product is a major challenge for asymmetric synthesis of amines and β -amino acids. Seo and coworkers published an exact examination for the asymmetric synthesis of (*S*)- α -methylbenzylamine (pyruvate as ketone byproduct) with acetophenone as a substrate and L-alanine as an amino donor [154]. They investigated the half reactions of transamination by detecting the reaction rate and velocity to form the PMP-enzyme (E-PMP) complex for the amino donor and to form the PLP-enzyme complex (E-PLP) for the amino acceptor. (*S*)- α -methylbenzylamine (MBA) has a high reaction rate for the formation of E-PMP and is therefore considered a good amino donor. Pyruvate shows high reaction rates to form E-PLP which makes it a good amino acceptor. Contrary, alanine shows conversion rates of 70 % for forming E-PMP (compared to (*S*)-MBA) and acetophenone is an unsuitable amino acceptor in this constellation due to low E-PLP formation rates. This leads to the conclusion that the emerging PLP (formed with acetophenone) immediately reacts back to PMP due to the high reactivity of the corresponding MBA. This means that the low conversion yield of MBA in the asymmetric synthesis is caused by low amination rate to acetophenone and high deamination rate of MBA, which shifts the equilibrium to the acetophenone side. Therefore, in this work, we can assume that the reaction rate of the (*S*)- β -phenylalanine is

higher compared to the reaction rate of the emerging product amino donor isopropylamine or 3-aminobutanoic acid. Hence, suitable substrate pairs had to be found which show no substrate or product inhibition. From those observations it can be concluded that the kinetic hindrances in the reaction generated by substrate pairs and the inability of the aminotransferase to convert β -keto acid esters are the reason why no product was synthesized in figure 4.21, as well as the problems with the intermediate substrate emerging by hydrolysis of β -keto acid ester which is instable. However, to successfully conduct asymmetric synthesis of β -amino acids it is necessary to find a suitable amino donor, due to the fact that the amino acceptor is already defined. The reaction rate of the substrate amino donor has to be higher than the reaction rate of the product amino donor, as well as the reaction rate of substrate amino acceptor has to be higher than the reaction rate of the product amino acceptor. Therefore a substrate amino donor has to be found with a higher reaction rate than the reaction rate of (S)- β -phenylalanine. Another possibility to achieve asymmetric synthesis could be protein engineering of the β -amino acid aminotransferase with the ability to convert β -keto acid esters and thus avoid the formation of the instable intermediate β -keto acid.

In 2007, Kim and coworkers proved that asymmetric synthesis is possible with the above mentioned enzyme cascade (figure 4.17) [68]. The β -transaminase from the *Mesorhizobium* sp strain LUK and the lipase from *Candida rugosa* was used and a reaction yield of 20 % was achieved. The β -keto acid (3-oxo-3-phenyl propionate) was freshly prepared, since it is instable. In figure 4.22 the stability of the substrate (the β -keto acid) for the transamination was investigated by scanning the spectrum after 0 h, 1 h, 24 h and after freezing and thawing. Due to the fact that the substrate should convert to acetophenone (absorption max. 250 nm, figure 4.22 B) it is supposed to shift its absorption peak to 250 nm. This may happen after 1 h hour as shown in figure 4.22 A, but the shift is minimal and not significantly exhibiting the spectrum of acetophenone. Hence, it cannot be assumed that this β -keto acid converts to acetophenone faster than it is used as a prochiral amino donor for the aminotransferase. This leads to the conclusion that either the ordered sodium 3-oxo-3-phenyl propionate is not the correct substrate or the β -keto acid is more stable as anticipated. Mathew demonstrated as well successful asymmetric synthesis of aromatic β -amino acids derivatives with different residues and showed reaction rates up to 90 % [69]. They used an ω -transaminase from *Polaromonas* sp JS666 and the lipase from *Candida rugosa*. The best ratio of lipase:aminotransferase in U/mg was found to be 3.3:4 and the amino donor leading to the highest yields was (S)- α -methylbenzylamine. The substrate concentration was 10 mM and the amino donor concentration was 50 mM.

The activity toward amines was not determined for the aminotransferase, immobilized in this work. Hence, it may be possible that α -methylbenzylamine is not accepted as amino donor for

asymmetric synthesis of β -amino acids. In contrast, the kinetic resolution of 3-aminobutanoic acid was shown for the β -amino acid aminotransferase [116]. Therefore, there is a chance of successful asymmetric synthesis of β -amino acids utilizing 3-aminobutanoic acid as amino donor.

Finally, the results of this work give preconditions for asymmetric synthesis of β -amino acids with the immobilized β -amino acid aminotransferase from *Variovorax paradoxus* and the lipase from *Candida rugosa*. The immobilized aminotransferase was found to be active toward a variety of β -amino acids even after adding DMSO (figure 7.4). In further experiments an amino donor has to be found which is accepted by the immobilized aminotransferase. Furthermore, it is also required that the substrate amino donor exhibit higher reaction rates than the product amino donor which also applies to the reaction rates of the amino acceptor.

5.3 CHARACTERIZATION OF TRANSAMINASE ACTIVITY OF *BURKHOLDERIA PHYTOFIRMANS* SPEC.

The transaminase activity of *Burkholderia phytofirmans* strain BS115 was mentioned for the first time in 2011 [67]. It was shown that resting cells and the crude cell extract of this strain were able to convert β -phenylalanine after adding PLP and α -ketoglutarate. Therefore, it was assumed that the enzyme which is responsible for the conversion should be a transaminase. The strain showed a strict (S)-selectivity for the chosen substrate. Furthermore, it was observed that the expression of the responsible enzyme for conversion of β -phenylalanine is induced by substrate, meaning that conversion of β -phenylalanine was shown when a β -amino acid were added to the cultivation medium. This leads to the assumption that the enzyme which is expressed after induction with β -amino acids may not be an α -transaminase but rather an ω -transaminase. For α -proteobacteria, for example the *Mesorhizobium sp* strain LUK transaminase activity toward (S)- β -phenylalanine was observed [168], as well as for several β -proteobacteria like *Variovorax paradoxus* [116, 169] and *Alcaligenes denitrificans* [65]. The genome of the *Burkholderia phytofirmans* strain PsJN was completely sequenced from Weilharter and coworkers [109], which is useful for purification of the enzyme with transaminase activity based on genetics due to the fact that the strain used in this work showed 99 % homology to the strain PsJN. Transaminases are useful biocatalysts for kinetic resolution or asymmetric synthesis of β -amino acids which can be applied as peptidomimetics or as compounds in pharmaceutical drugs. For cultivation or fermentation of the *Burkholderia* strain BS115 almost no information is given so far. Therefore, the focus of this work laid on finding suitable cultivation conditions and on establishing a fermentation process for controlled cultivation of the *Burkholderia phytofirmans* strain BS115. Moreover, the substrate scope of the enzyme with transaminase activity was examined as well as the amino acceptor spectrum.

Finally, first attempts for purification of this enzyme were conducted with ammonium sulfate precipitation and purification via anion exchange chromatography (AEX).

5.3.1 Cultivation of *Burkholderia phytofirmans spec* with β -amino acid as sole nitrogen source

The first cultivation of the *Burkholderia phytofirmans* strain BS115 was performed in shaking flasks with minimal medium, *rac*- β -phenylalanine as sole nitrogen and glucose as carbon source. As an amino donor, α -ketoglutarate was utilized and PLP was added as the indispensable cofactor. The experiments were conducted at 30° C and 120 rpm. Several concentrations of *rac*- β -phenylalanine and glucose were deployed and the specific growth rate (μ /h), as well as the consumption rates (R) for both enantiomers and glucose were determined. Figure 4.23 illustrates the cultivation process for all cultivation conditions. Assessing, the $\ln(\text{OD}_{600})$ for the cultivation with different concentrations of *rac*- β -phenylalanine and glucose, it is observable that the growth phases in the experiments are differing. This can be explained by the precultures which were inoculated by picking a culture from an agar plate or by inoculating with culture from a glycerol stock. However, care was taken that the precultures were growing for a similar period of time. It can be presented that (S)-enantiomer concentrations of 2.5 mM and 5 mM are both completely consumed after 21 h (figure 4.23 A and B). For starting concentrations of 10 mM (S)- β -phenylalanine, it is shown that only 5 mM substrate is converted after 21 h (figure 4.23 C). An explanation is found in enzyme kinetics. Considering the fact that 2.5 mM and 5 mM substrate is degraded in 21 h hours, the velocity for the conversion of 2.5 mM substrate is lower compared to the velocity for the conversion of 5 mM substrate. That means that, for 2.5 mM the substrate saturation was not reached, but with a concentration of 5 mM the enzyme is saturated and the maximum velocity can be achieved. By utilizing 10 mM (S)- β -phenylalanine only 5 mM is converted in 21 h, this confirms the latter assumption as the turnover rate does not increase for this substrate concentration in 21 h. The results given in figure 4.23 A and B give a suggestion for the K_M value of this enzyme located in the crude cell extract, which may be lower than 5 mM. The K_M values of purified ω -transaminases or β -transaminases for the substrate (S)- β -phenylalanine are differing: the K_M of the β -amino acid aminotransferase from *Variovorax paradoxus* is 0.3 mM [116], the K_M of the ω -transaminase from *Polarimonas sp* is 0.83 [170], the K_M of the ω -transaminase from *Mesorhizobium sp.* LUK is 1.2 [24] and the K_M of an ω -transaminase from *Burkholderia graminis* toward this substrate is 2.88 mM [66]. In all latter works pyruvate was used as an amino acceptor. In this work α -ketoglutarate was used as amino donor, which has also an impact on the K_M of the transaminase.

Another aspect which should be considered is the acetophenone concentration. As presented in figure 4.1, the (R)-enantiomer is enriched in kinetic resolution of *rac*- β -phenylalanine,

whereas the (S)-enantiomer is converted into an unstable β -keto acid. Hence, the product emerging out of the conversion of (S)- β -phenylalanine is acetophenone. It is assumed that if 2.5 mM or 5 mM of the (S)-enantiomer is converted, 2.5 mM or 5 mM of acetophenone occur, respectively. But this is not the case for all cultivations performed in this work (figure 4.23). For the cultivation with 2.5 mM (S)- β -phenylalanine, 1.5 mM acetophenone emerges, for cultivation with 5 mM (S)- β -phenylalanine, 2 mM and for cultivation with 10 mM (S)- β -phenylalanine (in which only 5 mM (S)- β -phenylalanine was converted), 3 mM acetophenone occurs. The highest concentration of acetophenone is reached after ~25 h for all cultivations. After the concentration peak at ~25 h, the concentration of acetophenone subsequently decreases. There is no information if and how the *Burkholderia phytofirmans* strain BS115 can metabolize acetophenone. For *Arthrobacter spec* a proposed pathway for acetophenone metabolism is the β -oxoadipate pathway, where acetophenone is converted to catechol by an acetophenone oxygenase and a phenyl acetate esterase [171]. The expression of the enzymes is induced after the strain grows on agar plates containing acetophenone as sole carbon source. Referring this to the results shown in figure 4.23, it can be assumed that the cultivation with acetophenone may induce expression of enzymes able to convert acetophenone, resulting in a decreasing acetophenone concentration after 25 h. To metabolize the substrate, the microbe expresses the needed enzyme. The β -oxoadipate pathway is a chromosomally encoded pathway for aromatic substrate degradation. It is widely distributed and highly conserved for bacteria like *Pseudomonas putida* or *Burkholderia cepacia* [172, 173]. Thus, it is obvious that the *Burkholderia phytofirmans* strain BS115 can also express this pathway for metabolizing the emerging acetophenone.

Furthermore, the conversion of the (R)-enantiomer of *rac*- β -phenylalanine has to be considered. For the cultivations in which the (S)-enantiomer is completely converted, the (R)-enantiomer starts to decrease (figure 4.23 D). In contrast, when the (S)-enantiomer is not completely degraded the (R)-enantiomer still has its starting concentration of 10 mM (figure 4.23 C). It seems that the *Burkholderia* strain BS115 is able to convert both enantiomers. Experiments with crude cell extract exhibited that no conversion was detected for the (S)- or the (R)-enantiomer if no PLP and an amino acceptor like α -ketoglutarate was added. Furthermore, it was observed that only the (S)-enantiomer is converted after adding PLP and an amino acceptor in an equimolar ratio to β -phenylalanine. Hence, a transaminase is responsible for conversion of the (S)-enantiomer [117], but not for the conversion of the (R)-enantiomer. Conversion of (R)- β -phenylalanine will be discussed more extensively in the following chapter 5.3.2

5.3.2 Fermentation of *Burkholderia phytofirmans spec*

The fermentation of the *Burkholderia phytofirmans* strain BS115 was performed to gain further understanding of the metabolism of β -amino acids in bacterial cells and more precisely, the growth behavior of the *Burkholderia phytofirmans* strain BS115 with *rac*- β -phenylalanine as sole nitrogen source. Furthermore, for further application of the transaminase responsible for the conversion of (*S*)- β -phenylalanine the enzyme has to be purified. Since the desired enzyme is not overexpressed a high amount of crude cell extract is needed and can be achieved via high cell density fermentation. The fermentation was conducted in a benchtop reactor (Minifors) with a total volume of 1 l in minimal medium containing 10 mM *rac*- β -phenylalanine, 5 mM α -ketoglutarate, 100 mM glucose and PLP. The temperature was set to 30° C, the air flow to 1 lpm and the stirrer to 120 rpm. The pH and pO₂ were only recorded, not controlled.

Assessing the $\ln(\text{OD}_{600})$ an exponential growth behavior is shown for the first 25 h until the (*S*)-enantiomer is completely consumed (consumption rate of 0.02 g/h, table 4.5). After complete consumption of the (*S*)- β -phenylalanine the culture is still growing, but the growth is not exponential anymore and the culture is slowly entering the stationary phase (figure 4.24 A). After 25 h, when the (*S*)-enantiomer is completely consumed, the degradation of the (*R*)-enantiomer begins, starting from 5 mM and ending up at 1.8 mM after 52 h. The stationary phase is reached after ~50 h. From these results, it can be assumed that the *Burkholderia phytofirmans* strain BS115 is able to degrade the (*R*)-enantiomer, if no alternative nitrogen source is available. However, the culture is growing slower with (*R*)- β -phenylalanine. After the stationary phase is reached the medium still contains about 3 g/l glucose (figure 4.24 B). Hence, the termination of bacterial growth is induced by lack of other essential nutrients in the medium, rather than lacking the carbon source glucose or the nitrogen source (*R*)- β -phenylalanine. For subsequent fermentation, the medium has to be optimized and higher concentrations of essential nutrients have to be utilized. Additionally, the pH can be controlled to prevent the decrease of the pH value. Longer fermentation times may result in the complete consumption of the (*R*)-enantiomer.

A feasible way for the conversion of the (*R*)- β -phenylalanine can be oxidative deamination catalyzed by a dehydrogenase. Mano and coworkers proved that the (*S*)-enantiomer of *rac*- β -phenylalanine is converted with a transaminase, whereas the (*R*)-enantiomer is degraded via oxidative deamination with a dehydrogenase [169]. In the latter work, the (*R*)-enantiomer was converted in the insoluble fraction under severe shaking, which indicates that O₂ might be necessary for the reaction. The assumption, that oxidative deamination is the reason for degradation of (*R*)- β -phenylalanine is supported by the emerging ammonia as a reaction product. Furthermore, only one strain (*Bacillus cereus*) is known so far to express two different ω -transaminases in one reaction [174]. Further examinations have to be carried to make sure

that oxidative deamination is the metabolic pathway of (*R*)- β -phenylalanine in the *Burkholderia phytofirmans* strain BS115. For example, it has to be examined if the insoluble fraction of the cells after centrifuging is able to convert (*R*)- β -phenylalanine and if ammonia is emerging as a reaction byproduct.

As it is not known if *Burkholderia phytofirmans* strain BS115 is able to convert (*R*)- β -phenylalanine with a transaminase, the bacterial strain should be cultivated with the (*R*)-enantiomer as the sole nitrogen source. The expression of the (*R*)-selective transaminase may be induced. Iwasaki showed the expression of an (*R*)-selective ω -transaminase from *Arthrobacter sp.* KNK168 after cultivation of the strain in a medium containing (*R*)- β -phenylalanine as sole nitrogen source [175, 176].

The concentration of acetophenone was determined as well and is pictured in figure 4.24 B. A concentration of nearly 5 mM acetophenone was achieved after 30 h. This concentration is expected for kinetic resolution of *rac*- β -phenylalanine with a (*S*)-selective ω -transaminase. Degradation of acetophenone starts at ~30 h (discussed in section 5.3.1).

The plots of the pH and pO₂ values are shown in figure 4.24 C. The (*S*)-enantiomer of *rac*- β -phenylalanine is completely converted, which correlates with the decrease of the pH starting at 6.7 to 5.7 in the first 25 h. This decrease is induced by metabolizing (*S*)- β -phenylalanine. An end product of the respiratory chain and also by product of the decarboxylation of the β -keto acid is the emerging CO₂. Dissolved in water it is a source of acidity. A further reason for the decrease of the pH value for the cultivation of *Burkholderia* strain BS115 may be acetate formation, which is shown for *E. coli*. Acetate formation is induced by O₂ limitation, NADH₂ accumulation, glucose surplus (overflow mechanism) or limitations of citrate cycle [177]. Subsequent conversion of the (*R*)-enantiomer does not result in further decrease of the pH. Between 25 h and 45 h, the pH slightly increases. The bacteria growth is diminished and no CO₂ or acetate is accumulating in the culture broth. If the (*R*)-enantiomer is effectively converted via oxidative deamination, α -ketoglutarate and NH₃ may accumulate before leaving to the urea cycle and slightly increase the pH [178].

The pO₂ was recorded (figure 4.24 C) and the graph shows correlation with the pH during the fermentation. A decrease in pO₂ is observed for the exponential growth phase in the first 25 h. In this phase, the organism needs the most O₂ for cell growth, enzyme activity and metabolism. The pO₂ value increases (as well as the pH value) after 25 h, since the (*S*)-enantiomer is completely consumed. The (*R*)-enantiomer is still available in the medium, however the (*R*)-enantiomer is not the preferred nitrogen source and its metabolism is much slower.

Table 4.5 summarize the cultivation in shaking flasks and the fermentations regarding μ_{\max} , t_d , the consumption rate of (*R*)- (*S*)- β -phenylalanine and glucose and the maximal OD₆₀₀. Via

fermentation the highest growth rate and OD_{600} of 0.16 and 8.35 are achieved, respectively. The higher OD_{600} of the culture cultivated in a benchtop reactor can be explained by the gas-liquid mass transfer and the suspension of the culture. The oxygen is introduced into the medium by a sparger with constant air flow. The air bubbles are dispersed via agitation with different types of stirrers (a Rushton turbine for example).

No data were available neither for the growth rate or the doubling time of *Burkholderia phytofirmans* nor for other *Burkholderia* species. *Burkholderia pseudomallei* seems to grow on agar plates consisting of different medium between 24 h and 48 h [179], what correlates with the time needed by *Burkholderia phytofirmans* to grow on agar plates. Information about fermentation was found for *Burkholderia spec. C20* for lipase production [180]. A benchtop bioreactor with a total volume of 5 l was used. Several aeration rates and agitation speeds were tested and it was observed that higher aeration rates of ~1.5 vvm increase the lipase production, whereas agitation speed, exceeding to 100 rpm did not increase the productivity due to the higher shear forces, which can have negative effects on cell growth and enzyme activity. In contrast to the lipase production in fungi or other bacteria, lipase production is not a growth-associated product in *Burkholderia*. The effect of pH was examined as well. It is shown that uncontrolled pH during fermentation increases the lipase productivity. Hence, to find the highest production rate of the ω -transaminase, the best aeration rate, agitation speed, and the best pH have to be found by conducting more fermentations.

It can be observed that the statistical error bars are increasing as of ~21 h. This can be explained with the occurring viscous layer at this time. The *Burkholderia phytofirmans* strain BS115 exhibits a viscous layer for all samples which were taken after 21 h. The cells are encapsulated which is shown for a cell dyed with ink in negative contrast microscopy after cultivation for 72 h (figure 4.25). According to literature, the length of a *Burkholderia phytofirmans* cell is ~3 μm and the encapsulated cell is 6.5 μm . The viscous layer was not observed for fermentation with TSB media, where the bacteria are not lacking essential nutrients (data not shown). This phenomenon is known for *Burkholderia pseudomallei*, *Burkholderia mallei* and *Burkholderia thailandensis* and seems to be a layer of polysaccharides around the cells [181–183]. It seems that the *Burkholderia phytofirmans* strain BS115 starts its encapsulation as soon as the easy accessible nutrients are consumed and the bacterial strain is getting deficiency symptoms. These capsular polysaccharides are highly hydrated and contain 95 % water, which makes it plausible that the bacteria are using it to protect themselves from drying out. This is correlating to the statistical error of the OD_{600} in figure 4.24 A. Due to the viscous layer it was not possible to measure the OD_{600} correctly, since it was not possible to dilute the sample accurately. Therefore, the samples were centrifuged several times, before

measuring the OD₆₀₀. No precise examinations are given so far, concerning the benefit or cause of this polysaccharides encapsulation of *Burkholderia phytofirmans*.

It is necessary to mention that, to achieve high biomasses, fermentation has to be conducted with full medium like TSB. Fermentation with TSB medium attained an OD₆₀₀ of 20, a wet cell weight of 9 g and 126 mg protein after cell disruption via sonication (data not shown).

Summarizing, new information on the consumption of β -amino acids, growth rates and metabolism of the *Burkholderia phytofirmans* strain BS115 were gained. Furthermore, an ω -transaminase was detected, which will be characterized with more details in the following sections.

5.3.3 Substrate scope and choice of amino acceptor of the transaminase from *Burkholderia phytofirmans spec*

The substrate scope and the activity with different amino acceptors were investigated for a more precise characterization of the ω -transaminase expressed in the *Burkholderia phytofirmans* strain BS115. β -Phenylalanine was the model substrate during the cultivation of this strain. Table 4.6 shows the tested β -amino acids utilized as amino donors. The relative activity of 100 % refers to 0.23 U/mg with (S)- β -phenylalanine. For biotransformation, 0.2 mg/ml of crude cell extract, 10 mM of substrate (except for entry 3, entry 4 and entry 5 where 2 mM were utilized), 5 mM amino acceptor and extra PLP were utilized. The reaction was conducted at 30° C in 50 mM Tris/HCl buffer pH 8 for 24 h. Relative activity was determined after 30 min of reaction time and the conversion and ee were calculated after 24 h. Complete conversion of all utilized β -amino acids was shown after 24 h, except for entry 2, where no conversion occurred at all. High relative activity is achieved for entry 8 and entry 4 with 69 % and 61.3 %, respectively. Assuming that the size of the moiety attached to the phenyl ring may influence the activity, it is expected that the activity may be higher with smaller residues. Arranging the moieties by size, the highest activity has to be achieved with entry 1; followed by entry 2, entry 8, entry 4, entry 7, entry 3, entry 6 and the lowest activity has to be determined for entry 5. That has been observed for all tested substrates, except for entry 3, 6 and entry 5, which do not fit to this assumption. Since only 2 mM of substrate was utilized for entry 3, 4 and 5, the activities may be different with 10 mM of the substrate. As discussed in section 5.3.1 the K_M of the ω -transaminase from *Polarimonas sp* is 0.83 [170], the K_M of the ω -transaminase from *Mesorhizobium sp*. LUK is 1.2 [24] and the K_M of an ω -transaminase from *Burkholderia graminis* toward (S)- β -phenylalanine is 2.88 mM [66]. Therefore, it is possible that with concentrations of 2 mM of the *rac*- β -amino acid no substrate saturation is reached and v_{max} cannot be achieved. High ee between 91 % and 99 % were achieved for all converted substrates and the transaminase seems to be strictly (S)-selective for all tested β -

amino acids. (*R*)-selective ω -transaminases are rarely discussed in literature so far. Yet, only a few wildtype ω -transaminases are described to convert (*R*)-enantiomers, like the (*R*)-selective ω -transaminase from *Alcaligenes eutropophus* [184] and the (*R*)-selective ω -transaminase from the *Mycobacterium vanbaalenii* [185]. Most (*R*)-selective ω -transaminases are isolated from fungi like *Nectria haematococca* [26], *Aspergillus terreus* [27] or *Aspergillus fumigatus* [186]. The investigation of the substrate scope of the transaminase from *Burkholderia phytofirmans* strain BS115 confirms that the detected transaminase is an (*S*)-selective ω -transaminase. The only substrate (entry 2) which was not converted at all is β -homophenylalanine. This may be due to the additional carbon-group between the β -amino group and the phenyl ring, which can disturb the function of the transaminase. In order to prove this suggestion, a closer look has to be taken at the binding sites of ω -transaminases. A two binding site model is proposed, consisting of a large and a small pocket, which control the substrate recognition of the enzyme [187, 188]. The L-pocket shows recognition of a hydrophobic group and a carboxylate group of the substrate. The S-pocket receives moieties not larger than an ethyl group. This is illustrated in figure 5.1.

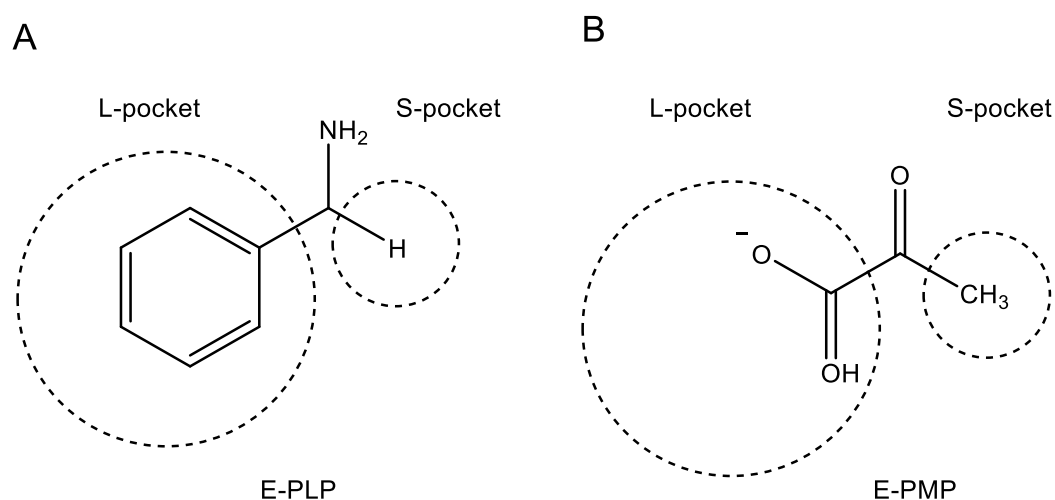


Figure 5.1: Binding pocket for substrate recognition of an ω -transaminase. Modified after Park and coworkers [187].

Since an extra carbon group between the amino group and the phenyl ring of β -homophenylalanine exists, undesired interactions may occur in the L-pocket of the active site. For successful transfer of the amino group, all substrate sites have to be within the pockets and only the amino group should be exposed. If the larger site of the substrate does not fit correctly into the L-pocket, β -homophenylalanine is not converted. To enlarge the pockets and broaden the substrate scope, a mutation approach and enzyme engineering has to be conducted. An example for successful enzyme evolution is given for the production of sitagliptin [13]. The large and the small binding pocket of an (*R*)-selective aminotransferase

from *Arthrobacter sp.*, were effectively engineered for activity toward pro-sitagliptin ketone, the substrate for sitagliptin production.

Furthermore, several amino acceptors were tested to classify the transaminase (figure 4.26). Biotransformation conditions were 10 mM of *rac*- β -phenylalanine, 5 mM of the amino acceptor, 0.2 mM of PLP and 0.2 mg/ml crude cell extract in 50 mM Tris/HCl buffer, pH 8, at 30° C. Activity is determined for α -ketoglutarate, pyruvate and oxaloacetate as amino donors, whereas acetone and acetophenone are not used as amino donors at all. Activity with α -ketoglutarate was shown before by Brucher [117]. Classification based on the substrate scope of this ω -transaminase assigns it to subgroup II and fold type I based on B6 database of PLP dependent enzymes. Assessing the influence of amino acceptors this enzyme shows similarity with the β -amino acid aminotransferase from *Variovorax paradoxus* (discussed in section 5.1.3.3) and the β -transaminase from the *Mesorhizobium species* strain LUK [68]. This enzyme shows high activity for pyruvate, α -ketoglutarate and a slightly lower activity for oxaloacetate. Crismaru showed for the β -amino acid aminotransferase activity with pyruvate and α -ketoglutarate. The immobilized β -amino acid aminotransferase described in this work shows activity with pyruvate, oxaloacetate and α -ketoglutarate (chapter 4.1 and 5.1). The differences in activity cannot be explained, but it is known that every enzyme exhibits its own substrate specification. With acetophenone as amino acceptor no activity was detected at all. A possible reason for that is described in detail in chapter 5.1.3.3 and 5.2.2. In literature, the activity of (*S*)-selective transaminases with acetone as amino acceptor has not been mentioned yet. But for an (*R*)-selective ω -transaminase from *Mycobacterium vanbaalenii*, kinetic resolution of α -methylbenzylamine was successfully performed with acetone as amino acceptor [189].

The latter results indicate that the enzyme which is responsible for the transaminase activity from the *Burkholderia phytofirmans* strain BS115 is an (*S*)-selective ω -transaminase. It belongs to the fold type I based on the B6 enzyme database and to subgroup II classified by its substrate range. The enzyme is able to convert a variety of aromatic β -amino acids with different moieties and uses different amino acceptors. Furthermore, the enzyme demonstrates the same properties regarding its substrate scope and enantioselectivity as the β -amino acid aminotransferase from *Variovorax paradoxus* and the β -transaminase from *Mesorhizobium species* LUK. The logical next step is the purification of this enzyme and to demonstrate if the properties of the purified enzyme and the enzyme in crude cell extract are comparable.

5.3.4 Protein enrichment

Purification of the detected (*S*)-selective ω -transaminase from *Burkholderia phytofirmans* is necessary, since no characterization for this purified enzyme is given in literature. The enzyme was enriched by ammonium sulfate precipitation and anion exchange chromatography. The

first approach for enzyme purification was the enrichment via ammonium sulfate precipitation (chapter 4.3.4). The cultivation of *Burkholderia phytofirmans* was conducted in 2 l TSB medium and the cell disruption was performed via sonication. The specific activities are illustrated in figure 4.27 and it is shown that the highest activity is achieved between 35 % and 55 % ammonium sulfate saturation. In these fractions, a recovery of 14.5 %-19.22 % was achieved and the enzyme enrichment was 1.35-1.54 fold. The fractions between 35 % and 55 % ammonium sulfate saturation were pooled and utilized for anion exchange chromatography. The saturation spectrum between 35 % and 55 % is given for enrichment of several wild type ω -transaminases [22, 176, 190]. The enrichment of the enzyme in this work is in the same range as for the transaminases from *Vibrio fluvialis*, *Arthrobacter species* KNK168 and *Pseudomonas fluorescense*. For the *Mesorhizobium* strain LUK the purification was 3.7 fold. A loss of protein and activity of 50 % and 60 % is observed for the transaminase from *Burkholderia phytofirmans*, compared to the latter purifications with a loss of 30 %. This may be induced by a short time without extra PLP, which is needed to maintain enzyme stability [65]. Furthermore, BCA may not be accurate for protein determination out of the crude cell extract. The low protein content obtained for 2 l culture broth can be explained by the poor cell disruption via sonication. Shin and coworkers also received only 1240 mg protein for 30 l cultivation broth disrupted via sonication, which is 82.67 mg with regard to 2 l cultivation broth [22]. For cell disruption with glass beads, 6480 mg were detected for 1.5 l cultivation broth, which seems to be a really efficient method for cell disruption [176]. For cell disruption via French press 1620 mg protein could be obtained for 4 l cultivation broth [190].

The enriched fractions were further purified with anion exchange chromatography with a linear NaCl-gradient (chapter 4.3.5). After elution off the column, only one fraction (elution with 35 % elution buffer) showed transaminase activity. The purification was 9.48 fold. The purification of the transaminase from *Vibrio fluvialis* was 23 fold after AEX with Q-sepharose [22]. The purification of the transaminase from *Pseudomonas fluorescense* was 18.7 fold [191] and purification of the transaminase from *Arthrobacter specie* KNK168 was 36.6 fold, using a DEAE-sepharose column [176]. The enrichment of the ω -transaminase from *Mesorhizobium species* LUK with Q-sepharose was 54 fold [190].

Both purification approaches were successfully performed for enrichment of the (S)-selective ω -transaminase from the *Burkholderia phytofirmans* strain BS115. Since higher purification fold and recovery were obtained for the purification of other transaminases, several crucial points have to be improved for this attempt. The first point is cell disruption of the cultivation broth. It is clearly shown that cell disruption via sonication is inefficient, thus cell disruption with glass beads seems to be the best and most efficient alternative. The poor recovery and purification fold after enrichment with AEX may be induced through enzyme precipitation

during the process or missing stabilizing PLP, which can be prevented by immediate addition of PLP after elution. Moreover, the linear gradient may be optimized for enhanced elution. Furthermore, additional purification steps have to be performed after AEX, like purification and polishing steps with hydrophobic interaction chromatography (HIC), with phenyl sepharose or butyl sepharose columns and size exclusion chromatography (SEC) in order to achieve a high resolution of the desired enzyme. Another way for the purification of the wild type ω -transaminase may be with a pyridoxal-5'-phosphate affinity column. This is described for a tyrosine aminotransferase purified with pyridoxamine phosphate bound to sepharose [192] and for phosphate kinase and pyridoxamine-5-phosphate oxidase with a pyridoxal sepharose column [193].

6 REFERENCES

- [1] Dold, S.-M., Syldatk, C., Rudat, J., Transaminases and Its Applications, in: Patel, R. (Ed.), *Green Biocatalysis*, 1. ed., WILEY-VCH Verlag, 2016, pp. 715–746.
- [2] Maur, J., Mikrobielle Umsetzung aromatischer β -Aminosäuren, Karlsruhe Institute of Technology, Institute of Process Engineering in Life Sciences Section II: Technical Biology (master thesis), 2012.
- [3] Needham, D.M., A quantitative study of succinic acid in muscle: Glutamic and aspartic acids as precursors. *Biochem. J.* 1930, *24*, 208–227.
- [4] Taylor, P.P., Pantaleone, D.P., Senkpeil, R.F., Fotheringham, I.G., Novel biosynthetic approaches to the production of unnatural amino acids using transaminases. *Trends Biotechnol.* 1998, *16*, 412–418.
- [5] Koszelewski, D., Tauber, K., Faber, K., Kroutil, W., omega-Transaminases for the synthesis of non-racemic alpha-chiral primary amines. *Trends Biotechnol.* 2010, *28*, 324–332.
- [6] Tufvesson, P., Lima-Ramos, J., Jensen, J.S., Al-Haque, N., et al., Process considerations for the asymmetric synthesis of chiral amines using transaminases. *Biotechnol. Bioeng.* 2011, *108*, 1479–1493.
- [7] Hwang, B.Y., Cho, B.K., Yun, H., Koteshwar, K., et al., Revisit of aminotransferase in the genomic era and its application to biocatalysis. *J. Mol. Catal. B-Enzymatic* 2005, *37*, 47–55.
- [8] Rudat, J., Brucher, B.R., Syldatk, C., Transaminases for the synthesis of enantiopure beta-amino acids. *AMB Express* 2012, *2*, 11.
- [9] Mathew H., S.. Y., ω -Transaminases for the Production of Optically Pure Amines and Unnatural Amino Acids. *Am. Chem. Soc.* 2012, *2*, 993–1001.
- [10] Thomsen, M., Skalden, L., Palm, G.J., Höhne, M., et al., Crystallization and preliminary X-ray diffraction studies of the (*R*)-selective amine transaminase from *Aspergillus fumigatus*. *Acta Crystallogr. Sect. F Struct. Biol. Cryst. Commun.* 2013, *69*, 1415–1417.
- [11] Höhne M., Bornscheuer, U., Application of Transaminases, in: Drauz H., K.. G. (Ed.), *Enzyme Catalysis in Organic Synthesis*, Wiley-VCH Verlag GmbH & Co. KGaA, Weinheim, Germany 2012.
- [12] Fuchs, M., Koszelewski, D., Tauber, K., Kroutil, W., et al., Chemoenzymatic asymmetric total synthesis of (*S*)-Rivastigmine using omega-transaminases. *Chem Commun* 2010, *46*, 5500–5502.
- [13] Savile, C.K., Janey, J.M., Mundorff, E.C., Moore, J.C., et al., Biocatalytic Asymmetric Synthesis of Chiral Amines from Ketones Applied to Sitagliptin Manufacture. *Science*, 2010, *329*, 305–309.
- [14] Jansonius, J.N., Structure, evolution and action of vitamin B6-dependent enzymes. *Curr. Opin. Struct. Biol.* 1998, *8*, 759–769.
- [15] Eliot, A.C., Kirsch, J.F., Pyridoxal phosphate enzymes: Mechanistic, structural, and evolutionary considerations. *Annu. Rev. Biochem.* 2004, *73*, 383–415.
- [16] Toney, M.D., Aspartate aminotransferase: an old dog teaches new tricks. *Arch. Biochem. Biophys.* 2014, *544*, 119–127.
- [17] Goto, M., Miyahara, I., Hayashi, H., Kagamiyama, H., et al., Crystal structures of branched-chain amino acid aminotransferase complexed with glutamate and glutarate: true reaction intermediate and double substrate recognition of the enzyme. *Biochemistry* 2003, *42*, 3725–3733.
- [18] Hayashi, H., Mizuguchi, H., Miyahara, I., Nakajima, Y., et al., Conformational change in aspartate aminotransferase on substrate binding induces strain in the catalytic group and enhances catalysis. *J. Biol. Chem.* 2003, *278*, 9481–9488.
- [19] Kirby, A.J., Enzymatic Reaction Mechanisms. Von Perry A. Frey und Adrian D. Hegeman, in: *Angew Chem Int Ed Engl*, WILEY-VCH Verlag, 2007, pp. 8068–8070.
- [20] Humble, M.S., Cassimjee, K.E., Hakansson, M., Kimbung, Y.R., et al., Crystal structures of the *Chromobacterium violaceum* beta-transaminase reveal major structural rearrangements upon binding of coenzyme PLP. *Febs J.* 2012, *279*, 779–792.
- [21] Cassimjee, K.E., Humble, M.S., Land, H., Abedi, V., et al., *Chromobacterium violaceum*

- omega-transaminase variant Trp60Cys shows increased specificity for (*S*)-1-phenylethylamine and 4'-substituted acetophenones, and follows Swain-Lupton parameterisation. *Org. Biomol. Chem.* 2012, 10, 5466–5470.
- [22] Shin, J.S., Yun, H., Jang, J.W., Park, I., et al., Purification, characterization, and molecular cloning of a novel amine:pyruvate transaminase from *Vibrio fluvialis* JS17. *Appl Microbiol Biotechnol* 2003, 61, 463–471.
- [23] Shin, J.S., Kim, B.G., Substrate inhibition mode of omega-transaminase from *Vibrio fluvialis* JS17 is dependent on the chirality of substrate. *Biotechnol. Bioeng.* 2002, 77, 832–837.
- [24] Wybenga, G.G., Crismaru, C.G., Janssen, D.B., Dijkstra, B.W., Structural Determinants of the beta-Selectivity of a Bacterial Aminotransferase. *J. Biol. Chem.* 2012, 287, 28495–28502.
- [25] Höhne, M., Schätzle, S., Jochens, H., Robins, K., et al., Rational assignment of key motifs for function guides in silico enzyme identification. *Nat. Chem. Biol.* 2010, 6, 807–813.
- [26] Sayer, C., Martinez-Torres, R.J., Richter, N., Isupov, M.N., et al., The substrate specificity, enantioselectivity and structure of the (*R*)-selective amine: pyruvate transaminase from *Nectria haematococca*. *FEBS J* 2014, 281, 2240–2253.
- [27] Lyskowski, A., Gruber, C., Steinkellner, G., Schurmann, M., et al., Crystal structure of an (*R*)-selective omega-transaminase from *Aspergillus terreus*. *PLoS One* 2014, 9, e87350.
- [28] Wybenga, G.G., Crismaru, C.G., Janssen, D.B., Dijkstra, B.W., Structural determinants of the beta-selectivity of a bacterial. *J. Biol. Chem.* 2012, 287, 28495–28502.
- [29] Höhne, M., Bornscheuer, U.T., Biocatalytic routes to optically active amines. *ChemCatChem* 2009, 1, 42–51.
- [30] Nugent, T.C., El-Shazly, M., Chiral amine synthesis - Recent developments and trends for enamide reduction, reductive amination, and imine reduction. *Adv. Synth. Catal.* 2010, 352, 753–819.
- [31] Uenishi, J., Hamada, M., Aburatani, S., Matsui, K., et al., Synthesis of chiral nonracemic 1-(2-pyridinyl)ethylamines: Stereospecific introduction of amino function onto the 2-pyridinylmethyl carbon center. *J. Org. Chem.* 2004, 69, 6781–6789.
- [32] Chelucci, G., Baldino, S., Synthesis of 4-diphenylphosphanylmethyl- and 4-phenylthiomethyl-1,4-methano-11,11-dimethyl-1,2,3,4-tetrahydroacridine: new N-P and N-S camphor-derived chiral ligands for asymmetric catalysis. *Tetrahedron-Asymmetry* 2006, 17, 1529–1536.
- [33] Koszelewski, D., Goritzer, M., Clay, D., Seisser, B., et al., Synthesis of Optically Active Amines Employing Recombinant omega-Transaminases in *E. coli* Cells. *ChemCatChem* 2010, 2, 73–77.
- [34] Yun, H., Cho, B.K., Kim, B.G., Kinetic resolution of (*R,S*)-sec-butylamine using omega-transaminase from *Vibrio fluvialis* JS17 under reduced pressure. *Biotechnol. Bioeng.* 2004, 87, 772–778.
- [35] Koszelewski, D., Clay, D., Rozzell, D., Kroutil, W., Deracemisation of alpha-Chiral Primary Amines by a One-Pot, Two-Step Cascade Reaction Catalysed by omega-Transaminases. *European J. Org. Chem.* 2009, 2289–2292.
- [36] Klätte, S., Wendisch, V.F., Redox self-sufficient whole cell biotransformation for amination of alcohols. *Bioorganic Med. Chem.* 2014, 22, 5578–5585.
- [37] Hintermann, T., Seebach, D., Synthesis of a beta-hexapeptide from (*R*)-2-aminomethyl-alkanoic acids and structural investigations. *Synlett* 1997, 437–&.
- [38] Hintermann, T., Seebach, D., The biological stability of beta-peptides: No interactions between alpha- and beta-peptidic structures. *Chimia (Aarau)*. 1997, 51, 244–247.
- [39] Seebach, D., Beck, A.K., Bierbaum, D.J., The World of b - and g -Peptides Comprised of Homologated Proteinogenic Amino Acids and Other Components 2 . From the Biopolymer Poly (b -hydroxybutyric acid ester) to beta -Peptides ± from Organic Synthesis to Departure into a New World 3 . Earlier Work o. *Chem. Biodivers.* 2004, 1, 1111–1239.
- [40] Mekhail, T.M., Markman, M., Paclitaxel in cancer therapy. *Expert Opin Pharmacother*

- 2002, 3, 755–766.
- [41] Ojima, I., Lin, S., Wang, T., Recent advances in the medicinal chemistry of taxoids with novel beta-amino acid side chains. *Curr Med Chem* 1999, 6, 927–954.
- [42] Crews, P., Manes, L. V., Boehler, M., Jasplakinolide, a Cyclodepsipeptide from the Marine Sponge, *Jaspis* Sp. *Tetrahedron Lett.* 1986, 27, 2797–2800.
- [43] Frackenpohl, J., Arvidsson, P.I., Schreiber, J. V, Seebach, D., The outstanding biological stability of beta- and gamma-peptides toward proteolytic enzymes: an in vitro investigation with fifteen peptidases. *Chembiochem* 2001, 2, 445–455.
- [44] Dieter Seebach, Jiirg V. Schreiber , Jennifer L. Matthews, Tobias Hintermann, and Bernhard Jaun, K.G., “Mixed” B-Peptides: A Unique Helical Secondary Structure in Solution. *Helv. Chim. Acta* 1997, Vol. 80, 2033–2038.
- [45] Arvidsson, P.I., Frackenpohl, J., Ryder, N.S., Liechty, B., et al., On the antimicrobial and hemolytic activities of amphiphilic beta-peptides. *Chembiochem* 2001, 2, 771–773.
- [46] Liu, M., Sibi, M.P., Recent advances in the stereoselective synthesis of β -amino acids. *Tetrahedron* 2002, 58, 7991–8035.
- [47] Weiner, B., Szymanski, W., Janssen, D.B., Minnaard, A.J., et al., Recent advances in the catalytic asymmetric synthesis of beta-amino acids. *Chem Soc Rev* 2010, 39, 1656–1691.
- [48] Ashfaq, M., Enantioselective Synthesis of beta-amino acids: A Review. *Med. Chem. (Los. Angeles)*. 2015, 5, 295–309.
- [49] Seebach, D., Overhand, M., Kohnle, F.N.M., Martinoni, B., et al., Beta-Peptides: Synthesis by Arndt-Eistert homologation with concomitant peptide coupling. Structure determination by NMR and CD spectroscopy and by X-ray crystallography. Helical secondary structure of a beta-hexapeptide in solution and its stability towards . *Helv. Chim. Acta* 1996, 79, 913–941.
- [50] Sibi, M.P., Deshpande, P.K., A new methodology for the synthesis of β -amino acids. *J. Chem. Soc. Perkin Trans. 1* 2000, 1461–1466.
- [51] A. Davis, F., Chen, B.-C., Asymmetric synthesis of amino acids using sulfinimines (thiooxime S-oxides). *Chem. Soc. Rev.* 1998, 27, 13.
- [52] Davis, F.A., Szewczyk, J.M., Reddy, R.E., An Efficient Synthesis of (S) - (+) -Ethyl - Amino-3-pyridinepropanoate Using Enantiopure Sulfinimines for the asymmetric synthesis of -amino acids 1 is of the asymmetric synthesis of (S) -ethyl -amino-3-pyridinefibrinogen and is an orally active antip. 1996, 2222–2225.
- [53] Davies, S.G., Walters, A.S., Asymmetric Synthesis of syn- α -Alkyl- p -amino Acids A3. *Reactions* 1994, 1141–1147.
- [54] Bunnage, M.E., Chernega, A.N., Sa, G.D., Goodwinc, C.J., et al., Asymmetric Synthesis of p -Amino- α -Hydroxy Acids. 1994.
- [55] Cimarelli, C., Palmieri, G., Stereoselective reduction of enantiopure beta-enamino esters by hydride: A convenient synthesis of both enantiopure beta-amino esters. *J. Org. Chem.* 1996, 61, 5557–5563.
- [56] Zhu, G., Chen, Z., Zhang, X., Highly Efficient Asymmetric Synthesis of β -Amino Acid Derivatives via Rhodium-Catalyzed Hydrogenation of β -(Acylamino)acrylates. *J. Org. Chem.* 1999, 64, 6907–6910.
- [57] Liu, H., Xu, J., Du, D.M., Asymmetric Friedel-Crafts alkylation of methoxyfuran with nitroalkenes catalyzed by diphenylamine-tethered bis(oxazoline)-Zn(II) complexes. *Org. Lett.* 2007, 9, 4725–4728.
- [58] Gedey, S., Liljeblad, A., Lázár, L., Fülöp, F., et al., Preparation of highly enantiopure β -amino esters by *Candida antarctica* lipase A. *Tetrahedron: Asymmetry* 2001, 12, 105–110.
- [59] Sánchez, V.M., Rebolledo, F., Gotor, V., *Candida antarctica* lipase catalyzed resolution of ethyl (\pm)-3-aminobutyrate. *Tetrahedron: Asymmetry* 1997, 8, 37–40.
- [60] Verkuijl, B.J. V, Szymański, W., Wu, B., Minnaard, A.J., et al., Enantiomerically pure β -phenylalanine analogues from α - β -phenylalanine mixtures in a single reactive extraction step. *Chem. Commun. (Camb)*. 2010, 46, 901.
- [61] Wu, B., Szymanski, W., Heberling, M.M., Feringa, B.L., et al., Aminomutases: mechanistic diversity, biotechnological applications and future perspectives. *Trends*

- Biotechnol.* 2011, 29, 352–362.
- [62] Groger, H., Trauthwein, H., Buchholz, S., Drauz, K., et al., The first aminoacylase-catalyzed enantioselective synthesis of aromatic beta-amino acids. *Org. Biomol. Chem.* 2004, 2, 1977–1978.
- [63] Rehdorf, J., Mihovilovic, M.D., Fraaije, M.W., Bornscheuer, U.T., Enzymatic synthesis of enantiomerically pure beta-amino ketones, beta-amino esters, and beta-amino alcohols with Baeyer-Villiger monooxygenases. *Chemistry (Easton)*. 2010, 16, 9525–9535.
- [64] Slomka, C. Engel, U.I, Syldatk, C. and Rudat, J., Hydrolysis of Hydantoins, Dihydropyrimidines, and Related Compounds, in: *Science of Synthesis: Biocatalysis in Organic Synthesis, Volume 1*, 2014, pp. 373–414.
- [65] Yun, H., Lim, S., Cho, B., Kim, B., ω -Amino Acid: Pyruvate Transaminase from *Alcaligenes denitrificans* Y2k-2 : a New Catalyst for Kinetic Resolution of β -Amino Acids and Amines *Appl. Environ. Microbiol.* 2004, 70, 2529–2534.
- [66] Mathew, S., Bea, H., Nadarajan, S.P., Chung, T., et al., Production of chiral beta-amino acids using omega-transaminase from *Burkholderia graminis*. *J. Biotechnol.* 2015, 196, 1–8.
- [67] Brucher, B., Syldatk, C., Rudat, J., Mikrobielle Umsetzung von β -Phenylalanin mittels neuer Transaminasen. *Chemie-Ingenieur-Technik* 2010, 82, 155–160.
- [68] Kim, J., Kyung, D., Yun, H., Cho, B.K., et al., Cloning and characterization of a novel beta-transaminase from *Mesorhizobium* sp. strain LUK: a new biocatalyst for the synthesis of enantiomerically pure beta-amino acids. *Appl. Environ. Microbiol.* 2007, 73, 1772–1782.
- [69] Mathew, S., Jeong, S.S., Chung, T., Lee, S.H., et al., Asymmetric synthesis of aromatic beta-amino acids using omega-transaminase: Optimizing the lipase concentration to obtain thermodynamically unstable beta-keto acids. *Biotechnol. J.* 2015.
- [70] Gaberc-Porekar, V., Menart, V., Perspectives of immobilized-metal affinity chromatography. *J. Biochem. Biophys. Methods* 2001, 49, 335–360.
- [71] Arnold, F.H., Metal-affinity separations: a new dimension in protein processing. *Biotechnology (N. Y.)*. 1991, 9, 151–156.
- [72] Hochuli, E., Döbeli, H., Schacher, A., New metal chelate adsorbent selective for proteins and peptides containing neighbouring histidine residues. *J. Chromatogr. A* 1987, 411, 177–184.
- [73] Sulkowski, E., Chro-, I.M.A., The Saga of IMAC and MIT. *BioEssays* 1989, 10, 170–175.
- [74] Porath, J., Carlsson, J., Olsson, I., Belfrage, G., Metal chelate affinity chromatography, a new approach to protein fractionation. *Nature* 1975, 258, 598–599.
- [75] Porath, J., Olin, B., Immobilized metal ion affinity adsorption and immobilized metal ion affinity chromatography of biomaterials. Serum protein affinities for gel-immobilized iron and nickel ions. *Biochemistry* 1983, 22, 1621–1630.
- [76] Hochuli, E., Bannwarth, W., Döbeli, H., Genetic Approach to Facilitate Purification of Recombinant Proteins with a Novel Metal Chelate Adsorbent. *Nat.* 1988, 6, 1321–1325.
- [77] David, N.E., Gee, M., Andersen, B., Naider, F., et al., Expression and purification of the *Saccharomyces cerevisiae* alpha-factor receptor (Ste2p), a 7-transmembrane-segment G protein-coupled receptor. *J. Biol. Chem.* 1997, 272, 15553–15561.
- [78] Seidler, A., Introduction of a histidine tail at the N-terminus of a secretory protein expressed in *Escherichia coli*. *Protein Eng.* 1994, 7, 1277–1280.
- [79] Khan, F., He, M., Taussig, M.J., Double-hexahistidine tag with high-affinity binding for protein immobilization, purification, and detection on Ni-nitrilotriacetic acid surfaces. *Anal. Chem.* 2006, 78, 3072–3079.
- [80] Grisshammer, R., Tucker, J., Quantitative evaluation of neurotensin receptor purification by immobilized metal affinity chromatography. *Protein Expr. Purif.* 1997, 11, 53–60.
- [81] Beitzinger, C., Stefani, C., Kronhardt, A., Rolando, M., et al., Role of N-Terminal His6-Tags in Binding and Efficient Translocation of Polypeptides into Cells Using Anthrax Protective Antigen (PA). *PLoS One* 2012, 7.
- [82] Bornhorst, J.A., Falke, J.J., Purification of Proteins Using Polyhistidine Affinity Tags.

- Methods Enzymol.* 2000, 326, 245–254.
- [83] Qu, X., Pu, X., Chen, F., Yang, Y., et al., Molecular cloning, heterologous expression, and functional characterization of an NADPH-cytochrome P450 reductase gene from *Camptotheca acuminata*, a camptothecin-producing plant. *PLoS One* 2015, 10.
- [84] Ralph, E.C., Xiang, L., Cashman, J.R., Zhang, J., His-tag truncated butyrylcholinesterase as a useful construct for in vitro characterization of wild-type and variant butyrylcholinesterases. *Protein Expr. Purif.* 2011, 80, 22–27.
- [85] Chhetri, G., Ghosh, A., Chinta, R., Akhtar, S., et al., Cloning, soluble expression, and purification of the RNA polymerase II subunit RPB5 from *Saccharomyces cerevisiae*. *Bioeng. Bugs* 2015, 6, 62–66.
- [86] Mateo, C., Palomo, J.M., Fernandez-Lorente, G., Guisan, J.M., et al., Improvement of enzyme activity, stability and selectivity via immobilization techniques. *Enzyme Microb. Technol.* 2007, 40, 1451–1463.
- [87] Bornscheuer, U.T., Immobilizing Enzymes: How to Create More Suitable Biocatalysts. *Angew. Chemie Int. Ed.* 2003, 42, 3336–3337.
- [88] Yiu, H.H.P., Keane, M. a., Enzyme-magnetic nanoparticle hybrids: New effective catalysts for the production of high value chemicals. *J. Chem. Technol. Biotechnol.* 2012, 87, 583–594.
- [89] Tuncagil, S., Kayahan, S.K., Bayramoglu, G., Arica, M.Y., et al., L-Dopa synthesis using tyrosinase immobilized on magnetic beads. *J. Mol. Catal. B Enzym.* 2009, 58, 187–193.
- [90] Bozhinova, D., Galunsky, B., Yueping, G., Franzreb, M., et al., Evaluation of magnetic polymer micro-beads as carriers of immobilised biocatalysts for selective and stereoselective transformations. *Biotechnol. Lett.* 2004, 26, 343–50.
- [91] Jia, H., Huang, F., Gao, Z., Zhong, C., et al., Immobilization of ω -transaminase by magnetic PVA-Fe₃O₄ nanoparticles. *Biotechnol. Reports* 2016.
- [92] Motejaded, H., Kranz, B., Berensmeier, S., Franzreb, M., et al., Expression, one-step purification, and immobilization of HaloTag™ fusion proteins on chloroalkane-functionalized magnetic beads. *Appl. Biochem. Biotechnol.* 2010, 162, 2098–2110.
- [93] Frommel, M., Nowak, J., Lazarovits, G., Growth Enhancement and Developmental Modifications of in Vitro Grown Potato (*Solanum tuberosum* spp. *tuberosum*) as Affected by a Nonfluorescent *Pseudomonas* sp. *Plant Physiol.* 1991, 96, 928–936.
- [94] Sessitsch, A., Coenye, T., Sturz, A. V., Vandamme, P., et al., *Burkholderia phytofirmans* sp. nov., a novel plant-associated bacterium with plant-beneficial properties. *Int J Syst Evol Microbiol* 2005, 55, 1187–1192.
- [95] Compant, S., Kaplan, H., Sessitsch, A., Nowak, J., et al., Endophytic colonization of *Vitis vinifera* L. by *Burkholderia phytofirmans* strain PsJN: From the rhizosphere to inflorescence tissues. *FEMS Microbiol. Ecol.* 2008, 63, 84–93.
- [96] Nowak, J., Benefits of in vitro “biotization” of plant tissue cultures with microbial inoculants. *Vitr. Cell. Dev. Biol. - Plant* 1998, 34, 122–130.
- [97] Sharma, V.K., Nowak, J., Enhancement of verticillium wilt resistance in tomato transplants by in vitro co-culture of seedlings with a plant growth promoting rhizobacterium (*Pseudomonas* sp. strain PsJN). *Can. J. Microbiol.* 1998, 44, 528–536.
- [98] Lazarovits, G., Nowak, J., Rhizobacteria for improvement of plant growth and establishment, in: *HortScience*, 1997, pp. 188–192.
- [99] Nowak, J., Asiedu, S.K., Bensalim, S., Richards, J., et al., From laboratory to applications: challenges and progress with in vitro dual cultures of potato and beneficial bacteria. *Plant Cell. Tissue Organ Cult.* 1998, 52, 97–103.
- [100] Wang, K., Conn, K., Lazarovits, G., Involvement of quinolinate phosphoribosyl transferase in promotion of potato growth by a *burkholderia* strain. *Appl. Environ. Microbiol.* 2006, 72, 760–768.
- [101] Ait Barka, E., Nowak, J., Clément, C., Enhancement of chilling resistance of inoculated grapevine plantlets with a plant growth-promoting rhizobacterium, *Burkholderia phytofirmans* strain PsJN. *Appl. Environ. Microbiol.* 2006, 72, 7246–7252.
- [102] Fernandez, O., Vandesteene, L., Feil, R., Baillieux, F., et al., Trehalose metabolism is activated upon chilling in grapevine and might participate in *Burkholderia phytofirmans* induced chilling tolerance. *Planta* 2012, 236, 355–369.

- [103] Fernandez, O., Theocharis, A., Bordiec, S., Feil, R., et al., *Burkholderia phytofirmans* PsJN acclimates grapevine to cold by modulating carbohydrate metabolism. *Mol. Plant-Microbe Interact.* 2012, 25, 496–504.
- [104] Su, F., Jacquard, C., Villaume, S., Michel, J., et al., *Burkholderia phytofirmans* PsJN reduces impact of freezing temperatures on photosynthesis in *Arabidopsis thaliana*. *Front. Plant Sci.* 2015, 6, 1–13.
- [105] Naveed, M., Mitter, B., Reichenauer, T.G., Wieczorek, K., et al., Increased drought stress resilience of maize through endophytic colonization by *Burkholderia phytofirmans* PsJN and *Enterobacter* sp. FD17. *Environ. Exp. Bot.* 2014, 97, 30–39.
- [106] Sheibani-Tezerji, R., Rattei, T., Sessitsch, A., Trognitz, F., et al., Transcriptome Profiling of the Endophyte *Burkholderia phytofirmans* PsJN Indicates Sensing of the Plant Environment and Drought Stress. *MBio* 2015, 6, e00621–15.
- [107] Zhao, S., Wei, H., Lin, C.-Y., Zeng, Y., et al., *Burkholderia phytofirmans* Inoculation-Induced Changes on the Shoot Cell Anatomy and Iron Accumulation Reveal Novel Components of *Arabidopsis*-Endophyte Interaction that Can Benefit Downstream Biomass Deconstruction. *Front. Plant Sci.* 2016, 7, 1–12.
- [108] Pinedo, I., Ledger, T., Greve, M., Poupin, M.J., *Burkholderia phytofirmans* PsJN induces long-term metabolic and transcriptional changes involved in *Arabidopsis thaliana* salt tolerance. *Front. Plant Sci.* 2015, 6, 1–17.
- [109] Weilharter, A., Mitter, B., Shin, M. V., Chain, P.S.G., et al., Complete genome sequence of the plant growth-promoting endophyte *Burkholderia phytofirmans* strain PsJN. *J. Bacteriol.* 2011, 193, 3383–3384.
- [110] Hussain, Z., Wiedner, R., Steiner, K., Hajek, T., et al., Characterization of two bacterial hydroxynitrile lyases with high similarity to cupin superfamily proteins. *Appl. Environ. Microbiol.* 2012, 78, 2053–2055.
- [111] Nojiri, M., Hibi, M., Shizawa, H., Horinouchi, N., et al., Imidase catalyzing desymmetric imide hydrolysis forming optically active 3-substituted glutaric acid monoamides for the synthesis of gamma-aminobutyric acid (GABA) analogs. *Appl. Microbiol. Biotechnol.* 2015, 99, 9961–9969.
- [112] Lal, R., Sukbuntherng, J., Tai, E.H.L., Upadhyay, S., et al., Arbaclofen placarbil, a novel R-baclofen prodrug: improved absorption, distribution, metabolism, and elimination properties compared with R-baclofen. *J. Pharmacol. Exp. Ther.* 2009, 330, 911–921.
- [113] Hampson, D.R., Adusei, D.C., Pacey, L.K.K., The neurochemical basis for the treatment of autism spectrum disorders and Fragile X Syndrome. *Biochem. Pharmacol.* 2011, 81, 1078–1086.
- [114] Vu, H.P., Mu, A., Moreau, J.W., Biodegradation of thiocyanate by a novel strain of *Burkholderia phytofirmans* from soil contaminated by gold mine tailings. *Lett. Appl. Microbiol.* 2013, 57, 368–372.
- [115] Iwanicka-Nowicka, R., Zielak, A., Cook, A.M., Thomas, M.S., et al., Regulation of sulfur assimilation pathways in *Burkholderia cenocepacia*: Identification of transcription factors CysB and SsuR and their role in control of target genes. *J. Bacteriol.* 2007, 189, 1675–1688.
- [116] Crismaru, C.G., Wybenga, G.G., Szymanski, W., Wijma, H.J., et al., Biochemical properties and crystal structure of a beta-phenylalanine aminotransferase from *Variovorax paradoxus*. *Appl. Environ. Microbiol.* 2013, 79, 185–195.
- [117] Brucher, B.S.C.R.J., Mikrobielle Umsetzung von b-Phenylalanin mittels neuer Transaminasen. *Chemie Ing. Tech.* 2010, 82, 155–160.
- [118] Aberhart, D.J., Separation by high-performance liquid chromatography of α - and β -amino acids: Application to assays of lysine 2,3-aminomutase and leucine 2,3-aminomutase. *Anal. Biochem.* 1988, 169, 350–355.
- [119] Brucher, B., Rudat, J., Syltatk, C., Vielhauer, O., Enantioseparation of Aromatic beta(A3)-Amino acid by Precolumn Derivatization with o-Phthaldialdehyde and N-Isobutyryl-L-cysteine. *Chromatographia* 2010, 71, 1063–1067.
- [120] Laemmli, U.K., Cleavage of structural proteins during the assembly of the head of bacteriophage T4. *Nature* 1970, 227, 680–685.
- [121] Scopes, R.K., Overview of protein purification and characterization. *Curr. Protoc.*

- Protein Sci.* 2001, *Chapter 1*, Unit 1.1.
- [122] Päiviö, M., Kanerva, L.T., Reusable ω -transaminase sol-gel catalyst for the preparation of amine enantiomers. *Process Biochem.* 2013, *48*, 1488–1494.
- [123] Truppo, M.D., Turner, N.J., Rozzell, J.D., Efficient kinetic resolution of racemic amines using a transaminase in combination with an amino acid oxidase. *Chem. Commun.* 2009, *16*, 2127–2129.
- [124] Tabor, S., Richardson, C.C., Polymerase/Promoter. 1985, *82*, 1074–1078.
- [125] Studier, F.W., Moffatt, B. a, Use of bacteriophage T7 RNA polymerase to direct selective high-level expression of cloned genes. *J. Mol. Biol.* 1986, *189*, 113–130.
- [126] Dubendorf, J.W., Studier, F.W., Controlling basal expression in an inducible T7 expression system by blocking the target T7 promoter with lac repressor. *J. Mol. Biol.* 1991, *219*, 45–59.
- [127] Wu, J., Filutowicz, M., Hexahistidine (His6)-tag dependent protein dimerization: A cautionary tale. *Acta Biochim. Pol.* 1999, *46*, 591–599.
- [128] Terpe, K., Overview of bacterial expression systems for heterologous protein production: From molecular and biochemical fundamentals to commercial systems. *Appl. Microbiol. Biotechnol.* 2006, *72*, 211–222.
- [129] Halliwell, C.M., Morgan, G., Ou, C.P., Cass, A.E., Introduction of a (poly)histidine tag in L-lactate dehydrogenase produces a mixture of active and inactive molecules. *Anal. Biochem.* 2001, *295*, 257–61.
- [130] Truppo, M.D., Rozzell, J.D., Moore, J.C., Turner, N.J., Rapid screening and scale-up of transaminase catalysed reactions. *Org. Biomol. Chem.* 2009, *7*, 395–398.
- [131] Svedendahl, M., Branneby, C., Lindberg, L., Berglund, P., Reversed Enantiopreference of an omega-Transaminase by a Single-Point Mutation. *ChemCatChem* 2010, *2*, 976–980.
- [132] Hohne, M., Schatzle, S., Jochens, H., Robins, K., et al., Rational assignment of key motifs for function guides in silico enzyme identification. *Nat Chem Biol* 2010, *6*, 807–813.
- [133] Humble, M.S., Cassimjee, K.E., Håkansson, M., Kimbung, Y.R., et al., Crystal structures of the *Chromobacterium violaceum* ω -transaminase reveal major structural rearrangements upon binding of coenzyme PLP. *FEBS J.* 2012, *279*, 779–792.
- [134] Kim, B., Park, O.K., Bae, J.Y., Jang, T., et al., Crystallization and preliminary X-ray crystallographic studies of β -transaminase from *Mesorhizobium* sp. strain LUK. *Acta Crystallogr. Sect. F. Struct. Biol. Cryst. Commun.* 2011, *67*, 231–3.
- [135] Lo, H., Chen, Y.-Z., Chi, M.-C., Lin, L.-L., Simultaneous Purification and Immobilization of Histidine-tagged *Bacillus licheniformis* Aldehyde Dehydrogenase on Metal Affinity Magnetic Beads. *J. Pure Appl. Microbiol.* 2012, *7*, 21–29.
- [136] Ha, E.J., Kim, K.K., Park, H.S., Lee, S.G., et al., One-step immobilization and purification of his-tagged enzyme using poly(2-acetamidoacrylic acid) hydrogel. *Macromol. Res.* 2013, *21*, 5–9.
- [137] Casella, L., Gullotti, M., Pacchioni, G., Coordination Modes. *J. Am. Chem. Soc.* 1982, *104*, 2386–2396.
- [138] Humble, M.S., Cassimjee, K.E., Hakansson, M., Kimbung, Y.R., et al., Crystal structures of the *Chromobacterium violaceum* omega-transaminase reveal major structural rearrangements upon binding of coenzyme PLP. *Febs J.* 2012, *279*, 779–792.
- [139] Stepuro II, Artsukevich, A.N., Solodunov, A.A., [Complexes of Cu²⁺ with pyridoxal-5'-phosphate and human and bovine serum albumin]. *Mol Biol* 1984, *18*, 813–820.
- [140] Arakawa, T., Timasheff, S.N., The stabilization of proteins by osmolytes. *Biophys. Soc.* 1985, *47*, 411–414.
- [141] Koszelewski, D., Muller, N., Schrittwieser, J.H., Faber, K., et al., Immobilization of omega-transaminases by encapsulation in a sol-gel/celite matrix. *J. Mol. Catal. B-Enzymatic* 2010, *63*, 39–44.
- [142] Martin, A.R., Shonnard, D., Pannuri, S., Kamat, S., Characterization of free and immobilized (S)-aminotransferase for acetophenone production. *Appl Microbiol Biotechnol* 2007, *76*, 843–851.
- [143] Mallin, H., Hohne, M., Bornscheuer, U.T., Immobilization of (R)- and (S)-amine

- transaminases on chitosan support and their application for amine synthesis using isopropylamine as donor. *J. Biotechnol.* 2014.
- [144] Nawani, N., Singh, R., Kaur, J., Immobilization and stability studies of a lipase from thermophilic *Bacillus* sp: The effect of process parameters on immobilization of enzyme. *Electron. J. Biotechnol.* 2006, 9, 559–565.
- [145] Yi, S.S., Lee, C.W., Kim, J., Kyung, D., et al., Covalent immobilization of omega-transaminase from *Vibrio fluvialis* JS17 on chitosan beads. *Process Biochem.* 2007, 42, 895–898.
- [146] Srinivasa Rao, R., Borkar, P.S., Khobragade, C.N., Sagar, a. D., Enzymatic activities of proteases immobilized on tri(4-formyl phenoxy) cyanurate. *Enzyme Microb. Technol.* 2006, 39, 958–962.
- [147] Atia, K.S., El-Batal, A., Preparation of glucose oxidase immobilized in different carriers using radiation polymerization. *J. Chem. Technol. Biotechnol.* 2005, 80, 805–811.
- [148] Kozlov, E.I., L'vova, M.S., Stability of water-soluble vitamins and coenzymes. Hydrolysis of pyridoxal-5-phosphate in acidic, neutral, and weakly alkaline solutions. *Pharm. Chem. J.* 1977, 11, 1543–1549.
- [149] Ugwu, S.O., Apte, S.P., The Effect of Buffers on Protein Conformational Stability. *Pharm. Technol.* 2004, 28, 86–109.
- [150] Mutaguchi, Y., Ohmori, T., Wakamatsu, T., Doi, K., et al., Identification, purification, and characterization of a novel amino acid racemase, isoleucine 2-epimerase, from *Lactobacillus* Species. *J. Bacteriol.* 2013, 195, 5207–5215.
- [151] Sung, M.H., Tanizawa, K., Tanaka, H., Kuramitsu, S., et al., Purification and Characterization of Thermostable Aspartate Aminotransferase from a Thermophilic *Bacillus* Species. *J. Bacteriol.* 1990, 172, 1345–1351.
- [152] Park, E., Kim, M., Shin, J.S., One-Pot Conversion of L-Threonine into L-Homoalanine: Biocatalytic Production of an Unnatural Amino Acid from a Natural One. *Adv. Synth. Catal.* 2010, 352, 3391–3398.
- [153] Malik, M.S., Park, E.S., Shin, J.S., Features and technical applications of omega-transaminases. *Appl Microbiol Biotechnol* 2012, 94, 1163–1171.
- [154] Seo, J.-H., Kyung, D., Joo, K., Lee, J., et al., Necessary and sufficient conditions for the asymmetric synthesis of chiral amines using ω -aminotransferases. *Biotechnol. Bioeng.* 2011, 108, 253–263.
- [155] Mateo, C., Palomo, J.M., Fernandez-Lorente, G., Guisan, J.M., et al., Improvement of enzyme activity, stability and selectivity via immobilization techniques. *Enzyme Microb. Technol.* 2007, 40, 1451–1463.
- [156] Palomo, J.M., Fernandez-Lorente, G., Mateo, C., Ortiz, C., et al., Modulation of the enantioselectivity of lipases via controlled immobilization and medium engineering: Hydrolytic resolution of mandelic acid esters. *Enzyme Microb. Technol.* 2002, 31, 775–783.
- [157] Kunz, W., Lo Nostro, P., Ninham, B.W., The present state of affairs with Hofmeister effects. *Curr. Opin. Colloid Interface Sci.* 2004, 9, 1–18.
- [158] Akkuş Çetinus, Ş., Nursevin Öztop, H., Immobilization of catalase into chemically crosslinked chitosan beads. *Enzyme Microb. Technol.* 2003, 32, 889–894.
- [159] Dessouki, A.M., Atia, K.S., Immobilization of adenosine deaminase onto agarose and casein. *Biomacromolecules* 2002, 3, 432–437.
- [160] Ni, K., Zhou, X., Zhao, L., Wang, H., et al., Magnetic catechol-chitosan with bioinspired adhesive surface: preparation and immobilization of omega-transaminase. *PLoS One* 2012, 7, e41101.
- [161] Martin, A.R., Shonnard, D., Pannuri, S., Kamat, S., Characterization of free and immobilized (S)-aminotransferase for acetophenone production. *Appl. Microbiol. Biotechnol.* 2007, 76, 843–851.
- [162] Morhardt, C., Ketterer, B., Heißler, S., Franzreb, M., Direct quantification of immobilized enzymes by means of FTIR ATR spectroscopy - A process analytics tool for biotransformations applying non-porous magnetic enzyme carriers. *J. Mol. Catal. B Enzym.* 2014, 107, 55–63.
- [163] Pleiss, J., Fischer, M., Schmid, R.D., Anatomy of lipase binding sites: The scissile fatty

- acid binding site. *Chem. Phys. Lipids* 1998, 93, 67–80.
- [164] Smith, L.C., Faustinella, F., Chan, L., Lipases: three-dimensional structure and mechanism of action. *Curr. Opin. Struct. Biol.* 1992, 2, 490–496.
- [165] Domínguez De María, P., Sánchez-Montero, J.M., Sinisterra, J. V., Alcántara, A.R., Understanding *Candida rugosa* lipases: An overview. *Biotechnol. Adv.* 2006, 24, 180–196.
- [166] Benjamin, S., Pandey, A., *Candida rugosa* lipases: Molecular biology and versatility in biotechnology. *Yeast* 1998, 14, 1069–1087.
- [167] Johnson, S.L., NoGeneral Base and Nucleophilic Catalysis of Ester Hydrolysis and Related Reactions, in: *Advances in Physical Organic Chemistry*, 1967, pp. 237–330.
- [168] Kim, J., Kyung, D., Yun, H., Cho, B.K., et al., Cloning and characterization of a novel omega-transaminase from *Mesorhizobium* sp. strain LUK: A new biocatalyst for the synthesis of enantiomerically pure beta-amino acids. *Appl. Environ. Microbiol.* 2007, 73, 1772–1782.
- [169] Mano, J., Ogawa, J., Shimizu, S., Microbial production of optically active beta-phenylalanine through stereoselective degradation of racemic beta-phenylalanine. *Biosci. Biotechnol. Biochem.* 2006, 70, 1941–6.
- [170] Bea, H.-S., Park, H.-J., Lee, S.-H., Yun, H., Kinetic resolution of aromatic β -amino acids by ω -transaminase. *Chem. Commun. (Camb)*. 2011, 47, 5894–5896.
- [171] Cripps, R.E., Noble, A.S., The Microbial Metabolism of Acetophenone. *Biochem J* 1975, 152, 233–241.
- [172] Harwood, C.S., Parales, R.E., The B -Ketoacid Pathway and the Biology of Self-Identity. *Annu. Rev. Microbiol.* 1996, 50, 553–590.
- [173] Daubaras, D., Saido, K., Chakrabarty, A., Purification of hydroxyquinol 1, 2-dioxygenase and maleylacetate reductase: the lower pathway of 2, 4, 5-trichlorophenoxyacetic acid metabolism by *Burkholderia cepacia* AC1100. *Appl. Environ. Microbiol.* 1996, 62, 4276–4279.
- [174] Nakano, Y., Tokunaga, H., Kitaoka, S., Two omega-amino acid transaminases from *Bacillus cereus*. *J. Biochem.* 1977, 81, 1375–1381.
- [175] Iwasaki, A., Yamada, Y., Kizaki, N., Ikenaka, Y., et al., Microbial synthesis of chiral amines by (*R*)-specific transamination with *Arthrobacter* sp. KNK168. *Appl Microbiol Biotechnol* 2006, 69, 499–505.
- [176] Iwasaki, A., Matsumoto, K., Hasegawa, J., Yasohara, Y., A novel transaminase, (*R*)-amine:pyruvate aminotransferase, from *Arthrobacter* sp. KNK168 (FERM BP-5228): purification, characterization, and gene cloning. *Appl Microbiol Biotechnol* 2012, 93, 1563–1573.
- [177] Han, K., Han, K., Lim, H.C., Lim, H.C., et al., Acetic acid formation in *Escherichia coli* fermentation. *Biotechnol. Bioeng.* 1992, 39, 663–671.
- [178] Krebs, H.A., Metabolism of amino-acids: Deamination of amino-acids. *Biochem. J.* 1935, 29, 1620–44.
- [179] Peacock, S.J., Chieng, G., Cheng, A.C., David, A., et al., Comparison of Ashdown 's Medium , *Burkholderia cepacia* Medium , and *Burkholderia pseudomallei* Selective Agar for Clinical Isolation of *Burkholderia pseudomallei*. *Society* 2005, 43, 5359–5361.
- [180] Liu, C.H., Chen, C.Y., Wang, Y.W., Chang, J.S., Fermentation strategies for the production of lipase by an indigenous isolate *Burkholderia* sp. C20. *Biochem. Eng. J.* 2011, 58-59, 96–102.
- [181] Reckseidler-zenteno, S.L., Devinney, R., Woods, D.E., The Capsular Polysaccharide of *Burkholderia pseudomallei* Contributes to Survival in Serum by Reducing Complement Factor C3b Deposition. *Society* 2005, 73, 1106–1115.
- [182] Reckseidler, S.L., Capsular Polysaccharides Produced by the Bacterial Pathogen *Burkholderia pseudomallei*. *The Complex World of Polysaccharides* 2012, 128–152.
- [183] Hatcher, C.L., Muruato, L.A., Torres, A.G., Recent Advances in *Burkholderia mallei* and *B. pseudomallei* Research. *Curr. Trop. Med. Reports* 2015, 2, 62–69.
- [184] Banerjee, A., Chase, M., Clayton, R.A., Landis, B., Methods for the stereoselective synthesis and enantiomeric enrichment of b-amino acids. 2005.
- [185] Shin, G., Mathew, S., Yun, H., Kinetic resolution of amines by (*R*)-selective omega-

- transaminase from *Mycobacterium vanbaalenii*. *J. Ind. Eng. Chem.* 2015, 23, 128–133.
- [186] Park, E.S., Dong, J.Y., Shin, J.S., Active site model of (*R*)-selective omega-transaminase and its application to the production of D-amino acids. *Appl Microbiol Biotechnol* 2014, 98, 651–660.
- [187] Park, E.S., Shin, J.S., Free energy analysis of omega-transaminase reactions to dissect how the enzyme controls the substrate selectivity. *Enzyme Microb. Technol.* 2011, 49, 380–387.
- [188] Hirotsu, K., Goto, M., Okamoto, A., Miyahara, I., Dual substrate recognition of aminotransferases. *Chem. Rec.* 2005, 5, 160–172.
- [189] Shin, G., Mathew, S., Yun, H., Kinetic resolution of amines by (*R*)-selective omega-transaminase from *Mycobacterium vanbaalenii*. *J. Ind. Eng. Chem.* 2015, 23, 128–133.
- [190] Kim, J., Kyung, D., Yun, H., Cho, B.K., et al., Screening and purification of a novel transaminase catalyzing the transamination of aryl beta-amino acid from *Mesorhizobium* sp. LUK. *J. Microbiol. Biotechnol.* 2006, 16, 1832–1836.
- [191] Ito, N., Kawano, S., Hasegawa, J., Yasohara, Y., Purification and characterization of a novel (*S*)-enantioselective transaminase from *Pseudomonas fluorescens* KNK08-18 for the synthesis of optically active amines. *Biosci. Biotechnol. Biochem.* 2011, 75, 2093–8.
- [192] Miller, J., Cuatrecasa, P., Thompson, B., PURIFICATION OF TYROSINE AMINOTRANSFERASE BY AFFINITY CHROMATOGRAPHY. *Biochim. Biophys. Acta* 1972, 276, 407–415.
- [193] Cash, C.D., Maitre, M., Rumigny, J.F., Mandel, P., Rapid purification by affinity chromatography of rat brain pyridoxal kinase and pyridoxamine-5-phosphate oxidase. *Biochem. Biophys. Res. Commun.* 1980, 96, 1755–60.

7 APPENDICES

7.1 SEQUENCE OF THE β -AMINO ACID AMINOTRANSFERASE

Sequence with the restriction sites Nde I and Xho I for the vector pET21b

```
CATATGACCCATGCCGCCATAGACCAGGCCCTTGCCGATGCGTACCGGCGCTTCACCGAC
GCCAATCCGGCCAGCCAGCGCCAGTTCGAGGGCGCAGGCGCGCTACATGCCCGAGCCAAC
AGCCGCTCCGTGCTGTTCTACGCGCCGTTCCCCCTGACCATCGCCAGGGGCGAAGGCGCC
GCGCTGTGGGACGCCGACGGCCACCGCTACGCCGACTTCATTGCCGAGTACACGGCCGGT
GTCTACGGCCACTCCGCGCCGAAATCCGCGATGCGGTCATCGAGGCGATGCAGGGCGGC
ATCAACCTCACCGGGCACAACCTGCTCGAAGGACGGCTGGCCCGGCTGATCTGCGAGCGC
TTTCCGAGATCGAGCAGCTGCGCTTCACCAACTCGGGCACCGAGGCCAACCTGATGGCG
CTCACGGCGGGCGCTGCACTTCACGGGGCGCAGGAAGATCGTCGTGTTCTCGGGCGGCTAC
CACGGCGGGGTGCTGGGCTTCGGCGCCAGGCCTTCGCCGACCACCGTGCCGTTTCGACTTT
CTCGTGCTGCCCTATAACGACGCGCAAACGGCCCCGCGCAGATCGAACGGCACGGCCCC
GAGATCGCCGTGGTATTGGTCGAGCCGATGCAGGGCGCGAGCGGCTGCATTCCGGGGCAA
CCCGACTTCCTGCAGGCCCTGCGCGAGTTCGGCCACGCAGGTGGGCGCGCTGCTGGTCTTC
GACGAAGTCATGACCTCGCGGCTCGCGCCGATGGGCTGGCGAACAAGCTCGGCATCCGT
TCGGACCTGACCACGCTGGGCAAGTACATCGGCGGGCGGCATGTCTTTTGGTGCGTTCGGC
GGGCGCGCCGACGTGATGGCACTGTTTCGACCCGCGTACCGGTCCGCTGGCCCATTCGGGC
ACCTTCAACAACAACGTGATGACGATGGCGGCCGGCTATGCCGGGCTCACGAAGCTTTTC
ACGCCCCGAGGCGGCCGGTTCGCTGGCCGAGAGGGGCGAGGCGCTGCGCGCGCGGCTCAAC
GCGCTGTGCGCGAACGAGGGCGTCGCCATGCAGTTCACCGGCATCGGCTCGCTGATGAAC
GCGCATTTTCGTGCAGGGCGATGTACGCAGCAGCGAAGACCTGGCGGGCGGTCGACGGCCGG
CTGCGGCAGCTGTTGTTCTTCCACCTGCTGAACGAGGATATCTACAGCTCGCCGCGCGGC
TTCGTGCTGCTGTGCTGCCGCTGACGGATGCGGACATCGACCGCTACGTGGCCGCCATC
GGCAGCTTCATCGGCGGGCACGGGGCGCTGCTGCCCCGCGCGAACCTCGAG
```

Sequence with the restriction sites Nde I and BamH I for the vector pET11a

```
CATATGACCCATGCCGCCATAGACCAGGCCCTTGCCGATGCGTACCGGCGCTTCACCGAC
GCCAATCCGGCCAGCCAGCGCCAGTTCGAGGGCGCAGGCGCGCTACATGCCCGAGCCAAC
AGCCGCTCCGTGCTGTTCTACGCGCCGTTCCCCCTGACCATCGCCAGGGGCGAAGGCGCC
GCGCTGTGGGACGCCGACGGCCACCGCTACGCCGACTTCATTGCCGAGTACACGGCCGGT
GTCTACGGCCACTCCGCGCCGAAATCCGCGATGCGGTCATCGAGGCGATGCAGGGCGGC
ATCAACCTCACCGGGCACAACCTGCTCGAAGGACGGCTGGCCCGGCTGATCTGCGAGCGC
TTTCCGAGATCGAGCAGCTGCGCTTCACCAACTCGGGCACCGAGGCCAACCTGATGGCG
CTCACGGCGGGCGCTGCACTTCACGGGGCGCAGGAAGATCGTCGTGTTCTCGGGCGGCTAC
CACGGCGGGGTGCTGGGCTTCGGCGCCAGGCCTTCGCCGACCACCGTGCCGTTTCGACTTT
CTCGTGCTGCCCTATAACGACGCGCAAACGGCCCCGCGCAGATCGAACGGCACGGCCCC
GAGATCGCCGTGGTATTGGTCGAGCCGATGCAGGGCGCGAGCGGCTGCATTCCGGGGCAA
CCCGACTTCCTGCAGGCCCTGCGCGAGTTCGGCCACGCAGGTGGGCGCGCTGCTGGTCTTC
GACGAAGTCATGACCTCGCGGCTCGCGCCGATGGGCTGGCGAACAAGCTCGGCATCCGT
TCGGACCTGACCACGCTGGGCAAGTACATCGGCGGGCGGCATGTCTTTTGGTGCGTTCGGC
GGGCGCGCCGACGTGATGGCACTGTTTCGACCCGCGTACCGGTCCGCTGGCCCATTCGGGC
ACCTTCAACAACAACGTGATGACGATGGCGGCCGGCTATGCCGGGCTCACGAAGCTTTTC
ACGCCCCGAGGCGGCCGGTTCGCTGGCCGAGAGGGGCGAGGCGCTGCGCGCGCGGCTCAAC
GCGCTGTGCGCGAACGAGGGCGTCGCCATGCAGTTCACCGGCATCGGCTCGCTGATGAAC
GCGCATTTTCGTGCAGGGCGATGTACGCAGCAGCGAAGACCTGGCGGGCGGTCGACGGCCGG
CTGCGGCAGCTGTTGTTCTTCCACCTGCTGAACGAGGATATCTACAGCTCGCCGCGCGGC
TTCGTGCTGCTGTGCTGCCGCTGACGGATGCGGACATCGACCGCTACGTGGCCGCCATC
GGCAGCTTCATCGGCGGGCACGGGGCGCTGCTGCCCCGCGCGAACCTAGGGATCC
```

7.2 PLASMID CARD

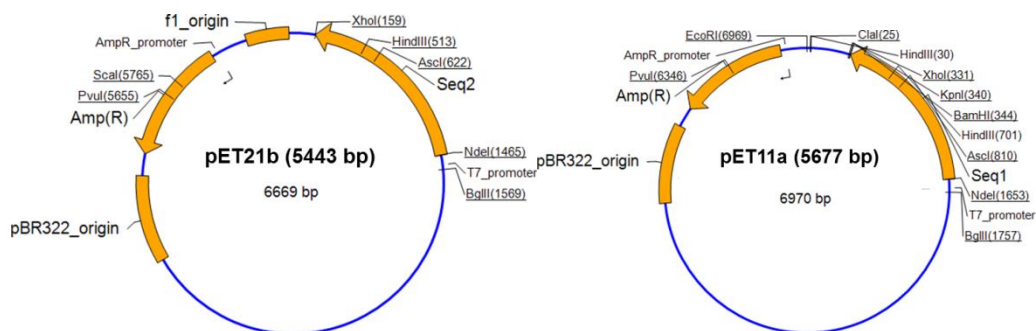


Figure 7.1: Plasmid card of plasmid pET21b and pET11a containing the encoding gene of the β-amino acid aminotransferase from *Variovorax paradoxus* (Seq 2).

7.3 FREEZING AND THAWING

Freezing and thawing of the immobilized aminotransferase and the crude cell extract.

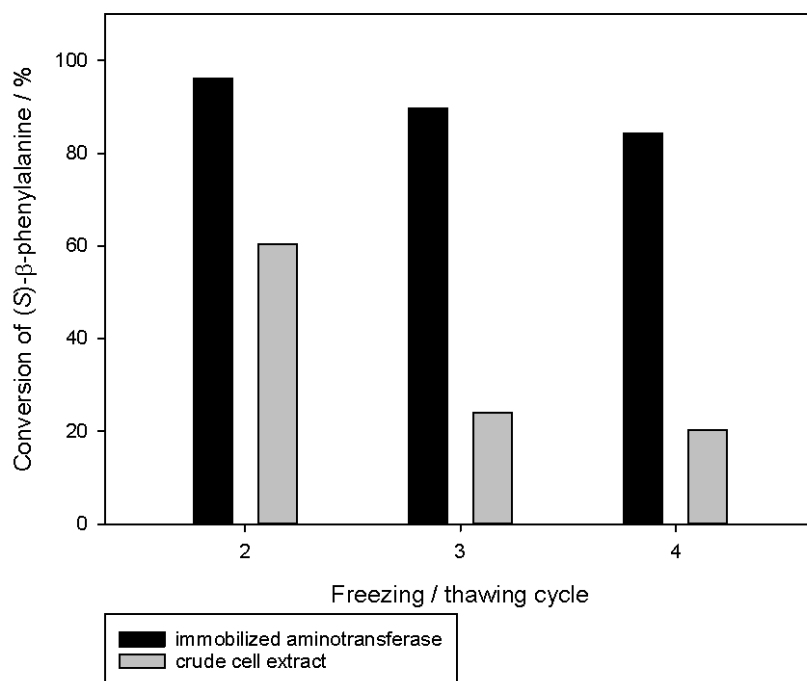


Figure 7.2: Freezing and thawing of the immobilized aminotransferase and the crude cell extract. Freezing was performed by incubating with liquid nitrogen.

7.4 CONVERSION OF *RAC*- β -PHENYLALANINE WITH β -AMINO ACID AMINOTRANSFERASE

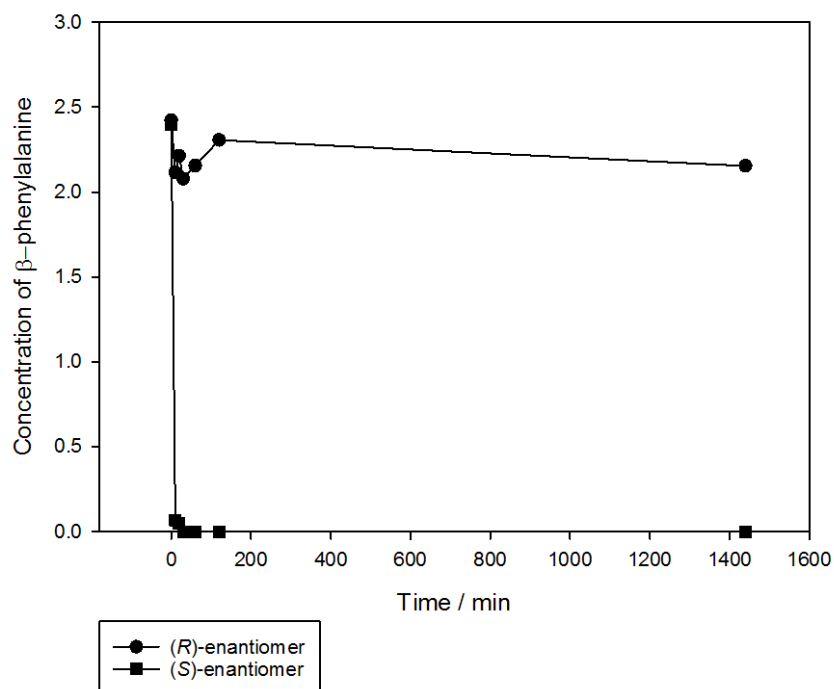


Figure 7.3: Conversion of the *rac*- β -phenylalanine with the His-tagged β -amino acid aminotransferase. The reaction conditions were: 5 mM *rac*- β -phenylalanine, 5 mM α -ketoglutarate, 0.2 mM PLP and 1 mg aminotransferase. The (*R*)-enantiomer is not converted at all, the (*S*)-enantiomer is converted after 10 min.

7.5 ACTIVITY OF THE AMINOTRANSFERASE IN THE PRESENCE OF DMSO

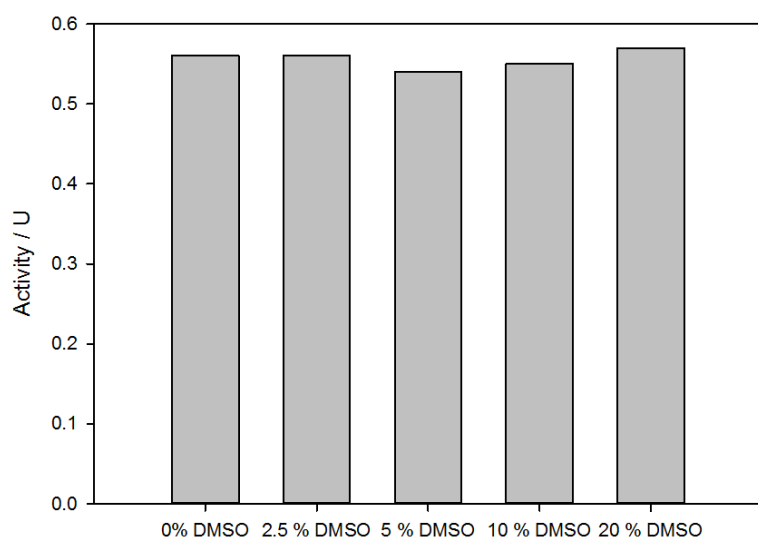


Figure 7.4: Activity of aminotransferase in the presence of several DMSO concentrations.

7.6 ASYMMETRIC SYNTHESIS STARTING WITH THE PROCHIRAL KETONE 3-OXO-3-PHENYL PROPIONATE

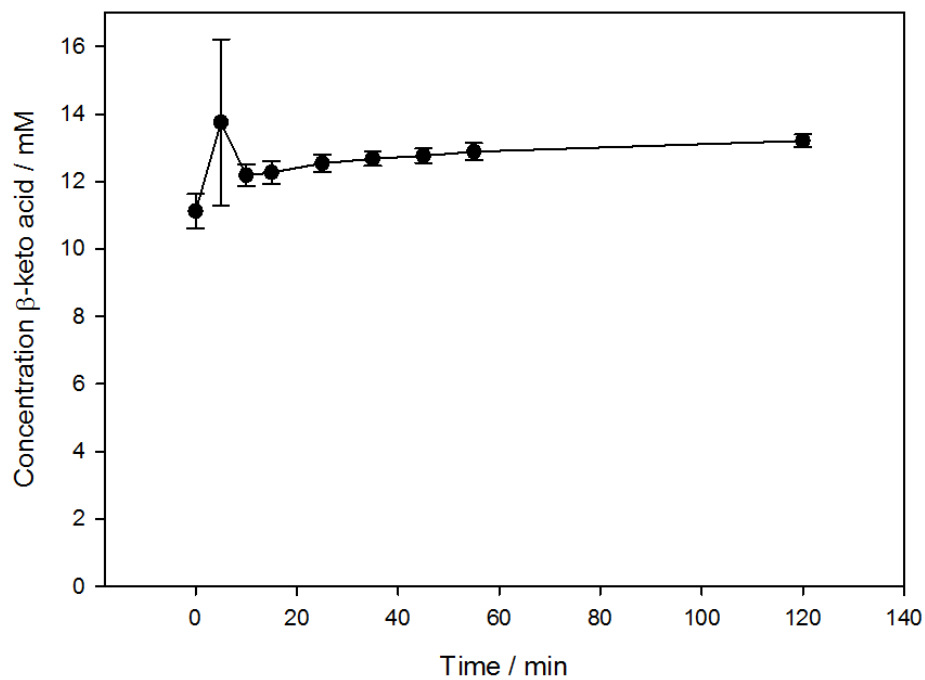


Figure 7.5: Concentration of the β -keto acid 3-oxo-3-phenyl propionate over time.

7.7 SDS-PAGE AFTER INCUBATION OF THE IMMOBILIZED ENZYME ON MAGNETIC BEADS AT 90 °C

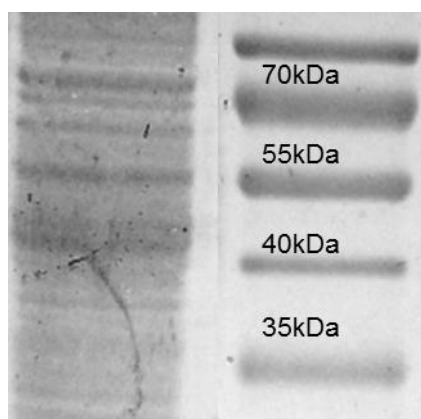


Figure 7.6: SDS-PAGE of immobilized enzyme on magnetic beads after incubation in 1 % SDS at 90 °C. 20 mg/ml beads.

7.8 ACETOPHENONE AND RAC-B-PHENYLALANINE AS CARBON SOURCE

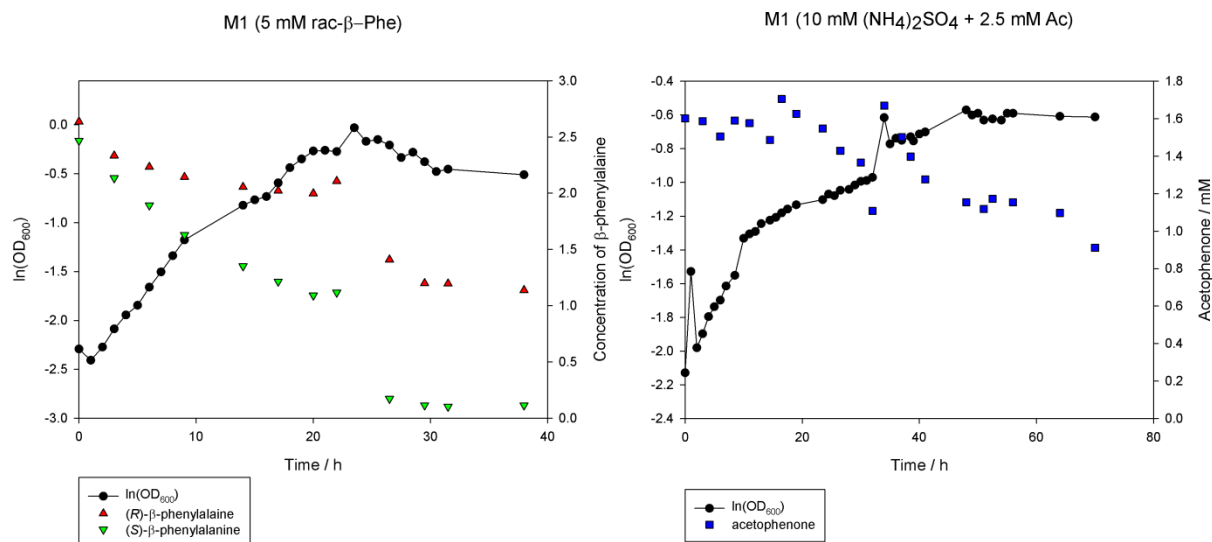


Figure 7.7: Acetophenone as sole carbon source and *rac*-β-phenylalanine as carbon and nitrogen source. For cultivation of the *Burkholderia phytofirmans* strain BS115

FIGURE LEGEND

Figure 1.1: Transaminase catalyzed reaction mechanism.	1
Figure 1.2: Reaction mechanism of transaminases with pyridoxal-5'-phosphate (PLP) as external co-factor via ping-pong bi-bi mechanism.	5
Figure 1.3: General synthesis strategies for transaminase-catalyzed reactions.	8
Figure 1.4: The structures of α - and β -amino acids.	9
Figure 1.5: Overview of the β -amino acids examined in this work	10
Figure 1.6: Solid matrix functionalized with iminodiacetic acid (IDA) and covalently bound nickel (A) and functionalized nitriloacetic acid (NTA) with a covalently bound nickel (B).	14
Figure 1.7: Protein with His-tag, binding onto nickel-chelate complex with functionalized magnetic beads.	16
Figure 3.1: Bioreactor containing a Rushton turbine, a pH sensor, a pO ₂ sensor and a temperature sensor.	33
Figure 3.2: Gradient for elution of the enzyme via IMAC purification of the His-tagged aminotransferase.	37
Figure 4.1: Kinetic resolution to synthesize enantiopure β -amino acids.	46
Figure 4.2: Agarose gel electrophoresis of plasmid pET21b and pET11a.	47
Figure 4.3: Relative conversion of (S)- β -phenylalanine catalyzed by the β -amino acid aminotransferase from <i>Variovorax paradoxus</i> for different expression conditions.	49
Figure 4.4: Chromatogram of the protein purification via IMAC.	50
Figure 4.5: Specific activity of the fractions after IMAC purification.	51
Figure 4.6: SDS-PAGE gel for the fractions of the IMAC purification.	52
Figure 4.7: Specific activity of the fractions after elution of the β -amino acid aminotransferase off the magnetic M-PVA beads.	53
Figure 4.8: SDS-PAGE gel for the fractions after elution of β -amino acid aminotransferase off the magnetic M-PVA beads.	54
Figure 4.9: Relative activity of the immobilized His-tagged β -amino acid aminotransferase.	56
Figure 4.10: Relative activity of immobilized aminotransferase and crude cell extract toward the substrate (S)- β -phenylalanine at different temperatures.	57
Figure 4.11: Specific activity of the immobilized β -amino acid aminotransferase and crude cell extract at different pH.	59
Figure 4.12: Relative activity of the immobilized β -amino acid aminotransferase and the crude cell extract for biotransformation with different amino acceptors.	60

Figure 4.13: Activity/ Specific activity of immobilized β -amino acid aminotransferase after incubation of different bead concentrations with crude cell extract.	63
Figure 4.14: Activity/ Specific activity of immobilized β -amino acid aminotransferase after incubation of 20 mg magnetic beads with various crude cell extract concentrations.	63
Figure 4.15: Relative activity of the immobilized β -amino acid aminotransferase and the crude cell extract for storage at 4° C for 38 days.	65
Figure 4.16: Relative activity of the immobilized β -amino acid aminotransferase, immobilized with nickel, cobalt and copper as affinity metal ions using 20 mg magnetic M-PVA beads for 7 recycling steps.	66
Figure 4.17: Enzyme cascade for the asymmetric synthesis of β -amino acids.	67
Figure 4.18: Specific activity of the lipase from <i>Rhizomucor miehei</i> , <i>Thermomyces lanuginosus</i> and <i>Candida rugosa</i> toward various β -keto acid esters with different moieties.	68
Figure 4.19: Conversion of ethyl benzoylacetate by a lipase from <i>Candida rugosa</i> and the concentration of ethanol during the reaction.	69
Figure 4.20: Amino donors for asymmetric synthesis of β -amino acids.	70
Figure 4.20: Concentration of ethyl benzoylacetate and β -phenylalanine synthesized via synthesized via asymmetric synthesis in an enzyme cascade.	71
Figure 4.22: Wavelength scan of 3-oxo-3-phenyl propionate and acetophenone.	72
Figure 4.23: Shaking flask experiments with <i>rac</i> - β -phenylalanine as sole nitrogen and glucose as carbon source.	77
Figure 4.24: Fermentation of <i>Burkholderia phytofirmans</i> strain BS115 in minimal medium containing <i>rac</i> - β -phenylalanine.	78
Figure 4.25: Negative contrast of an ink-stained bacteria cell culture (<i>Burkholderia phytofirmans</i> strain BS115) under phase-contrast microscope.	80
Figure 4.26: Relative activity of transaminase from <i>Burkholderia phytofirmans</i> strain BS115 with different amino acceptors.	82
Figure 4.27: Specific activity of the fractions of ammonium sulfate saturation.	83
Figure 4.28: Chromatogram of the protein purification via anion exchange chromatography (AEX).	85
Figure 5.1: Binding pocket for the substrate recognition of an ω -transaminase.	109
Figure 7.1: Plasmid card of plasmid pET21b and pET11a containing the encoding gene of β -amino acid aminotransferase from <i>Variovorax paradoxus</i> .	124
Figure 7.2: Freezing and thawing of the immobilized aminotransferase and the crude cell extract.	124

Figure 7.3: Conversion of the <i>rac</i> - β -phenylalanine with His-tagged β -amino acid aminotransferase.	125
Figure 7.4: Activity of aminotransferase in the presence of various DMSO concentration.	125
Figure 7.5: Concentration of the β -keto acid 3-oxo-3-phenyl propionate over time.	126
Figure 7.6: SDS-PAGE of immobilized enzyme on magnetic beads after incubation in 1 % SDS at 90° C.	126
Figure 7.7: Acetophenone as carbon source and <i>rac</i> - β -phenylalanine as carbon and nitrogen source.	127

TABLE LEGEND

Table 1.1: Classification of transaminases based on their evolutionary relationship as pyridoxal-5'-phosphate dependent enzymes.	2
Table 3.1: Devices.	20
Table 3.2: <i>Rac</i> - β -amino acids.	21
Table 3.3: Deployed amino acceptors.	21
Table 3.4: Deployed amino donors.	21
Table 3.5: Columns for enzyme purification	22
Table 3.6: General substances for biotransformation and regeneration of magnetic beads.	22
Table 3.7: β -Keto acid esters.	22
Table 3.8: Deployed enzymes.	22
Table 3.9: Strains with activity toward β -amino acids	23
Table 3.10: Expressing strain and introduced plasmids.	23
Table 3.11: Parameters for analysis of ethanol with GC.	29
Table 3.12: Temperature program (GC).	30
Table 3.13: Restriction enzymes for DNA digestion.	31
Table 3.14: SDS-gel preparation for 2 gels.	36
Table 3.15: Standard substrates for biotransformation.	41
Table 4.1: Description of entries shown in Figure 4.3.	48
Table 4.2: Quantification of enzyme purification via IMAC of the His-tagged β -amino acid aminotransferase.	52
Table 4.3: Quantification of the His-tagged β -amino acid aminotransferase purification Using magnetic M-PVA beads.	55
Table 4.4: Substrate scope of the immobilized enzyme and crude cell extract.	62
Table 4.5: Comparison of μ_{\max} / h, t_d / h, the consumption rates of (<i>R</i>)- β -phenylalanine / g/h (R_R), (<i>S</i>)- β -phenylalanine / g/h (R_S) and of glucose / g/h (R_{Glc}) and the maximal OD at 600 nm for shaking flask experiments (SF) and fermentation (Fer) of <i>Burkholderia phytofirmans</i> strain BS115.	79
Table 4.6: Transaminase substrate scope of the <i>Burkholderia phytofirmans</i> strain BS115	80
Table 4.7: Quantification of enzyme purification via ammonium sulfate precipitation.	84
Table 4.8: Protein content before and after purification of a transaminase from <i>Burkholderia phytofirmans</i> strain BS115.	86
Table 4.9: Quantification of purification with ammonium sulfate and subsequent purification via anion exchange chromatography of a transaminase from <i>Burkholderia phytofirmans</i> strain BS115.	86

Table 5.1: Residual activity after incubating the magnetic beads with crude cell extract. 97